NATIONAL ADVISORY COMMITTEE
FOR AERONAUTICS

TECHNICAL NOTE

No. 1013

STRESSES IN AND GENERAL INSTABILITY OF MONOCOQUE CYLINDERS

WITH CUTOUTS

I - EXPERIMENTAL INVESTIGATION OF CYLINDERS WITH A

SYMMETRIC CUTOUT SUBJECTED TO PURE BENDING

By N. J. Hoff and Bruno A. Boley
Polytechnic Institute of Brooklyn

NACA

Washington
June 1946

NATIONAL ADVISORY COMMITTEE FOR AERONAUTICS

TECHNICAL NOTE NO. 1013

STRESSES IN AND GENERAL INSTABILITY OF MONOCOQUE CYLINDERS

WITH CUTOUTS

I — EXPERIMENTAL INVESTIGATION OF CYLINDERS WITH A SYMMETRIC CUTOUT

SUBJECTED TO PURE BENDING

By N. J. Hoff and Bruno A. Boley

SUMMARY

Ten 24S—T alclad cylinders of 20—inch diameter, 45—:-
or 58—inch length, and 0.012—inch wall thickness, reinforced
with 24S—T aluminum alloy stringers and rings were tested in
pure bending. In the middle of the compression side of the
cylinders there was a cutout extending over 19 inches in the
longitudinal direction, and over an angle of 45°, 90°, or 135°
in the circumferential direction. The strain in the stringers
and in the sheet covering was measured with metalectric strain
gages.

The stress distribution in the cylinders deviate con-
siderably from the linear law valid for cylinders without a
cutout. The maximum strain measured was about four—thirds
of the value calculated from the Mc/I formula when I
was taken as the moment of inertia of the cross section of
the portion of the cylinder where the cutout was situated.
A diagram is presented containing the strain factors defined
as the ratios of measured strain to strain calculated with
the Mc/I formula.

All the 10 cylinders tested failed in general instability.
Two symmetric and one antisymmetric pattern of buckling were
observed and the buckling load appeared to be independent
of the method of manufacture and the length of the cylinder.
The buckling load of the cylinders having cutouts extending
over 45°, 90°, and 135° was 66, 47, and 31 percent, respec-
tively, of the buckling load of the cylinder without a cut-
out.

INTRODUCTION

In the past 15 years a great deal of work has been done in order to clarify the stress distribution in and the failure of reinforced monocoque structures. Most of this work has been devoted to the problems of circular cylinders with cross-sectional properties constant over their length. However, actual monocoque fuselages deviate considerably from this idealized type of structure, one of the most important deviations resulting from the necessity to cut out portions of the shell in order to provide openings for doors, windows, and military equipment.

Two major effects of the cutouts in monocoque cylinders are to be noted. One is the redistribution of stress in the neighborhood of the opening. In this report results of strain measurements are presented which were obtained at the Polytechnic Institute of Brooklyn with 10 circular cylinders tested in pure bending. A later report will contain theoretical calculations and a comparison of the theory with experiment. It may be mentioned here, however, that good agreement has been obtained between the theoretical and experimental axial stresses.

The second item investigated is the effect of the cutout upon the failure of the cylinder. This effect is included in the one first mentioned if failure occurs in the form of material failure, local buckling of some thin-walled element, or buckling of a stringer between two adjacent frames. An entirely new problem arises, however, when failure is caused by general instability.

General instability is defined as the simultaneous buckling of the longitudinal and circumferential reinforcing elements of a monocoque cylinder together with the sheet attached to them. This type of buckling of reinforced circular monocoque cylinders subjected to pure bending has been recently investigated in some detail at the Polytechnic Institute of Brooklyn and the California Institute of Technology under the sponsorship of the National Advisory Committee for Aeronautics (references 1 to 8).

It is rather obvious that a cutout in a monocoque cylinder makes general instability possible under a load smaller than the buckling load of a complete cylinder. The second purpose of the investigations described in this report was to collect data regarding the buckled shape and the

buckling load of cylinders with cutouts of different sizes.
In a later report an attempt will be made to develop a
strain energy theory of the general instability of rein-
forced monocoque cylinders having a cutout.

LIST OF SYMBOLS

c	distance from neutral axis
d	stringer spacing measured along circumference
E	Young's modulus
G	shear modulus
I	moment of inertia of cylinder cross section with respect to neutral axis
I_c	moment of inertia with respect to the neutral axis of the cross section of the portion of the cylinder where the cutout is situated
I_o	moment of inertia with respect to the neutral axis of the cross section of the complete cylinder (no cutout)
M	applied bending moment
M_{cr}	critical bending moment (at general instability)
R	strain factor $(R = \epsilon_{exp}/\epsilon_{calc})$
t	thickness of sheet covering
y_c	distance from neutral axis of cylinder cross section with cutout

y_0 distance from neutral axis of cylinder cross section
            without cutout

$2w$ effective width of flat panel

$2w'$ effective width of curved panel

γ shear strain

ϵ normal strain

ϵ_c normal strain in sheet in circumferential direction

ϵ_{calc} calculated normal strain in axial direction

ϵ_{curved} buckling strain of non-reinforced circular cylinder
            under uniform axial compression

ϵ_{exp} experimental normal strain in axial direction

ϵ_{flat} buckling strain of flat panel under uniform com-
            pression

ϵ_{str} axial strain in stringer

ϵ_x normal strain in sheet covering in axial direction

μ Poisson's ratio

σ_c normal stress in sheet in circumferential direction

σ_x normal stress in sheet covering in axial direction

τ shear stress

TEST SPECIMENS, RIG, AND PROCEDURE

The test cylinders are shown in figures 1 and 2. They
consist of a 24S-T alclad sheet covering of 0.012-inch thick-
ness, 16 24S-T aluminum alloy stringers of 3/8-inch square
section, and a number of 24S-T aluminum alloy rings of
1/8 by 3/8 rectangular section. The diameter of the cylinder
is 20 inches, and the length either 45 inches, or 58 inches.
Each cylinder has a cutout in its middle extending over
three ring fields and two, four, or six stringer fields.
Altogether 10 specimens were tested. They were numbered
consecutively from 16 to 25. The characteristics of each
are given in table 1.

The cylinders were constructed in a manner similar to
that described in reference 2. Differences worth mention-
ing are the use of rivets spaced 0.643 inch apart in all
but the first cylinder of the present series instead of
machine screws spaced 0.714 inch apart, and the increased
ring spacing as compared to that of the cylinders of refer-
ence 2. Further details may be found in figures 1 and 2
as well as in table 1.

The test rig and the attachment of the cylinders to the
rig are very much the same as those used in the tests de-
scribed in reference 2. Figure 3 shows that the cutout is
always on the lower, or compression, side of the cylinder.
The figure also contains the designation of the ring fields
and stringers.

The photograph of figure 4 shows all the parts of the
rig that differ from the original ones used in the ex-
periments of reference 2. They are the strengthened type
of loading head, the heavier end rings, and the stronger
stringer grip fittings attached to the end rings by 3/4-
inch diameter bolts. Each grip fitting contains a surface
with machined and case-hardened serrations to prevent any
sliding of the stringer relative to the end ring.

As in the earlier tests the load was applied by means
of a mechanical jack, and its magnitude was measured by
Baldwin-Southwark SR-4 metalectric strain gages type A-1
cemented to a calibrated load link. The strain in the test
cylinders was measured in every stringer in two end bands
$5\frac{1}{2}$ inches from the edge of the end rings, and in the middle
band in the plane of symmetry of the cylinder. The measure-
ments were made with two SR-4 type A-1 strain gages cemented
to opposite sides of the stringer and connected in series in
order to obtain the average normal strain in the stringer.
Additional pairs of gages were arranged in other locations
when more information was desired regarding the strain
distribution along a stringer. In cylinder 24 the axial
strain was also measured in the sheet in the middle band
in the center of each stringer field by 10 additional pairs
of strain gages.

In four cylinders the strain distribution in the sheet
was surveyed in more detail by the use of pairs of SR-4
type R-4 equilateral strain rosettes. Six to twelve pairs
of rosettes were cemented to the sheet covering of these
cylinders in the neighborhood of the cutout. The strain
in the A-1 type strain gages was measured with the aid of

an SR—4 portable strain indicator, which is an electronics
device. The strains in the rosettes and the load link
were measured with an SR—4 control box, which contains a
Wheatstone bridge. Switching was done by two Shallcross
multiple switching units and by the tapered brass socket
and plug arrangement used in the earlier tests.

During the tests the load was changed in increments of
90 to 625 pounds, using greater values with cylinders having
a small cutout and in the initial stages of loading, smaller
values with cylinders having a large cutout and when the
load was near the failing load. About 1/2 to 3 minutes were
required to complete the change from one load to the next.
The time necessary for taking readings and check readings
was 20 to 40 minutes at each stage of loading. A complete
test to failure took from 4 to 10 hours and was always com—
pleted within 1 day.

The accuracy of the strain measurements was checked by
tests made with a cantilever beam to which pairs of gages
were cemented. The maximum error was found to be about
$\pm10 \times 10^{-6}$ inch per inch. The applied load was measured
with an error of less than ±50 pound.

ANALYSIS AND DISCUSSION OF TEST RESULTS

Presentation of Test Results

Results of the strain measurements in the stringers
are presented for each of the two end bands and for the
middle band of each cylinder. The presentation is in the
form of diagrams in which the strain is plotted against
the distance of the stringer from the horizontal diameter
of the cylinder. These basic data are contained in figures 5
to 34.

The strain measured in the sheet and the stress in the
sheet calculated from the measured strain are recorded in
the diagrams of figures 35 to 40.

The variation of the strain set up in the stringers
and sheet by the various operations of fastening the test
specimen proper to the end rings and the rig is shown in
figures 41 to 45.

The axial force and the bending moment calculated from the strain readings are compared in table 2 with the corresponding values obtained from the measurement of the applied load.

The effect upon the strain distribution of the length of the cylinder and of the differences in its construction is presented in figures 46 to 51. Figures 52 to 57 give the variation of the strain along the edge stringer (the one bordering the cutout) and the stringer next to it in the various stages of loading. The axial strain distribution in the entire cylinder is shown in figures 58 to 63 for an applied bending moment of 35,000 inch-pounds. The variation of the strain in the most highly compressed stringers with moment is presented in figures 64 to 72.

The effect of the size of the cutout upon the strain is given in four groups of drawings. In the first, figures 73 to 75, the strains are plotted against the distance of the stringer from the horizontal diameter of the cylinder. Figures 76 to 78 contain plots of the changes in strain in individual stringers. The ratios of calculated and observed stringer strain are presented for the convenience of the designer in figures 79 to 82. Finally, figure 83 shows the shift of the neutral axis.

The changes in the size of the cutout caused by the application of the loads also were measured. The values obtained are plotted in figures 84 and 85.

Figures 86 to 89 show the variation of the maximum strain with the size of the cutout and the applied moment. In figure 90 the maximum moment (at buckling) is plotted against the size of the cutout. Data regarding the buckling of the cylinders are assembled in table 3, data concerning the behavior after buckling in table 4.

Non-Linearity of the Normal Strain Distribution

It is customary in airplane stress analysis, and entirely justified, to assume that the normal stress is distributed according to a linear law, and that the neutral axis is the horizontal diameter of the cylinder, when a pure bending moment is applied in a vertical plane to a reinforced monocoque cylinder. The linearity of the stress distribution is a consequence of the assumption that plane sections perpendicular to the axis of the unloaded cylinder remain

plane and perpendicular to the axis when the cylinder is distorted by the applied moment. The stress distribution remains linear even when the sheet covering buckles on the compression side of the cylinder but the neutral axis shifts toward the tension side. The normal stress still can be calculated by the simple Mc/I formula, provided in all those panels where the sheet is in a buckled state the effective width of the sheet rather than the total width is considered when the centroid and the moment of inertia of the section are determined.

These conclusions were borne out by the experiments described in reference 2. The situation is entirely different, however, when there is a cutout in the monocoque cylinder. Stringers of which portions are cut out offer little resistance to axial displacement so that the stress distribution in the cylinder is not linear when the end sections of the cylinder remain plane during the distortions. Conversely, if the stress is applied to the end sections of the cylinder corresponding to the linear pattern assumed in bending theory, then during the ensuing distortions of the cylinder the end sections do not remain plane.

In the experiments presented here the end sections of the cylinder were forced to remain plane during the tests. In the tests of reference 2 some shimming was necessary in order to achieve linearity of the displacements and this linearity could be checked with the aid of the strain gage readings. In the present tests no direct check of the linearity of the displacements was possible, since a plane end section did not correspond to a linear strain distribution. Nevertheless, the rigidities of the end rings and the loading head are believed to have been sufficient, because these elements were materially heavier than those used in the tests described in reference 2, while the maximum applied moments were considerably smaller.

An indirect proof of the plane distortion pattern at the end rings was obtained analytically. The stresses in the stringers were calculated on the basis of the assumption that the end rings remain plane, and the strain distribution obtained was in good agreement with that measured. Details of these calculations and comparisons will be given in a separate report.

If there is a cutout in a reinforced monocoque cylinder, at some distance from the cutout in the axial direction both the displacements and the stresses will be distributed linearly

within the accuracy required in engineering calculations.
It appears, however, that this distance is considerable,
probably greater than the length of the portion of any
actual fuselage that can be regarded as uniform and cylin-
drical. This statement holds if the size of the cutout is
of the order of magnitude of those investigated. In any
section closer to the cutout than the distance at which
the effect of the cutout becomes negligible, as a rule,
neither the displacements nor the stresses are distributed
linearly. In the present tests linearity of the displace-
ments was stipulated at the end sections, since it is con-
sidered to be in better agreement with reality than a
linearity of the stress distribution and also since it is
easier to realize in experiment.

As in reference 2, the fundamental strain data obtained
in the tests are presented in a number of diagrams. In fig-
ures 5 to 34 the ordinate is the distance of any individual
stringer from the horizontal diameter of the cylinder, and
the abscissa is the strain measured in the stringer. The
following observations may be made in connection with these
diagrams:

1. On the tension side of the cylinder the strain, and
consequently the stress, is distributed according to a linear
law in good approximation.

2. The neutral axis is shifted considerably toward the
upper side. (It should be remembered that the cutout is
situated on the lower side.) The amount of shift increases
with increasing size of the cutout and with increasing bend-
ing moment.

3. On the compression side of the cylinder close to the
neutral axis the strain (and stress) distribution is sensibly
linear. The slope of the straight line is often greater than
that of the line on the tension side.

4. In the middle of the cylinder, that is, in the middle
band, the compressive strain increases, as a rule, more rapidly
than according to a straight line farther away from the neu-
tral axis. The deviation from linearity, however, is not
substantial as long as the applied bending moment is not
large. Close to the maximum load the curvature of the
strain line often reverses and the deviations from linearity
become large.

5. At the ends of the cylinder, that is, in the end bands, the strain, and thus also the stress, increases less rapidly than according to a straight line farther away from the neutral axis. Up to the edge of the cutout the deviation from linearity is not substantial when the applied bending moment is not very large. Beyond the edge of the cutout the strain decreases rapidly.

6. The agreement is good between the strain values measured at the two ends of the cylinder. Such is the case also in regard to the strains measured in stringers situated symmetrically with respect to the vertical axial plane of symmetry.

Strain and Stress in the Sheet Covering

A check of the strain distribution in the sheet covering at the middle section of cylinder 24 was made possible by the application of a pair of strain gages to the middle of each panel. The measured values of the strain are shown in figure 30 together with the strain in the stringers. It may be seen that on the tension side the strain in the sheet plots exactly on the curves of the stringer strain for all loads. The coincidence is almost as good on the compression side for the two lower loads. Under the two higher loads, however, the strain in the sheet has about the same value as under the two lower loads. Apparently, the sheet buckled approximately at the second stage of loading and the higher applied moments did not increase the average strain in the sheet.

In cylinders 16, 17, 19, and 25 the strain was measured in some panels of the sheet by means of strain rosettes. The values obtained with the three different sizes of cutouts are given in figures 35, 37, and 39. The axial component of the strain in the sheet was found to be in good agreement with the strain in the stringers at low loads when the sheet was not in a buckled state. When the panels buckled, the compressive strain in the sheet lagged behind the strain in the stringers. Both the normal strain in the circumferential direction and the shear strain were calculated from the strain rosette data. The values are given in the figures mentioned. In general, these strains are small and decrease as the distance of the rosette from the stringer adjacent to the cutout increases. The circumferential strain is always tensile.

The stresses in the sheet were calculated with the aid
of the formulas

$$\sigma_x = [E/(1 - \mu^2)](\epsilon_x + \mu\epsilon_c)$$
$$\sigma_c = [E/(1 - \mu^2)](\epsilon_c + \mu\epsilon_x) \qquad (1)$$
$$\tau = G\gamma$$

where x and c refer to the axial and the circumferential
directions, respectively. The values computed are given in
figures 36, 38, and 40.

Initial Strains

The initial strains caused by attaching the cylinder
to the test rig were investigated in the case of two cylinders.
The results of the measurements made with cylinder 24 are
presented in figures 41 to 45. The effect of placing end
ring No. 1 on the cylinder and fastening it to the cylinder
by means of the stringer grip fittings and bolts is shown
in figure 41. The initial stress decreases rapidly along
the axis of the cylinder and becomes insignificant at the
other end.

The distribution of the initial strain caused by the
attachment of ring No. 2 is shown in figure 42. The curve
of the initial strain in the band next to ring No. 2 re-
sembles that in the band next to ring No. 1 presented in
figure 41, except for an unusually high maximum in stringer
16. The decrease of the initial stress along the cylinder
is slower than in the case discussed before. This can be
attributed to the effect of the rigid end ring at the other
end of the cylinder which prevented relative displacements
of the far ends of the stringers.

The attachment of the test specimen to the end stand
caused comparatively small stresses (fig. 43), its attach-
ment to the loading head insignificant stresses (fig. 44).

The total initial strains are presented in figure 45.
The corresponding maximum stresses amount to 3000 psi tension
in stringer 16 close to the loading head, 2700 psi com-
pression in the middle of the cylinder in the stringer at
the edge of the cutout, and 1250 psi tension in stringers
1 and 4 near the end stand.

In the middle band the initial strain was also measured in the sheet covering. In all the figures the values obtained in the sheet fall on the curves drawn for the stringers.

The initial stresses in stringers and sheet added up to zero resultant force and zero resultant moment in good approximation.

With cylinder 22 the initial strains were somewhat smaller. Moreover, the initial stress in the middle band in the edge stringers was tensile. It amounted to about 1,000 psi.

Although it is regrettable that the initial strains were so high, no method could be devised with the time and means available to reduce them to negligible quantities. To indicate the importance of the initial stress in relation to the stresses caused by the loading, it is noted that the maximum stress in the cylinders near buckling was of the order of 20,000 to 30,000 psi. The initial stress could not influence the stress distribution caused in the cylinder by the applied load at loads under which the sheet panels were not in a buckled state. No effect of the initial strain upon the buckling load of the cylinders in general instability was observed as follows from the uniformity of the critical bending moments with each size of cutout, and the smoothness of the curve (see fig. 90) connecting the points corresponding to the different sizes of cutouts. Moreover, cylinder 22, in which the edge stringer was in tension, failed under the lowest buckling load of its group, while the buckling load of cylinder 24, in which the edge of the cutout was in compression, was the highest of its group. The deviation of the critical bending moments of these cylinders from the group averages, however, amounted to only 3.8 and 3.0 percent, respectively.

Equilibrium of Forces and Moments

The resultant force and the resultant moment were calculated from the strain measurements in each band. They are listed in table 2 together with the values of the applied moment. In the calculations it was assumed that on the tension side the entire sheet was fully carrying, while on the compression side the effective width of sheet was determined with the aid of the formulas

$$2w' = 2w + (\epsilon_{curved}/\epsilon_{str})(d - 2w) \left.\vphantom{\begin{array}{c} \\ \\ \end{array}}\right\} \quad (2)$$

$$2w = [\epsilon_{flat}/(\epsilon_{str} - \epsilon_{curved})]^{1/3}d$$

As in reference 2, equations (4), the critical values of the strain were taken as

$$\epsilon_{flat} = 0.5 \times 10^{-4} \left.\vphantom{\begin{array}{c} \\ \\ \end{array}}\right\} \quad (3)$$

$$\epsilon_{curved} = 3 \times 10^{-4}$$

The agreement between the moments applied and calculated was found to be reasonably good. The axial force resultant was also small as compared to the total tensile force on the tension side and the total compressive force on the compression side of the cylinder the difference between which is the force resultant. There is a definite tendency for the calculated moment to decrease in the direction from the loading head to the end stand. The average decrease from one end band to the other is about 9 percent of the applied bending moment for the first load, and about 8 percent for the second load. As this fact was detected only when table 2 was set up after completion of the test series, it was not possible to establish definitely the reason for it.

Strain Variation with Length of Cylinder and Method of Construction

In figures 46 to 51 the strain diagrams obtained for the middle band and the average strain diagrams of the two end bands are presented for an applied bending moment of 35,000 inch-pounds. In each figure the diagrams corresponding to one size of cutout are shown to permit an evaluation of the effects upon the strain distribution of different total lengths of the cylinder and various methods of fabrication.

As far as the effect of the length is concerned, the following conclusions may be drawn:

1. The maximum strain in both the middle and end bands is smaller when the cylinder is longer.

2. The strain distribution in the end bands is slightly closer to the linear law of strength of materials when the cylinder is longer. This is to be expected since the linear law corresponds to the strain distribution in the end sections

of an infinitely long cylinder. The deviations from line-
arity are still very noticeable when the distance from the
edge of the cutout to the end ring is equal to the diameter
of the cylinder.

3. The effect of the variation of the length is more
noticeable when the circumferential length of the cutout is
small.

In 7 of the 10 test cylinders the rings were attached
to the sheet only at the intersections of the rings with
the stringers. In the remaining three cylinders three
additional equidistant rivets were used in each panel for
fastening together the sheet and the rings on the com-
pression side of the cylinder. The differences between the
strain diagrams of cylinders manufactured according to these
two methods were slight and inconclusive.

In cylinder 16 bolts were used throughout for fastening
together the sheet, stringers, and rings. The spacing of
the bolts was 0.714 inch. Cylinder 17 was built identically
with cylinder 16 except that it was riveted with a rivet
pitch of 0.643 inch. The strain distribution in the two
cylinders was similar with the bolted cylinder showing a
slightly closer approach to the straight line law valid for
cylinders without a cutout.

Strain Variation along Stringers

In figures 52 to 57 the strain along one of the edge
stringers and the strain along the stringer adjacent to it
are plotted for the different stages of loading. The curves
are symmetrical to the middle section of the cylinder in
good approximation. In most of the diagrams there is a
tendency toward slightly higher strains in band I than in
band A.

In figures 58 to 63 the strain distribution over the
entire cylinder is shown in the form of strain trajectories.
The cylinder is imagined to be cut along a stringer and
developed into the plane of the drawing. The location of
the stringers and rings is shown. Points in this surface
subjected to the same strain are connected with lines denoted
as trajectories. Since each trajectory represents a constant
value of strain, the trajectories were constructed by means
of linear interpolation between the measured values of the
strain.

The trajectories may be visualized as the contour lines of a topographic map of the strain surface. In figure 58 they show distinctly a hill of stress concentration along stringers 8 and 10 with a peak in the middle of the cylinder. There is a deep valley in the region of stringer 9 extending from the cutout to the end of the cylinder. The strain distribution on the tension side of the cylinder lacks noteworthy features. Figure 59 differs from figure 58 mainly by showing a definite increase of the strain from left to right.

The distinctive feature of figures 60 and 61 is the appearance of curves resembling parabolas in the regions between the cutout and the ends of the cylinder. These curves demonstrate that the reduction in the value of the strain at the cutout decreases with distance from the cutout, and that at some distance from the cutout the strain distribution may again correspond to the linear law. It is to be noted that in figures 60 and 61 corresponding to the 58- and 45-inch long cylinders, respectively, the values of the strain at the end rings are almost identical. This indicates that an increase in the total length of the cylinder increases the length of the parabolic trajectories. Hence it might be necessary to build much longer cylinders than the present ones if an approximately linear strain distribution at the end rings is desired.

It may be mentioned that the absence of the parabolic trajectories in figures 58 and 59 between the cutout and the end rings may be due to insufficient data for the strain in that region.

Figures 62 and 63 show that the stress concentration hill is higher, steeper, and more extended, and the valley between cutout and end ring deeper when the cutout is longer in the circumferential direction. With the medium size cutout the strain at the ends of stringer 9 is practically zero, while with the large cutout there appears even a small tensile strain in stringer 9 next to the end rings. It may be pointed out that the interval between the trajectories in figure 63 is twice that in figure 62. False conclusions will be avoided if this is kept in mind.

Variation of Strain With Applied Moment

The variation of the strain in the edge stringers and in those adjacent to the edge stringers was plotted against the applied moment for all the cylinders tested. Curves were also plotted for several additional stringers in some of the cylinders. The abscissa was the moment corrected for the weight of the loading arm. The curves were used to obtain by extrapolation the values of the strain at buckling.

In this report only the diagrams corresponding to cylinders 16 (figs. 64 to 66), 21 (figs. 67 to 69), and 22 (figs. 70 to 72) are included. The conclusions drawn from these figures are now stated so that they apply as well to the cylinders for which no curves are presented.

1. Curves drawn for strains measured in any one cylinder at locations symmetrically situated with respect to either vertical plane of symmetry of the cylinder show good agreement.

2. All the strain-moment curves are substantially straight up to about one-half the buckling load.

3. From about one-half to three-quarters of the buckling load the strains increase with moment more rapidly than in the initial stages of loading.

4. Above about three-quarters of the buckling load the strains change rapidly. In the end bands the strain in the edge stringer drops, that in the adjacent stringer increases. The curves corresponding to these stringers intersect so that the strain in the edge stringer is smaller at buckling than the strain in the adjacent stringer. In the middle band the strain in the edge stringer keeps increasing but at a lower rate than the strain in the adjacent stringer. In the case of cylinders 18, 23, and 25 the curves crossed so that the strain at buckling was lower in the edge stringer than in the adjacent one. In the other cylinders no crossing took place in the curves for the middle of the cylinder.

5. The statements under (4) are strictly valid only for the six cylinders that buckled both sides outward, for one of the two cylinders that buckled both sides inward, and for one of two cylinders that buckled one side inward and the other outward. The deviations from this normal behavior

were slight in the case of cylinder 23, which buckled both
sides inward; they were considerable in the case of cylinder
20 which buckled one side inward and the other outward.
With the latter the strain in the middle band dropped in
both the edge stringer and the one adjacent to it on the
side of the cylinder that buckled inward, and increased in
both stringers on the side that buckled outward. In the
end bands the strain in the stringer adjacent to the edge
stringer dropped on the side that buckled inward and in-
creased on the side that buckled outward. In the end bands
the strain in the edge stringers dropped on both sides.

6. The strain-moment curves for stringers on the tension
side of the cylinder also deviated from linearity but to a
much lesser degree than those corresponding to stringers on
the compression side.

Strain Variation with Size of Cutout

In figures 73 the strain diagrams of the end bands
are compared for cylinders having the three different sizes
of cutout. The same comparison based on the middle section
is presented in figure 74, while figure 75 contains the
strain distribution curves calculated for cylinders which
have a constant cross section identical with the cross
section of the portion of the actual cylinder where the cut-
out is situated. The calculation was carried out for an
applied moment of 35,000 inch-pounds, and the experimental
curves were reduced to correspond to the same bending moment.

The comparison shows that there is a reasonable agree-
ment between the experimental and the so-calculated strain
distribution in the cut middle section. The maximum ex-
perimental tensile strain is slightly smaller, and the maxi-
mum experimental compressive strain slightly larger than
the corresponding theoretical values.

In the complete end sections the strain distribution
above the horizontal diameter of the cylinder is very
similar to the distribution in the cut middle section. From
this line downward the experimental strain falls off the
theoretical straight line more and more rapidly. In this
region, therefore, the experimental strain is smaller than
the theoretical strain. The value of the experimental strain
actually decreases with distance from the horizontal diameter
in the region where the stringers are cut.

Both the maximum strain and the deviations from linearity increase rapidly with increasing size of the cutout.

The variation of the strain in each stringer with increasing size of the cutout is shown in figures 76 to 78. The first of these figures contains the experimental curves for the end bands, the second the experimental curves for the middle band, and the last one the calculated values corresponding to a cylinder of constant section identical with the section of the actual cylinder at the location of the cutout. Comparison of these figures shows that the strain in the cutout portion does not differ much from that calculated for the cutout cylinder on the basis of the Mc/I formula. The deviations in the end bands are substantial when the cutout is large.

Figures 79 to 82 were prepared for the convenience of the designer. They give the strain factors R defined as the ratios

$$R = \epsilon_{exp}/\epsilon_{calc} \qquad (4)$$

of the experimental strain to the fictitious calculated strain. In the curves of figures 79 to 80 the basis of the comparison is the strain in the complete cylinder:

$$\epsilon_{calc} = My_0/EI_0 \qquad (5)$$

where I_0 is the moment of inertia of the full cylindrical section, and y_0 is the distance of the stringer in which the strain is sought from the neutral axis of the cylinder in the same section.

The curves of figures 81 to 82 are based on the sectional properties of the portion of the cylinder where the cutout is located. The theoretical strain is

$$\epsilon_{calc} = My_c/EI_c \qquad (6)$$

where I_c is the moment of inertia of the cross section of the portion of the cylinder where the cutout is located about the horizontal centroidal axis of the section, and y_c is the distance of the stringer in question from the neutral axis of the section.

It may be seen from the diagrams that the strain factor
R deviates greatly from unity when the basis is the com-
plete cylinder, while its value is close to unity when the
basis is the cutout cylinder. Figures 79 and 80 are, there-
fore, considered reliable only in the case of cylinders
closely resembling those tested. On the other hand, it is
believed that stresses calculated with the aid of figures
81 and 82 should prove useful even with cylinders differ-
ing considerably from those tested as long as the stringers
are distributed uniformly around the perimeter, and the
stresses are sought for a bending moment not greater than
about one-half the critical bending moment in general in-
stability. This latter requirement does not eliminate the
usefulness of these figures since in many monocoque cylinders
with cutout failure does not occur by general instability.

It should be noted that the cross-sectional properties
must be based on the effective areas of the sheet cover-
ing in all those panels that are in a buckled state under
the action of the bending moment.

The strain diagrams showed a considerable amount of
shift of the neutral axis from the horizontal diameter of
the cylinder. In figure 83 the shift obtained from the ex-
perimental curves of the middle and end bands is plotted
against the size of the cutout. The figure corresponds to
an applied moment of 35,000 inch-pounds. The calculated
location of the centroid of the section of the cutout portion
is also shown. It is worth noting that the neutral axis of
the complete end sections differs little from that of the
middle section, and that both pass close to the centroid
of the cross section of the cutout portion.

Deflection Measurements

The changes of the linear dimensions of the cutout due
to loading were measured roughly, within about a sixty-fourth
of an inch, with the aid of a steel scale. The values ob-
tained are plotted against the applied moment for two repre-
sentative cylinders. The data shown in figure 84 refer to
cylinder 16,which buckled symmetrically in the outward
direction, those shown in figure 85 to cylinder 20,which
buckled one side in the inward and the other in the outward
direction.

Magnitude and Location of Maximum Stress

At low values of the applied moment the maximum strain
always occurred in the middle of the edge stringer. At
buckling the maximum strain was usually in the middle of
the edge stringer, but in the case of cylinders 18, 23, and
25 it occurred in the middle of the stringer adjacent to
the edge stringer.

The average maximum value of the strain in the three
groups of cylinders corresponding to the various sizes of
cutouts is plotted in figure 86 against the ratio of the
applied moment to the average buckling moment of each group.
For the sake of comparison the curve corresponding to
cylinder 11 of reference 2 which had no cutout is also
shown. The four curves are similar. They are almost
straight with a slight deviation in the upward direction
when the applied moment is large.

In figure 87 faired-in curves are presented for the
experimental average maximum strain in the cylinder as a
function of applied moment and size of cutout. The corre-
sponding calculated values are shown in figure 88, the ratios
experimental value divided by calculated value in figure 89.
Figures 87 and 88 are reasonably similar, but the lines in
figure 87 are more curved than those in figure 88. The
numerical values of the experimental strain are, as a rule,
higher than those of the calculated strain. Except for
very small loads the maximum strain occurs when the cutout
extends over an angle of about 100°.

The curves of the strain ratios vary greatly with
applied load. For small loads they resemble ellipses, for
high loads they have steep maxima for values of the cutout
angle close to 90°. When the cutout is small the strain
ratio first decreases, and then increases again with in-
creasing load. In the region of the maxima of the curves
the strain ratio increases steadily with increasing load.
The highest value of the strain factor in the diagram is 1.39.

General Instability

Each of the 10 cylinders investigated failed in general
instability. Three distortion patterns were observed at
failure. Two of them were symmetric, both edge stringers
buckling either in the inward or in the outward direction.
The third was antisymmetric, one edge stringer buckling in
the inward, the other in the outward direction.

    The instability data are collected in table 3. It
may be seen that only 2 cylinders showed the antisymmetric
pattern, and a comparison with table 1 reveals that both
of these cylinders had a small-size cutout. Moreover, of the
three cylinders in which the rings were also riveted to the
sheet, two buckled symmetrically in the inward direction,
and one antisymmetrically. No other cylinder buckled
symmetrically in the inward direction. The data contained
in table 3 show no correlation between the buckling pattern
on the one hand and the length of cylinder, size of cutout,
and method of construction on the other, except for the
two items mentioned above, which, however, may be just
incidental. It is believed possible that slight initial
deviations of the center line of an edge stringer from a
straight line determine whether the stringer will buckle in
the inward or the outward direction.

    The characteristic features of the pattern of buckling
are a main (inward or outward) bulge in the neighborhood of
the midpoint of the edge stringer accompanied by a secondary
bulge and four minor bulges. The crest of the secondary
bulge is situated at a distance of one or two stringer
spacings from the edge stringer in the circumferential direc-
tion. The amplitude of the secondary bulge is smaller than
or equal to that of the main bulge and the sense of the de-
flections is opposite to that of the main bulge. The crests
of the minor bulges are between the edge ring and the second
ring from the edge ring, their amplitudes are considerably
smaller than that of the main bulge, and the senses of their
deflections alternate. Details of the deflected shapes are
shown in the photographs contained in figures 91 to 110.

    With each cylinder deflections of the edge stringers
were observed well before buckling occurred. The deflections
increased gradually and attained substantial magnitudes be-
fore the cylinder failed. Buckling itself occurred suddenly
with 3 of the 10 cylinders, gradually with the others.
Two of the cylinders that failed suddenly buckled anti-
symmetrically, one symmetrically in the inward direction.

    A characteristic feature of sudden buckling of the
monocoque cylinder was the sudden buckling of the edge
ring in the inward direction. At this stage of the loading
the load link reading suddenly dropped, and there was a
loud report. In table 4 the maximum load and the load after
buckling are listed for cylinders 20 to 25. In the case
of gradual buckling a maximum load was reached which could
be maintained even though the deflections were greatly

increased by lowering the end point of the loading arm.
In such cases the test was continued until a drop in the
load was observed. With each cylinder the load could be
again increased after the test cylinders were left in the
loading rig under load overnight, but the maximum load
could never be reached again. When the load was entirely
released, and then again applied, the maximum value of the
load during the second loading was 83 to 94 percent of the
buckling load.

The critical bending moment of each cylinder is plotted
against the size of the cutout in figure 90. The value
corresponding to cylinder 11 of the test series of refer-
ence 2 is added in order to complete the diagram. It may
be seen that the averages of the groups of points can be
connected by a smooth curve. Moreover, the individual
points deviate but slightly from the group averages. The
percentage deviation is given in table 3. The maximum de-
viation is 2.5 percent with the group of cylinders having
the small cutout, 7.5 percent with that corresponding to
the medium cutout, and 3.0 percent with that corresponding
to the large cutout.

In each group there were cylinders of 45- and 58-
inch   length, and cylinders in which the rings were riveted
to the sheet covering. No correlation was found between
buckling load on the one hand, and length of cylinder and
method of construction on the other. As far as the effect
of the pattern of buckling upon the buckling load is con-
cerned, it may be observed that cylinders that buckled
antisymmetrically had the lowest buckling loads of their
group, while those which buckled symmetrically in the in-
ward direction showed the highest buckling loads of their
group.

                          CONCLUSIONS

     From the strain measurements the following conclusions
may be drawn:

     1. Considerable deviations from the commonly assumed
linear law for the stress distribution were observed in all
the sections of the cylinders, including the end sections
of the long cylinders the length of which was equal to
approximately three times the diameter of the cylinder.

2. On the tension side, and in the portion of the compression side adjacent to the neutral axis the strain varies approximately linearly with distance from the horizontal diameter of the cylinder. In most cylinders the slope of the straight lines is different on the tension and the compression sides. In the cutout portion of the cylinder the compressive strain increases more rapidly than according to the straight line in the neighborhood of the edge stringer. In the complete portions of the cylinder the compressive strain decreases rapidly beyond the edge stringer.

3. The axial strain in the sheet covering and that in the stringers were found to plot along the same curves as long as the sheet was in the non-buckled state.

4. The effect upon the strain distribution of the method of construction, namely the use of bolts or rivets, and the riveting of the sheet to the stringers alone or to both stringers and ring, was found to be slight.

5. Increasing the total length of the cylinder always slightly decreased the stress concentration caused by the cutout.

6. Up to about one-half the failing load the strain increases linearly in any one stringer with increasing applied moment. Beyond this load the strain increases more rapidly than according to the straight line. Above about three-quarters of the failing load the strain distribution changes considerably. In the cutout portion the increments in strain in the edge stringers tend to become smaller than those in the stringers adjacent to the edge stringers. In the complete portions of the cylinder the strain in the edge stringers decreases, that in the adjacent stringers increases rapidly.

7. In figures 79 to 82 strain factors are presented for each stringer and for any size of cutout from 0° to 135°. These factors are valid for loads not greater than one-half the failing load. The strain factors of figures 79 and 80 are ratios of the average measured strain to the strain calculated from the conventional Mc/EI formula with I representing the moment of inertia of the complete cylinder. Some of these strain factors are very high, the maximum value being 5.7. In figures 81 and 82 the strain factors are calculated in the same manner except that I is based on the section of the cutout portion. It may be seen from the diagrams that the Mc/EI formula represents a fair

seven gradually reached a maximum bending moment which re-
mained practically constant while the end point of the
loading arm was further lowered.

3. The buckling load was not influenced by the method
of manufacture and the length of the cylinder. It should
be noted that one cylinder was bolted while the other nine
were riveted. Six cylinders had the stringers alone riveted
to the sheet, while in three the rings were also attached
by rivets to the sheet on the compression side. Five cyl-
inders were 58 inches, and five 45 inches long.

4. Figure 90 presents the ratio of the buckling moment
of a cylinder having a cutout extending over 0° to 135° to
that of a cylinder not having a cutout. In the case of the
45°, 90°, and 135° cutouts the ratio was 0.66, 0.47, and
0.31, respectively.

5. The drop in the bending moment at failure was com-
paratively small, amounting to 9 percent on the average.
Moreover, the cylinders were able to carry this reduced
load overnight, and it was even possible to increase the
bending moment slightly on the following day.

Polytechnic Institute of Brooklyn,
    Brooklyn, N. Y., November 5, 1945.

REFERENCES

1. Hoff, N. J. and Klein, Bertram: The Inward Bulge Type
      Buckling of Monocoque Cylinders. I — Calculation of
      the Effect upon the Buckling Stress of a Compressive
      Force, a Nonlinear Direct Stress Distribution, and
      a Shear Force. NACA TN No. 938, 1944.

2. Hoff, N. J., Fuchs, S. J., and Cirillo, Adam J.: The
      Inward Bulge Type Buckling of Monocoque Cylinders.
      II — Experimental Investigation of the Buckling in
      Combined Bending and Compression. NACA TN No. 939,
      1944.

3. Hoff, N. J. and Klein, Bertram: The Inward Bulge Type
      Buckling of Monocoque Cylinders. III — Revised Theory
      Which Considers the Shear Strain Energy. NACA TN No.
      968, 1945.

4. Guggenheim Aeronautical Laboratory, California Institute
      of Technology: Some Investigations of the General
      Instability of Stiffened Metal Cylinders. I — Review
      of Theory and Bibliography. NACA TN No. 905, 1943.

5. Guggenheim Aeronautical Laboratory, California Institute
      of Technology: Some Investigations of the General
      Instability of Stiffened Metal Cylinders. II —
      Preliminary Tests of Wire—Braced Specimens and
      Theoretical Studies. NACA TN No. 906, 1943.

6. Guggenheim Aeronautical Laboratory, California Institute
      of Technology: Some Investigations of the General
      Instability of Stiffened Metal Cylinders. III —
      Continuation of Tests of Wire—Braced Specimens and
      Preliminary Tests of Sheet—Covered Specimens. NACA
      TN No. 907, 1943.

7. Guggenheim Aeronautical Laboratory, California Institute
      of Technology: Some Investigations of the General
      Instability of Stiffened Metal Cylinders. IV —
      Continuation of Tests of Sheet—Covered Specimens and
      Studies of the Buckling Phenomena of Unstiffened
      Circular Cylinders. NACA TN No. 908, 1943.

8. Guggenheim Aeronautical Laboratory, California Institute
      of Technology: Some Investigations of the General
      Instability of Stiffened Metal Cylinders. V — Stiffened
      Metal Cylinders Subjected to Pure Bending. NACA TN
      No. 909, 1943.

TABLE 1. CYLINDER CHARACTERISTICS

Cylinder Number	Cutout	Circumferential Length of Cutout	Length of Cylinder		Fasteners		Spacing of Stringer Fasteners	Ring Rivets (compression side only)	
	Degrees	Stringer fields	in.	bands	for Stringers	for Rings	in.	from Stringer	to Stringer
16	45	two	45	7	Screws	—	0.714	—	—
17	45	two	45	7	Rivets	—	0.643	—	—
18	45	two	58	9	Rivets	—	0.643	—	—
19	90	four	45	7	Rivets	—	0.643	—	—
20	45	two	45	7	Rivets	Rivets	0.643	5	13
21	135	six	45	7	Rivets	—	0.643	—	—
22	90	four	58	9	Rivets	—	0.643	—	—
23	90	four	58	9	Rivets	Rivets	0.643	5	13
24	135	six	58	9	Rivets	Rivets	0.643	4	14
25	135	six	58	9	Rivets	—	0.643	—	—

For all cylinders: Diameter: 20 in.
Length of each band: 6.43 in.
Length of cutout: 3 bands
1/8 in. machine screws for fastening stringers and rings at their intersection.
Number of stringers: 16
Thickness of sheet covering: 0.012 in.

TABLE 2. FORCE AND MOMENT EQUILIBRIUM

		Cylinder 16		Cylinder 17		Cylinder 18		Cylinder 19		Cylinder 20	
		Moment in.-lb.	Force lb.	Moment in.-lb.	Force lb.	Moment in.-lb.	Force lb.	Moment in.-lb.	Force lb.	Moment in.-lb.	Force lb.
First Load	(a)	27700	0	34700	0	35600	0	33300	0	37400	0
	(b)	23800	111	33400	-109	31200	269	34900	280	34500	-247
	(c)	24500	-83	37000	61	32800	89	35600	278	37100	-365
	(d)	26800	-61	39900	-81	34000	644	38200	-267	38400	-205
Second Load	(a)	59700	0	71100	0	71300	0	66600	0	73200	0
	(b)	54400	-166	69500	-294	65300	63	70200	-577	70600	-557
	(c)	54000	-107	73400	-43	66500	-194	67700	-462	72200	-649
	(d)	58800	-105	78900	-318	71300	401	74400	-642	75800	-452

		Cylinder 21		Cylinder 22		Cylinder 23		Cylinder 24		Cylinder 25	
		Moment in.-lb.	Force lb.	Moment in.-lb.	Force lb.	Moment in.-lb.	Force lb.	Moment in.-lb.	Force lb.	Moment in.-lb.	Force lb.
First Load	(a)	28300	0	32800	0	34600	0	16200	0	19140	0
	(b)	25100	-126	28500	-164	31100	32	14400	36	16200	87
	(c)	26700	-215	30200	-245	32300	-69	14900	74	17300	-18
	(d)	26400	-164	31700	-144	33400	-16	15900	109	16800	249
Second Load	(a)	44800	0	70300	0	71600	0	33700	0	38300	0
	(b)	38200	-298	63900	-460	68000	-93	30900	-65	32400	105
	(c)	43100	-369	64800	-357	67200	-85	31200	63	33000	-361
	(d)	42100	-436	68700	-353	71400	-235	33200	241	35100	59

Rows (a) - Applied load.
Rows (b) - Computed from strains in band A.
Rows (c) - Computed from strains in band D for 45 in. long cylinders, band E for 58 in. long cylinders.
Rows (d) - Computed from strains in band G for 45 in. long cylinders, band I for 58 in. long cylinders.

TABLE 3. INSTABILITY DATA

Cylinder Number	Maximum Jack Load (Not corrected for weight of loading arm) lb.	Maximum Moment in.-lb.	Maximum Jack Load (corrected for weight of loading arm) lb.	Maximum Moment in.-lb.	Percentage Deviation from Group Average	Collapse	Deflection of Stringers at edge of cutout (Stringer Number in parenthesis)	
16	2,540	182,900	2,665	191,900	−0.5	Gradual	out	out
17	2,620	188,600	2,745	197,600	+2.5	Gradual	out	out
18	2,530	182,200	2,655	191,200	−0.8	Sudden	in (8)	out (10)
19	1,690	121,700	1.815	130,700	−3.8	Gradual	out	out
20	2,520	181,400	2,645	190,400	−1.2	Sudden	in (8)	out (10)
21	1,088	78,300	1,213	87,300	−2.5	Gradual	out	out
22	1,690	121,700	1,815	130,700	−3.8	Gradual	out	out
23	1,910	137,000	2,035	146,000	+7.5	Sudden	in	in
24	1,156	83,200	1,281	92,200	+3.0	Gradual	in	in
25	1,110	79,900	1,235	88,900	−0.7	Gradual	out	out

Average maximum moment (corrected for loading arm) for 45° cutout − 192,800 in.-lb.
Average maximum moment (corrected for loading arm) for 90° cutout − 135,800 in.-lb.
Average maximum moment (corrected for loading arm) for 135° cutout − 89,500 in.-lb.

TABLE 4. BEHAVIOR AFTER COLLAPSE

Cylinder Number		Maximum Load	Load immediately after collapse	Load after overnight rest	Maximum load after overnight rest	
					Before decrease to zero	After decrease to zero
20	(a)	2,520	2,440	—	—	—
	(b)	2,645	2,565	—	—	—
	(c)	181,400	175,900	—	—	—
	(d)	190,400	185,000	—	—	—
21	(a)	1,088	1,055	960	995	960
	(b)	1,231	1,180	1,085	1,120	1,085
	(c)	78,300	76,000	69,100	71,600	69,100
	(d)	87,300	84,900	78,100	80,600	78,100
22	(a)	1,690	—	1,538	1,585	1,585
	(b)	1,815	—	1,663	1,710	1,710
	(c)	121,700	—	110,800	114,000	114,000
	(d)	130,700	—	119,800	123,000	123,000
23	(a)	1,910	1,505	1,495	1,575	1,575
	(b)	2,035	1,630	1,620	1,700	1,700
	(c)	137,000	108,300	107,500	113,300	113,300
	(d)	146,000	117,600	116,800	122,400	122,400
24	(a)	1,156	1,120	948	1,022	971
	(b)	1,281	1,245	1,073	1,147	1,096
	(c)	83,200	80,600	68,200	73,500	70,000
	(d)	92,200	89,500	77,300	78,900	82,600
25	(a)	1,110	930	—	—	—
	(b)	1,235	1,055	—	—	—
	(c)	79,900	67,000	—	—	—
	(d)	88,900	76,000	—	—	—

Rows (a) − Jack load, not corrected for weight of loading arm − lb.
Rows (b) − Jack load, corrected for weight of loading arm − lb.
Rows (c) − Moment, not corrected for weight of loading arm − in.-lb.
Rows (d) − Moment, corrected for weight of loading arm − in.-lb.
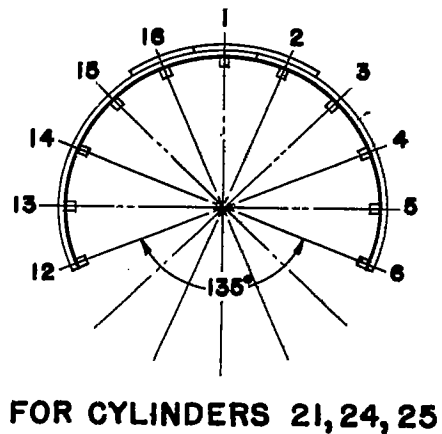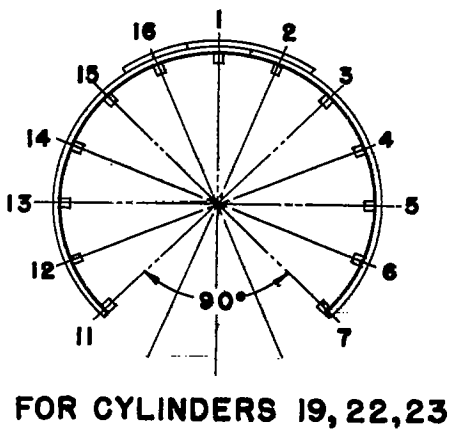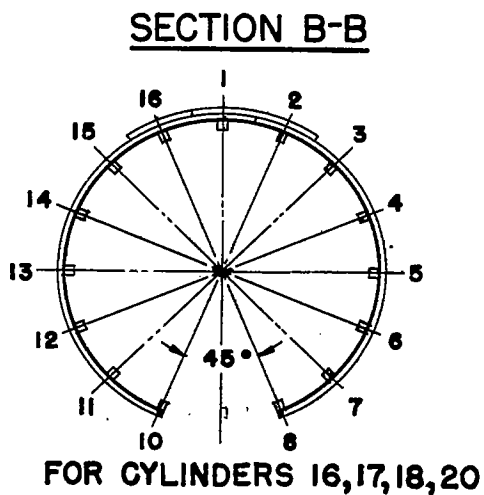
SECTIONS A-A AND B-B
ARE SHOWN IN FIG. 2.

SECTIONS

1/8" 3/8"

3/8" 3/8"

RING   STRINGER
24 ST ALUM. ALLOY

STRINGER CENTER LINES

6"43 10 EQ.SP. 6"43 10 EQ.SP. 6"43 10 EQ.SP. 6"43 10 EQ.SP. 6"43 10 EQ.SP. 6"43 10 EQ.SP. 6"43 10 EQ.SP. 6"43 10 EQ.SP.

62"00

57".87

18".915

18".915

45".00

49".00

20" O.D. SHEET

20" O.D. SHEET

1/8" 17 ST ALUM. ALLOY
ROUND HEAD RIVETS

1/8" MACHINE SCREW
ONLY AT INTERSECTION
OF STRINGERS AND RINGS

FIG.I. TEST SPECIMENS

Fig. 2   NACA TN No. 1013

LOCATION OF SECTIONS
SHOWN IN FIG. 1.

SECTION B-B

45°

FOR CYLINDERS 16,17,18,20

SECTION A-A

24 ST ALCLAD SHEET
t = 0.012
RING SPLICE

$22\frac{1}{2}°$

20" O.D. SHEET

FOR ALL CYLINDERS

90°

FOR CYLINDERS 19,22,23

135°

FOR CYLINDERS 21,24,25
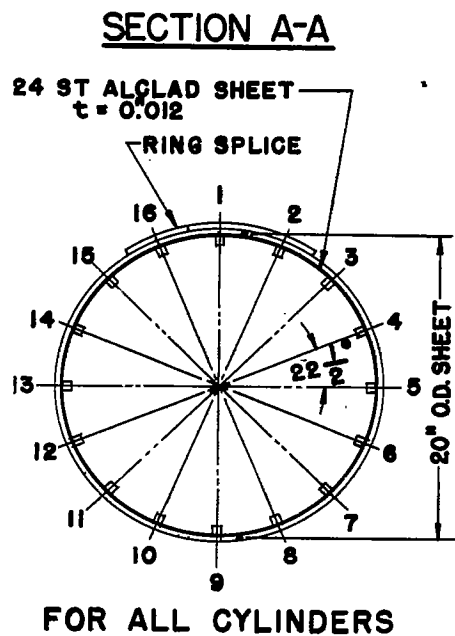
FIG.2. SECTIONS OF TEST SPECIMENS
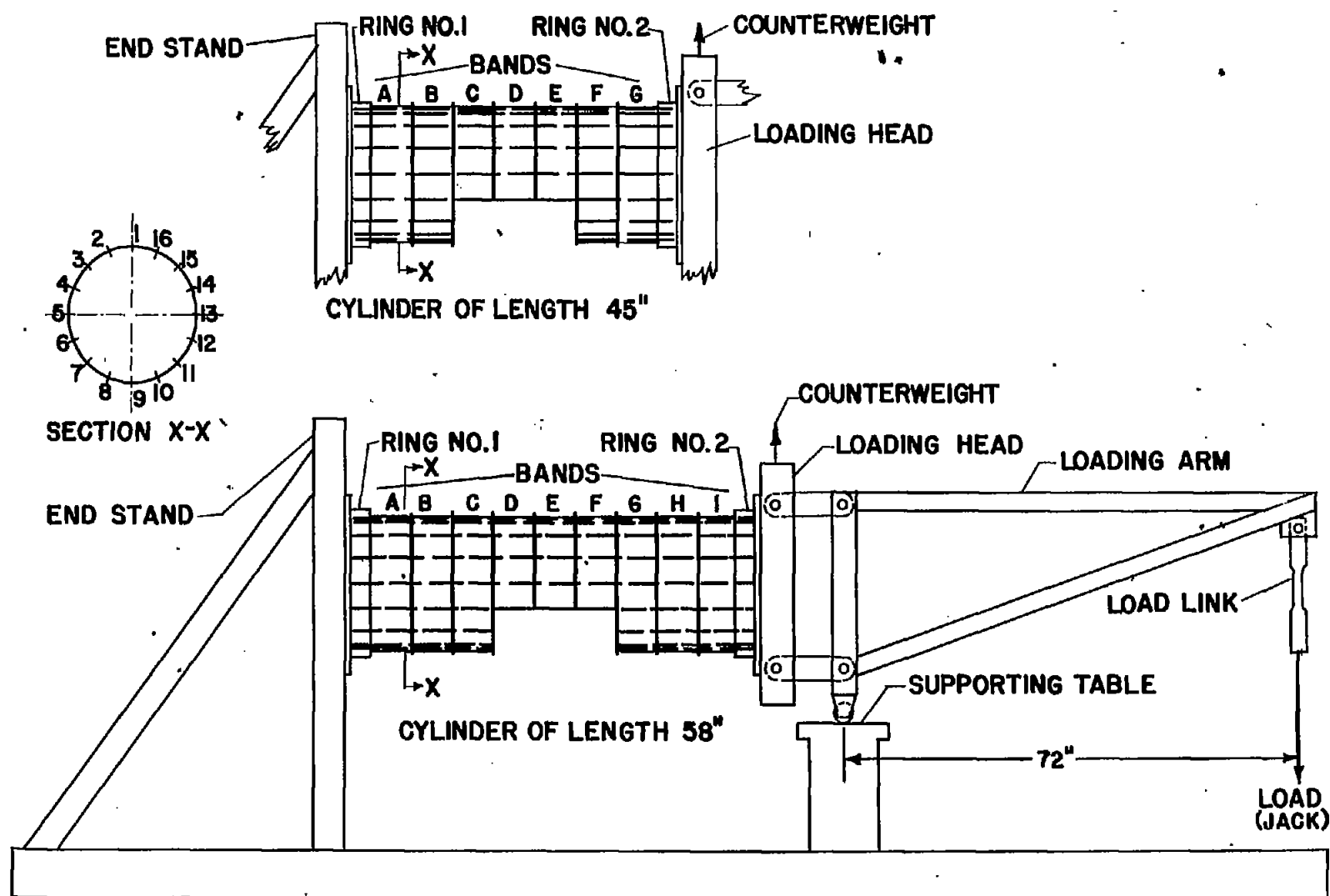
FIG. 3. DIAGRAM OF TEST SET-UP.

Fig. 3
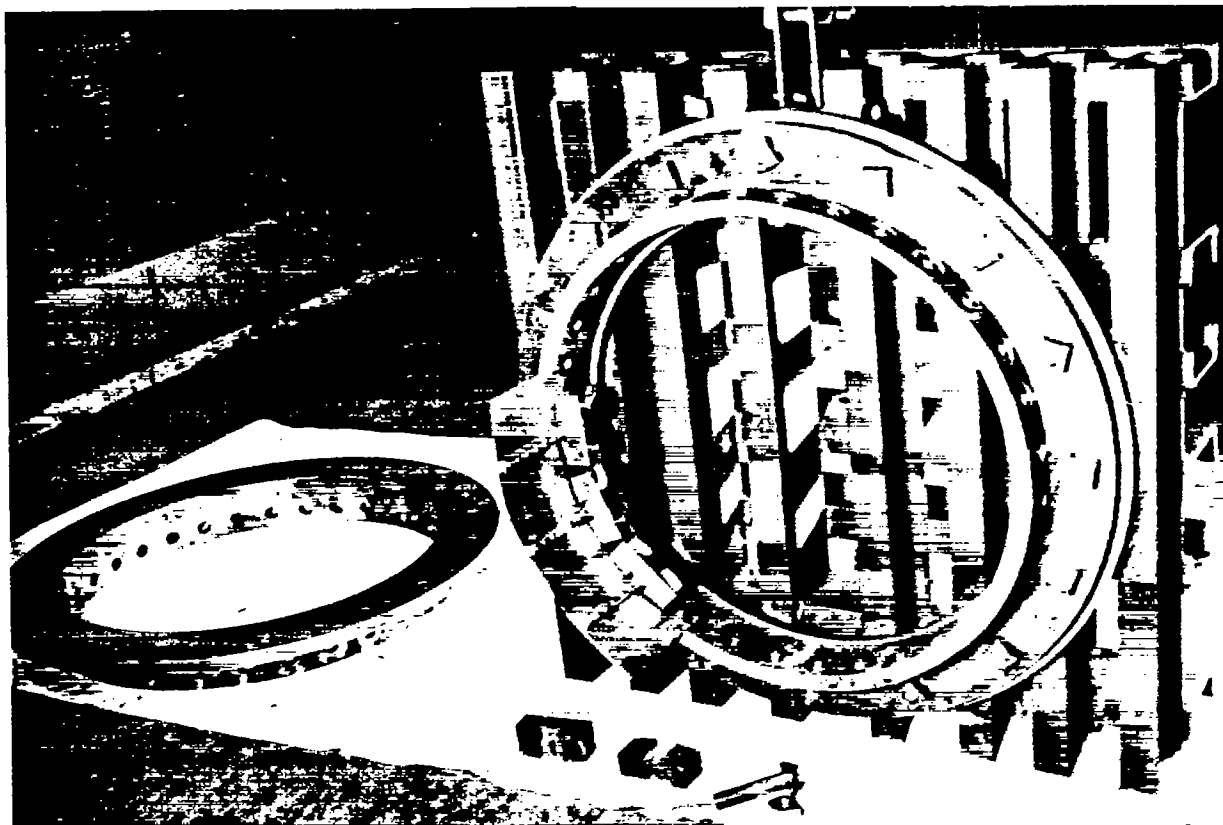
Figure 4.- Details of loading rig. A portion of the sheet
          covering and stringers is shown attached by means
of stringer grip fittings to end ring number 2, which in
turn is fastened to the loading head. Two stringer grip
fittings are in the foreground and end ring number 1 is on
the left.
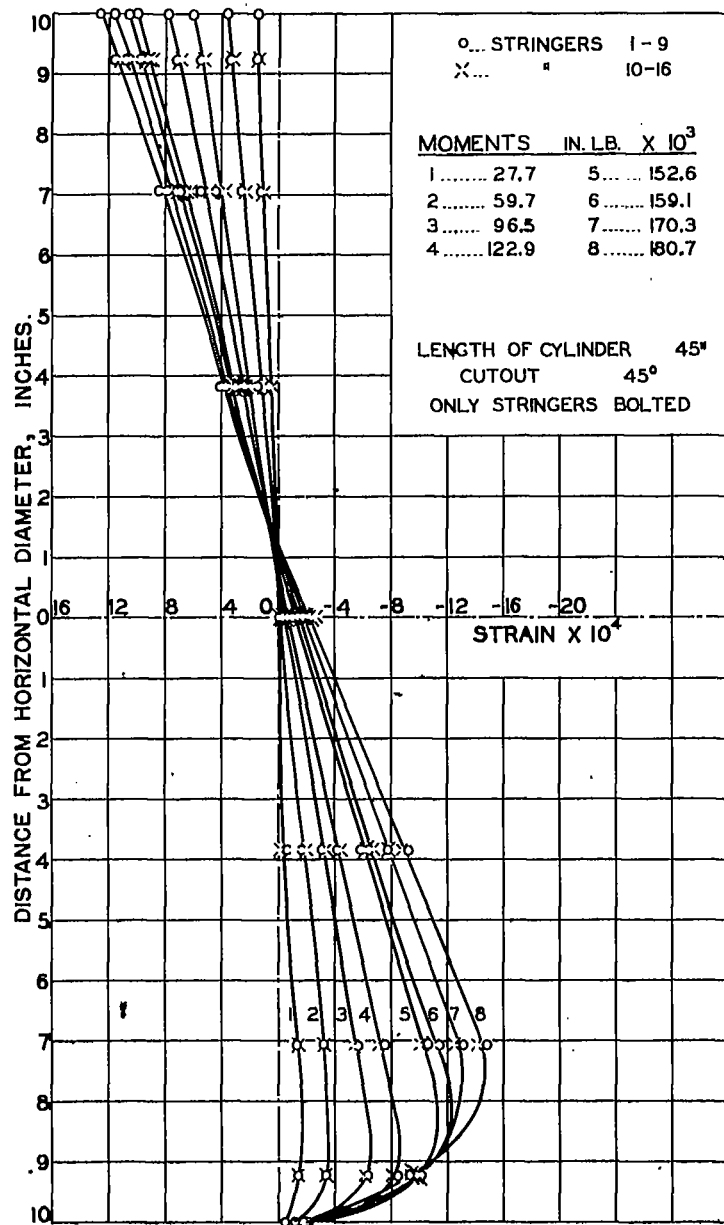
FIG. 5. STRAIN DIAGRAM OF CYLINDER 16 BAND A.
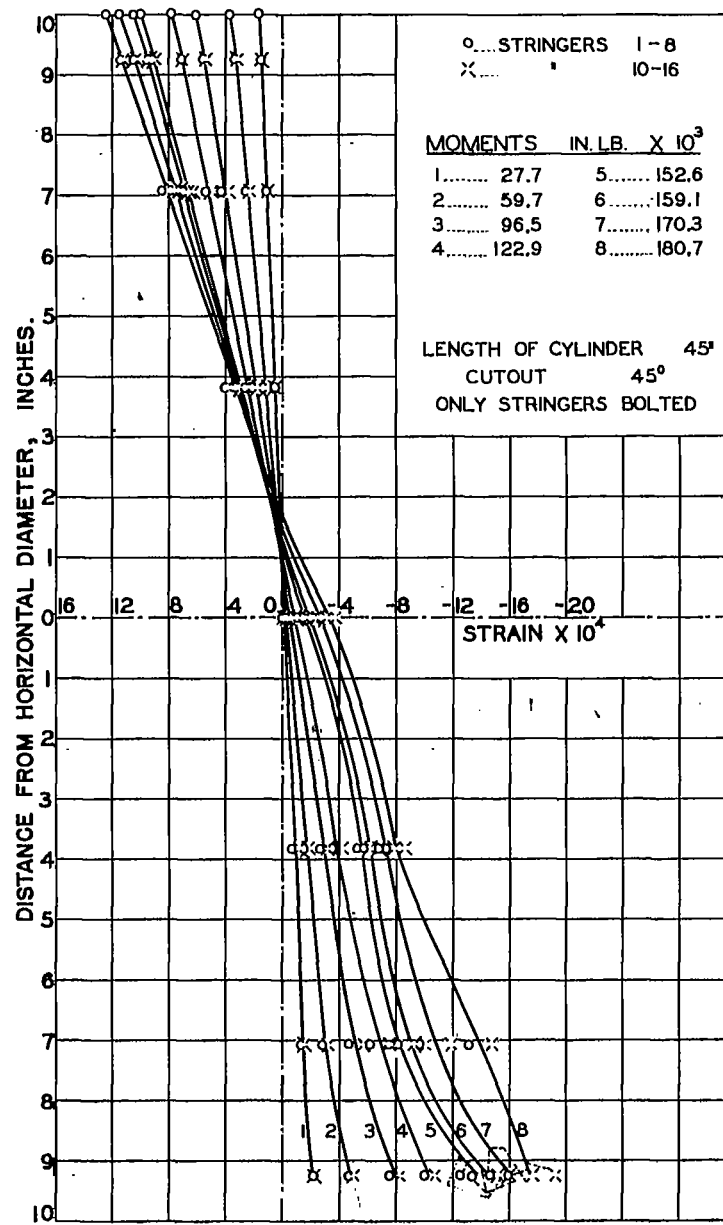
FIG. 6. STRAIN DIAGRAM OF CYLINDER 16 BAND D.
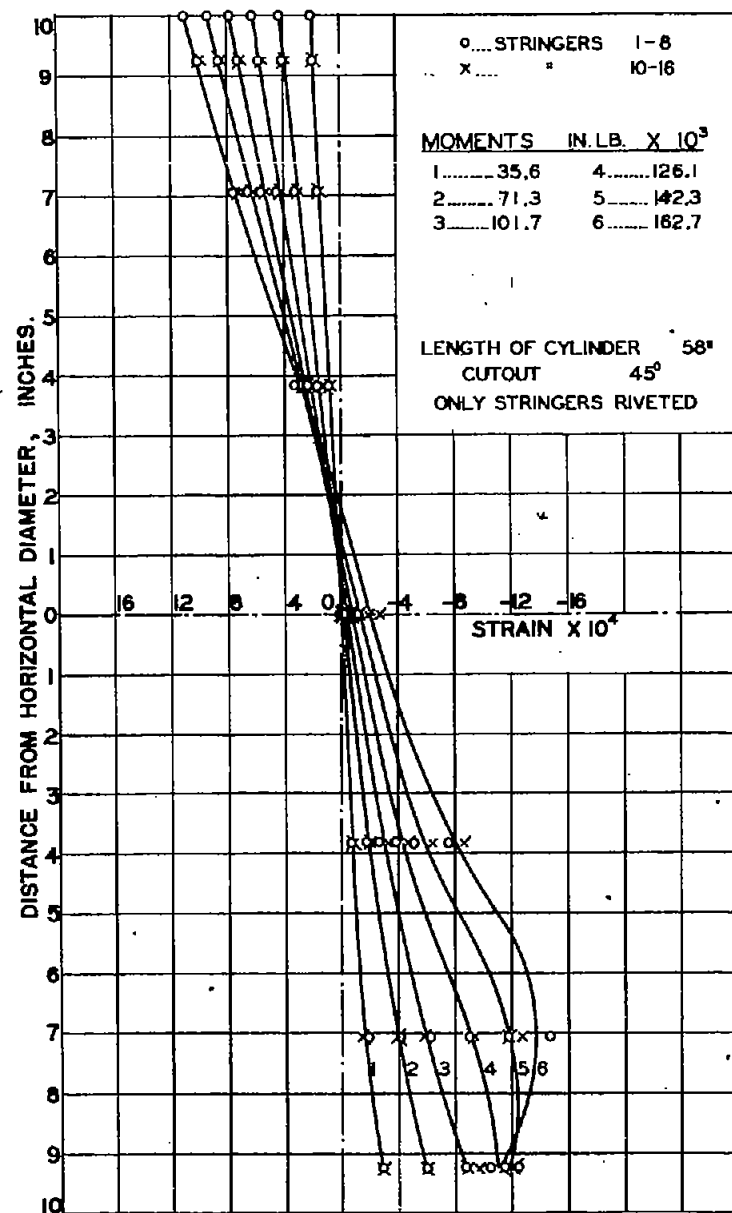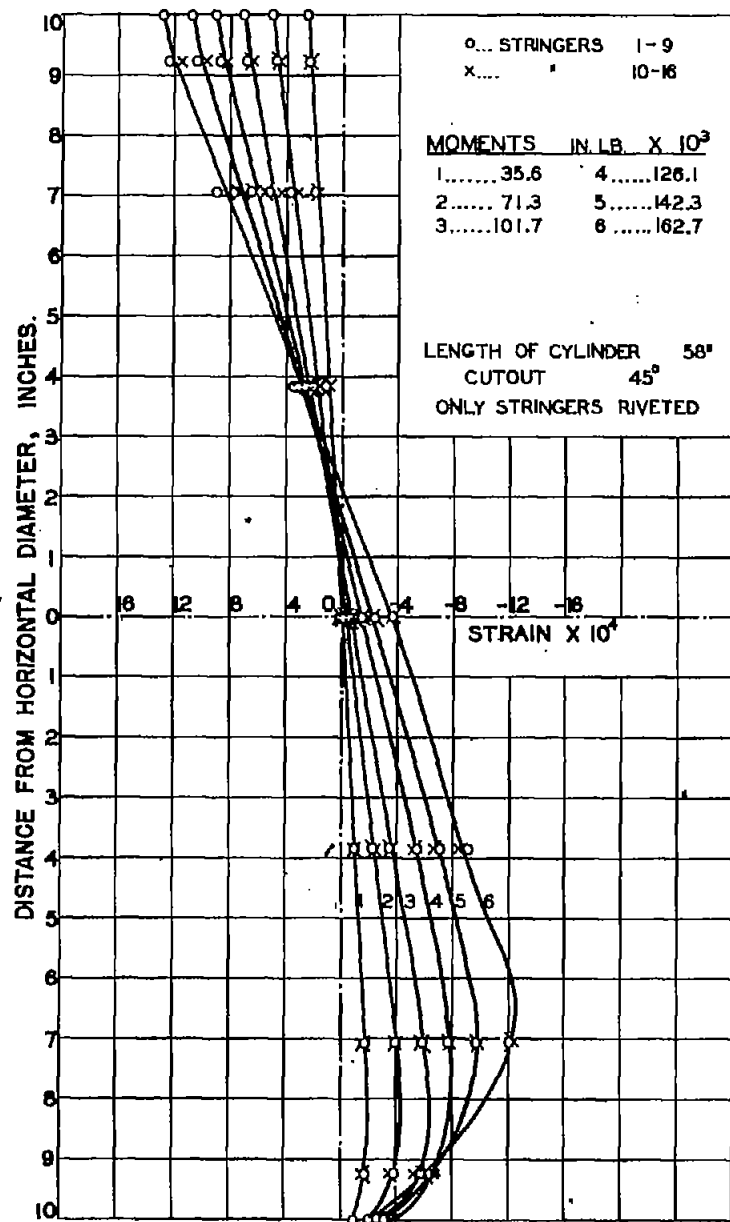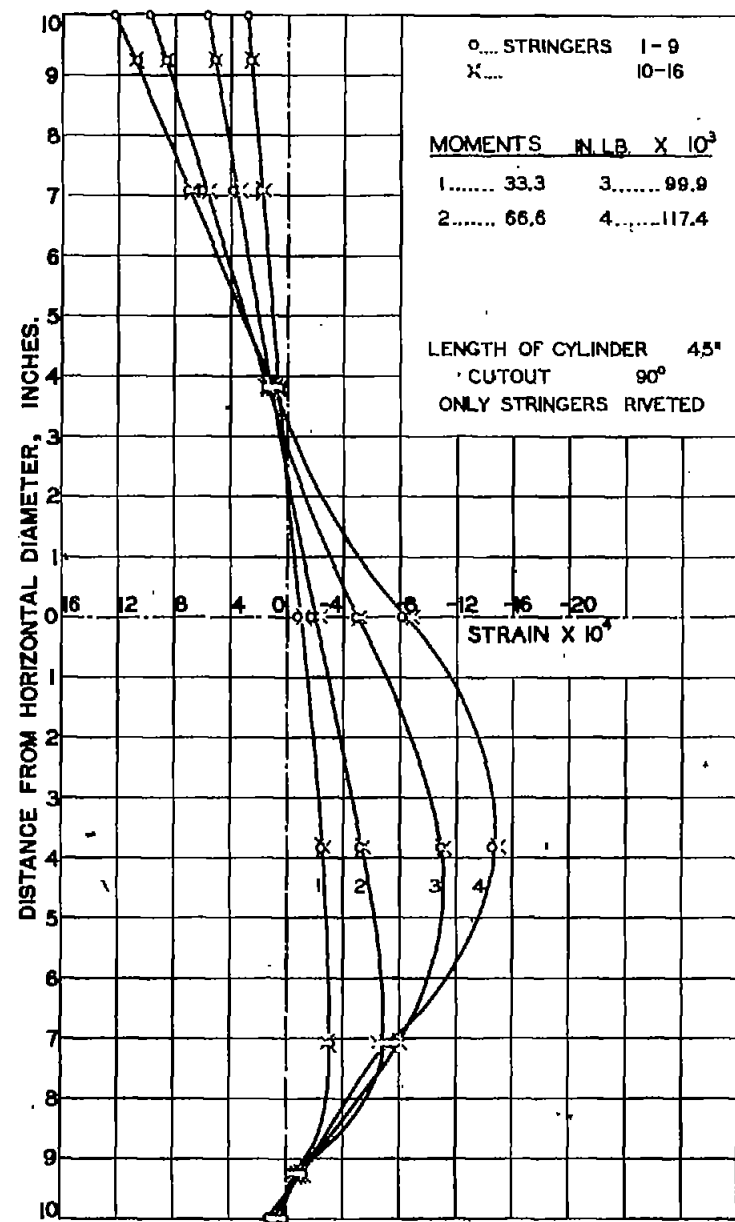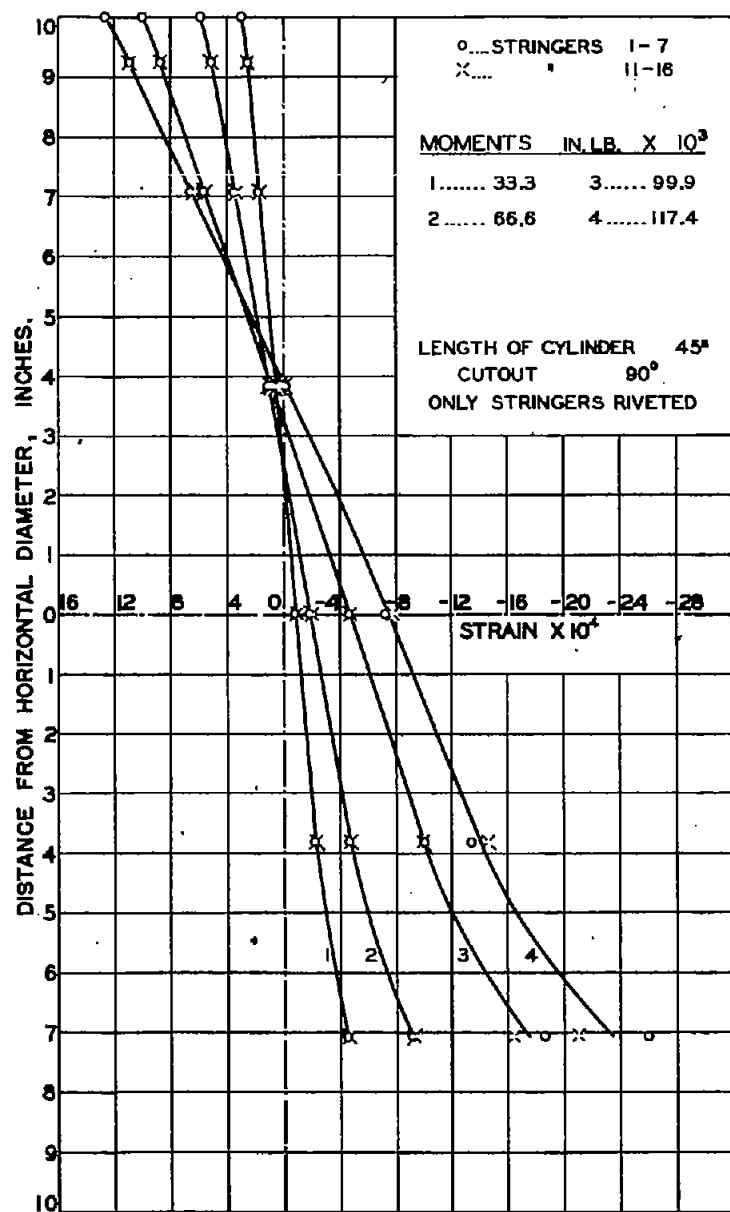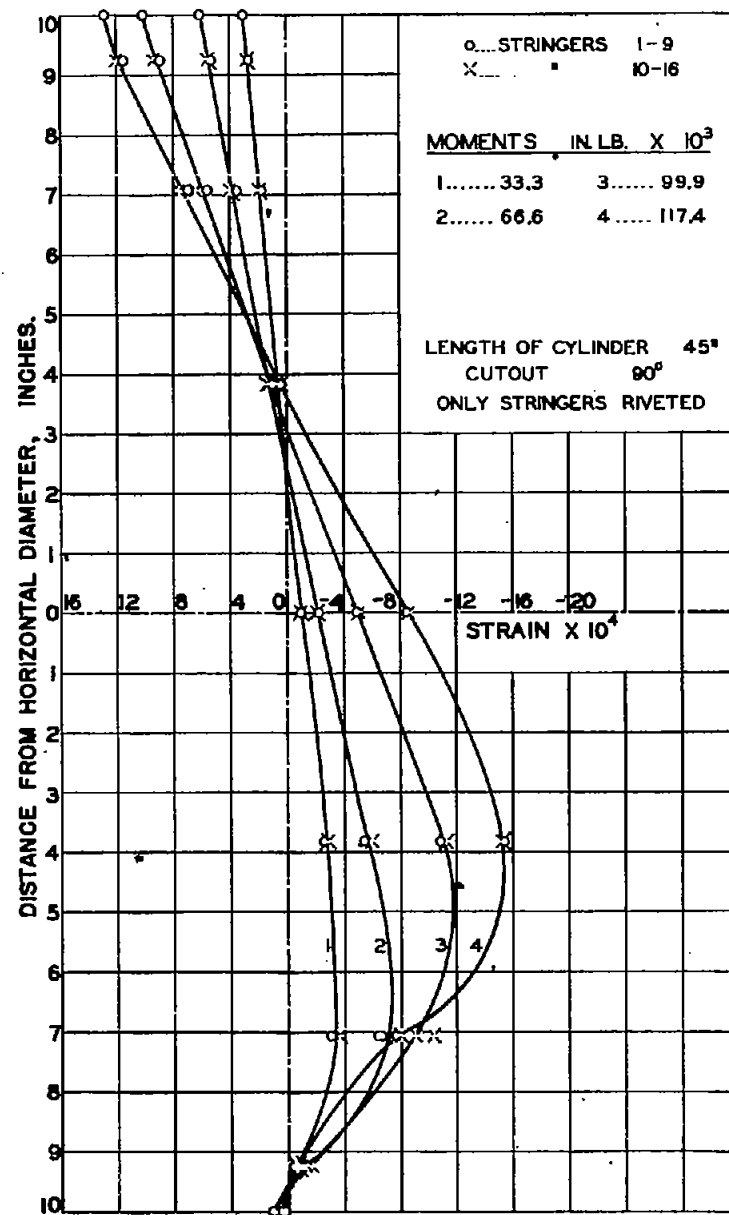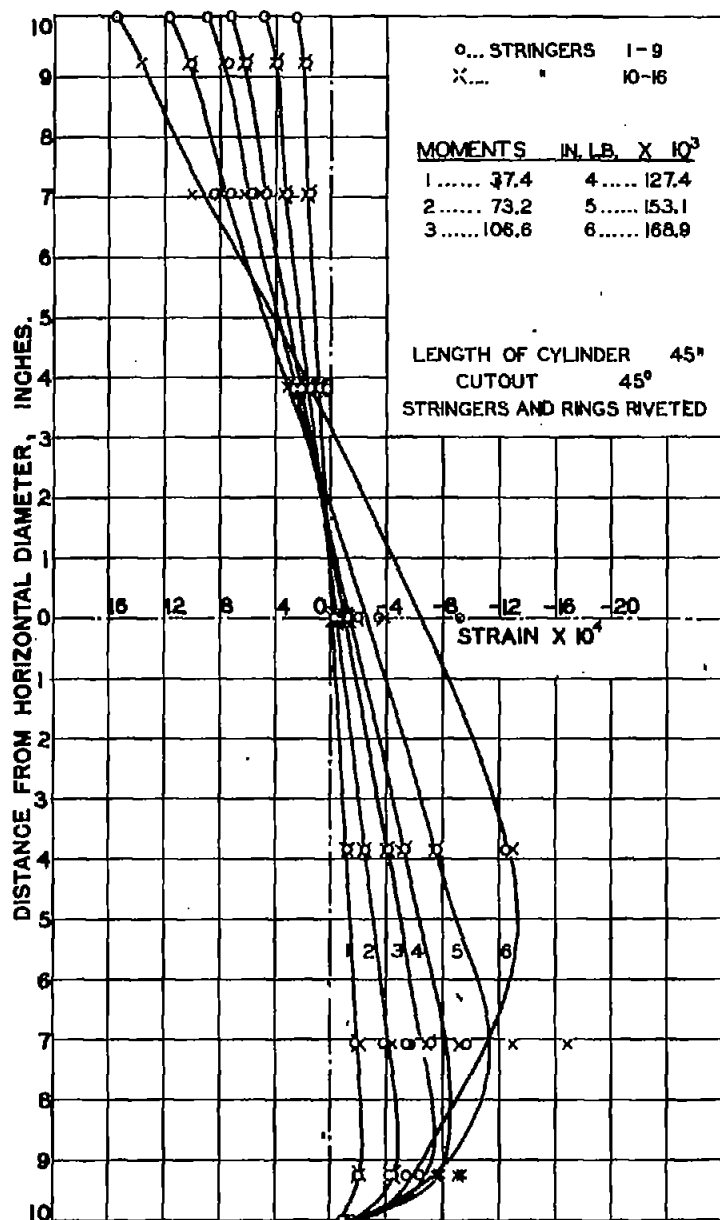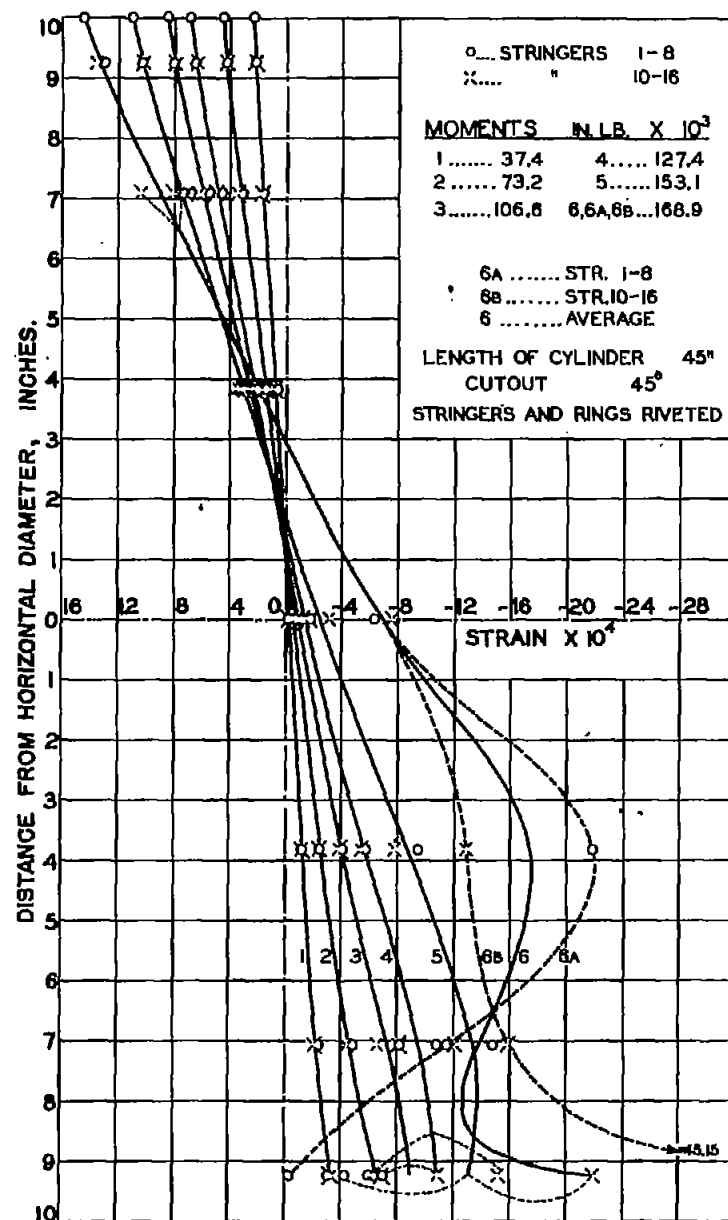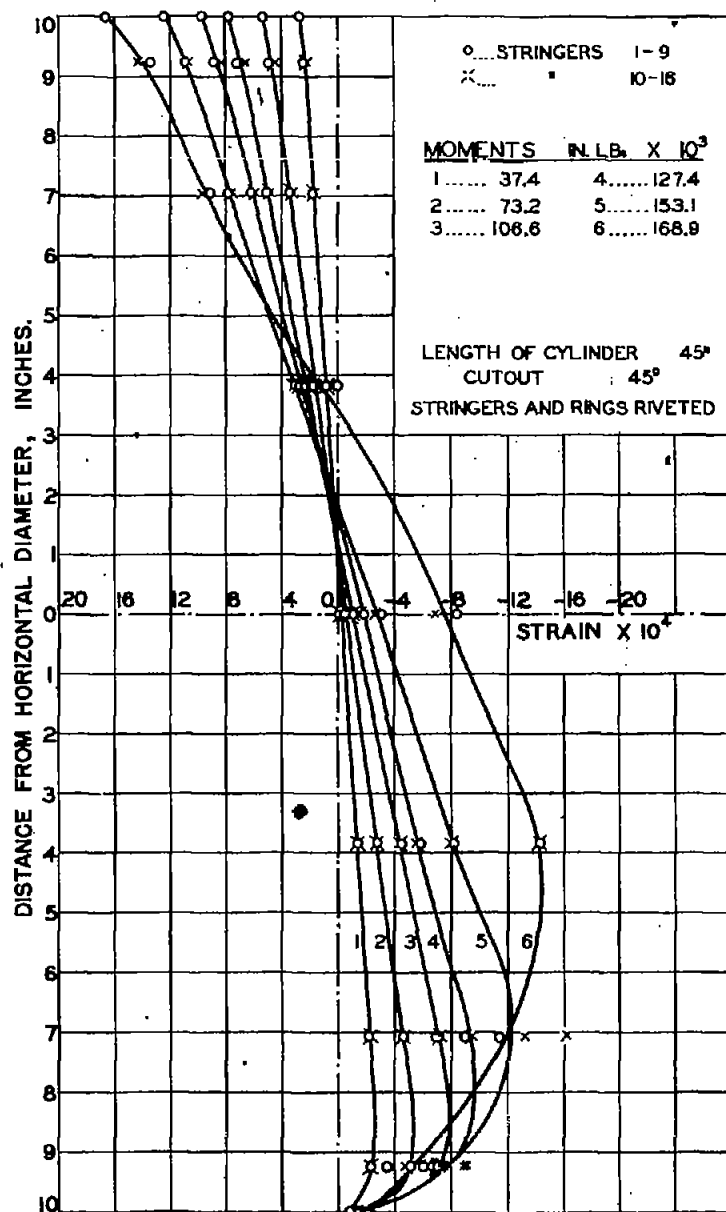
FIG. 7. STRAIN DIAGRAM OF CYLINDER 16 BAND G.

For Fig. 7:

o ... STRINGERS 1 - 9
x ... " 10-16

MOMENTS	IN. LB. X 10^3
1 .... 27.7	5 .... 152.6
2 .... 59.7	6 .... 159.1
3 .... 96.5	7 .... 170.3
4 .... 122.9	8 .... 180.7

LENGTH OF CYLINDER 45"
CUTOUT 45°
ONLY STRINGERS BOLTED

DISTANCE FROM HORIZONTAL DIAMETER, INCHES.
STRAIN X 10^4

FIG. 8. STRAIN DIAGRAM OF CYLINDER 17 BAND A.

For Fig. 8:

o ... STRINGERS 1 - 9
x ... " 10-16

MOMENTS	IN. LB. X 10^3
1 .... 34.7	4 ...... 132.0
2 ...... 71.1	5 ...... 144.1
3 ...... 116.1	6 ..... 159.6
	7 ...... 171.0

LENGTH OF CYLINDER 45"
CUTOUT 45°
ONLY STRINGERS RIVETED

DISTANCE FROM HORIZONTAL DIAMETER, INCHES.
STRAIN X 10^4

o....STRINGERS   1 - 8
X....   "   10-16

MOMENTS   IN. LB.   X 10³
1....... 34.7   4......132.0
2...... 71.1   5......144.1
3......116.1   6......159.6
         7....... 171.0

LENGTH OF CYLINDER   45"
CUTOUT   45°
ONLY STRINGERS RIVETED

STRAIN X 10⁴

DISTANCE FROM HORIZONTAL DIAMETER, INCHES.

FIG. 9. STRAIN DIAGRAM OF CYLINDER 17 BAND D.

o....STRINGERS   1 - 9
X....   "   10-16

MOMENTS   IN. LB.   X 10³
1........ 34.7   4......132.0
2........71.1   5......144.1
3......116.1   6......159.6
         7.........171.0

LENGTH OF CYLINDER   45"
CUTOUT   45°
ONLY STRINGERS RIVETED

STRAIN X 10⁴

DISTANCE FROM HORIZONTAL DIAMETER, INCHES.

FIG. 10. STRAIN DIAGRAM OF CYLINDER 17 BAND G.

o.... STRINGERS 1-9
x....   "   10-16

MOMENTS   IN. LB. X 10³

1 ...... 35.6   4 ...... 126.1
2 ...... 71.3   5 ...... 142.3
3 ...... 101.7   6 ...... 162.7

LENGTH OF CYLINDER   58"
      CUTOUT   45°
ONLY STRINGERS RIVETED

DISTANCE FROM HORIZONTAL DIAMETER, INCHES.

STRAIN X 10⁴

FIG. 11. STRAIN DIAGRAM OF CYLINDER 18 BAND A.

o.... STRINGERS 1-8
x....   "   10-16

MOMENTS   IN. LB. X 10³

1 ...... 35.6   4 ...... 126.1
2 ...... 71.3   5 ...... 142.3
3 ...... 101.7   6 ...... 162.7

LENGTH OF CYLINDER   58"
      CUTOUT   45°
ONLY STRINGERS RIVETED

DISTANCE FROM HORIZONTAL DIAMETER, INCHES.

STRAIN X 10⁴

FIG. 12. STRAIN DIAGRAM OF CYLINDER 18 BAND E.

FIG. 13. STRAIN DIAGRAM OF CYLINDER 18 BAND 1:

FIG. 14. STRAIN DIAGRAM OF CYLINDER 19 BAND A.

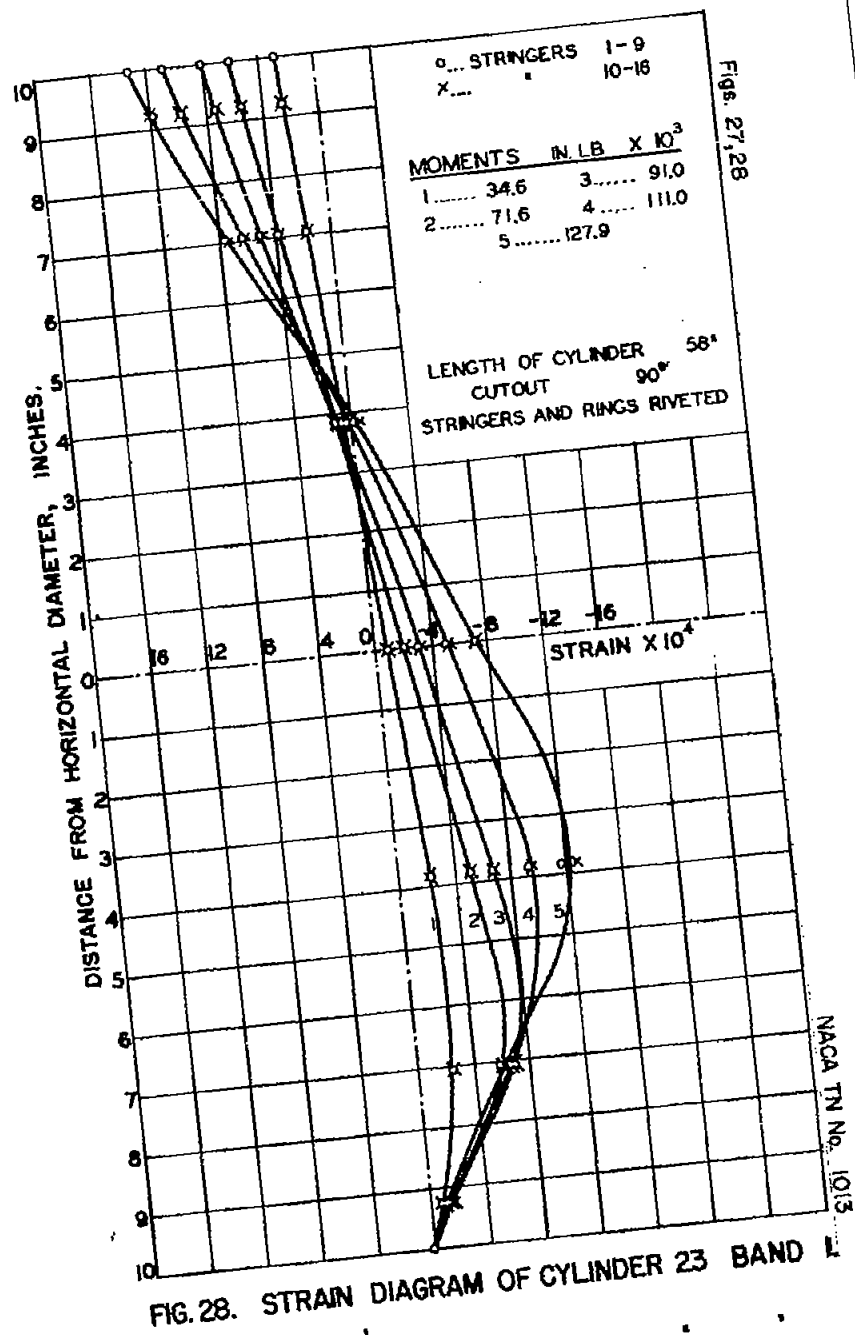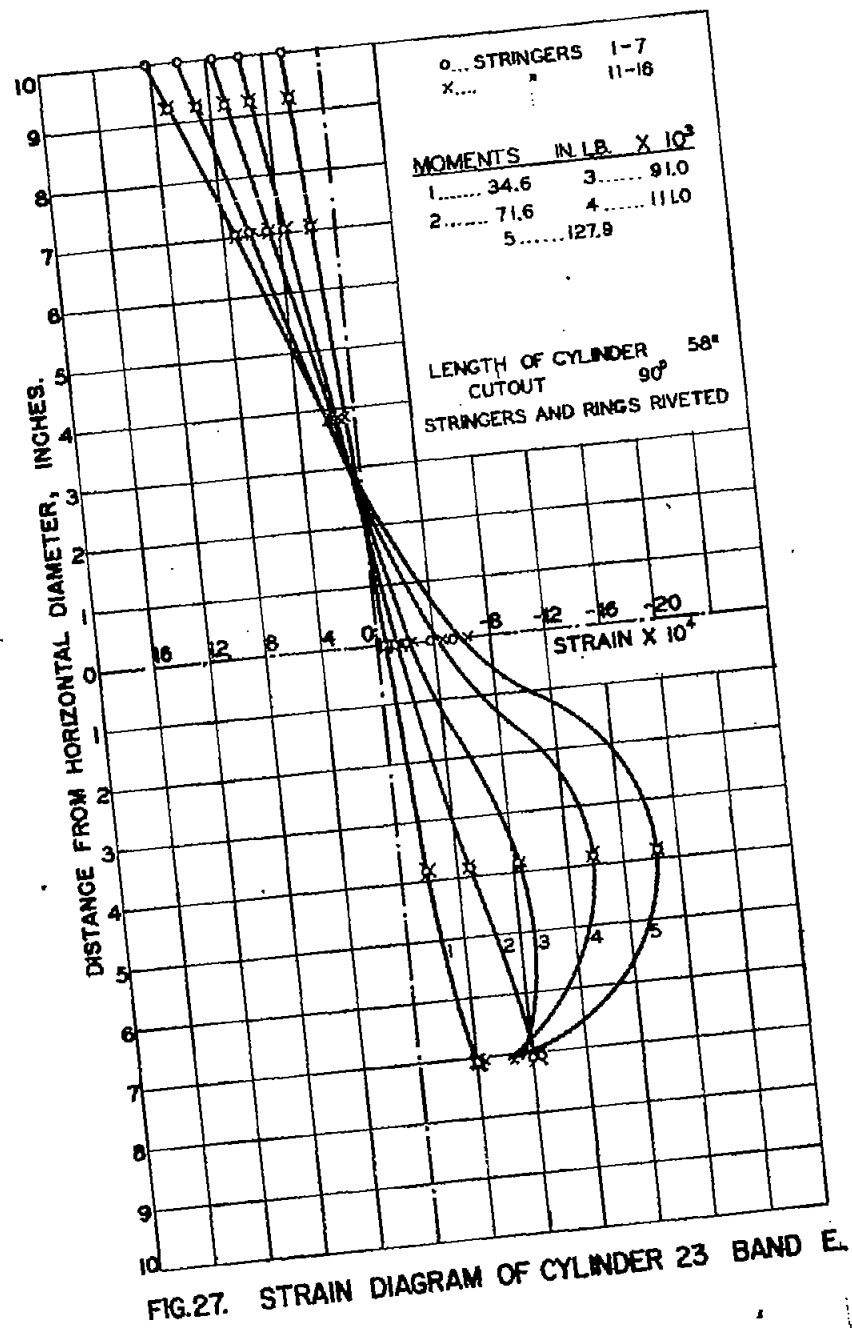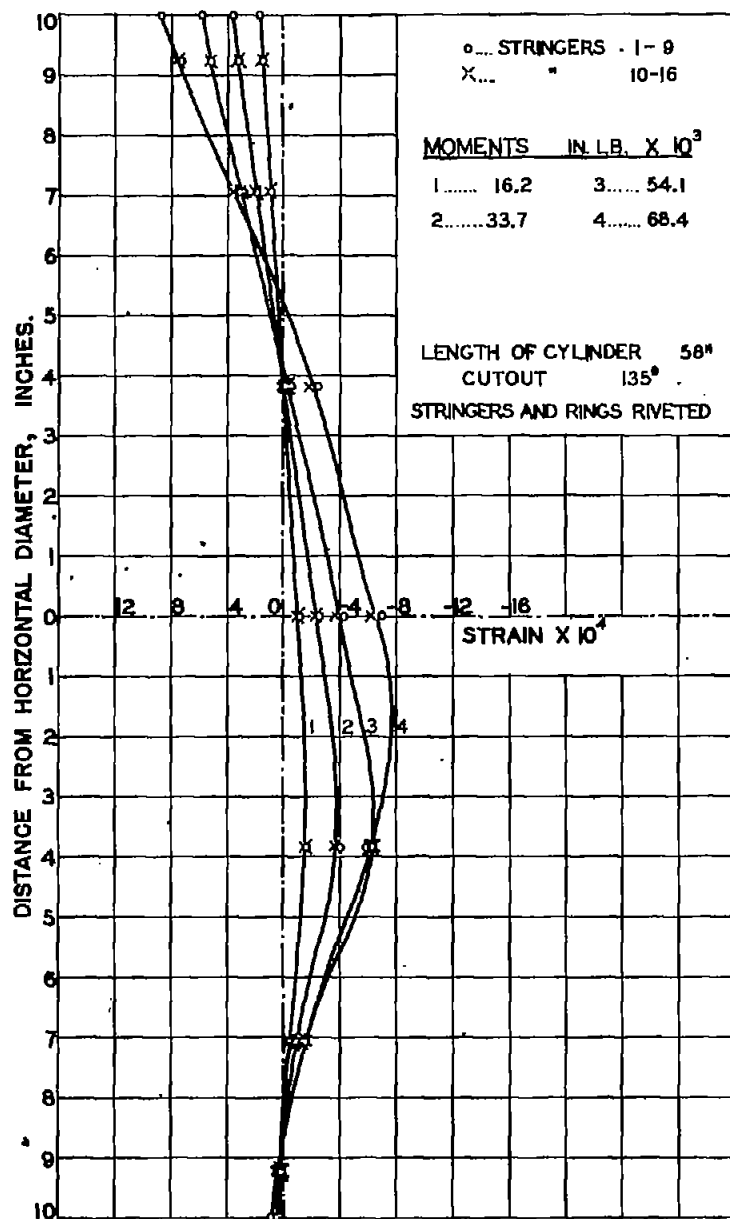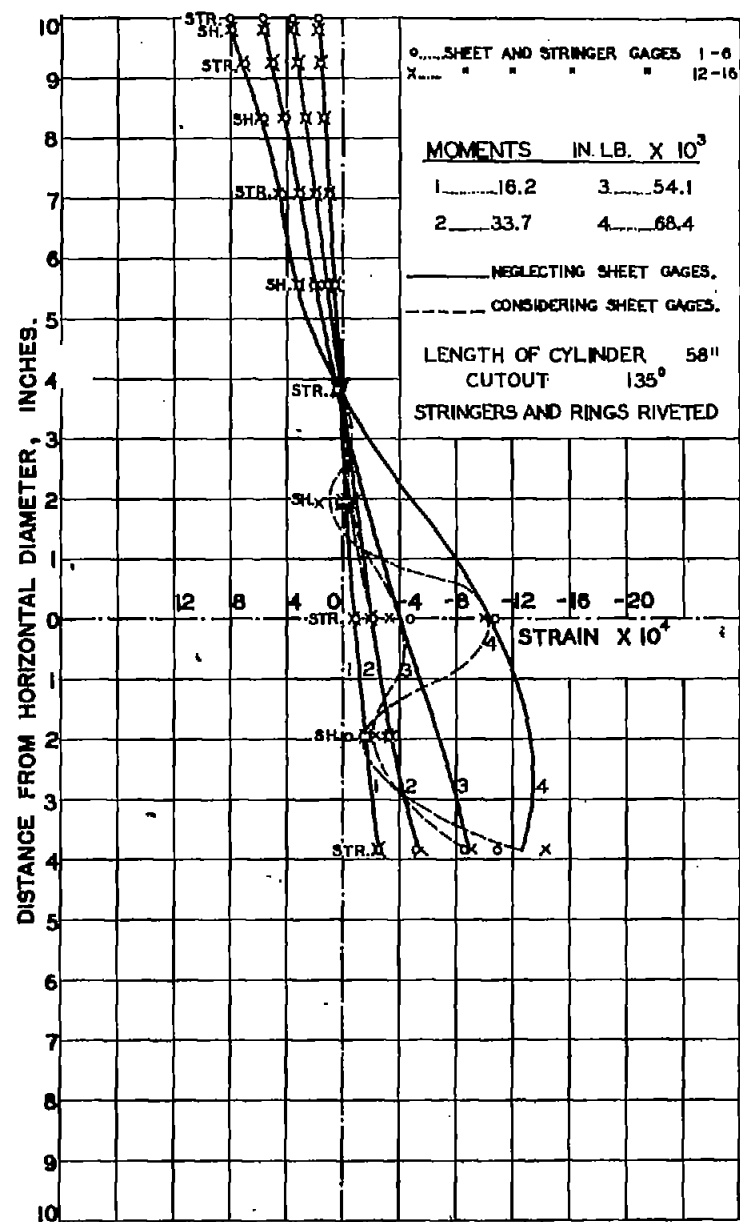o....STRINGERS   1-7
X....   "   11-16

MOMENTS   IN.LB. X 10³

1....... 33.3   3...... 99.9
2....... 66.6   4...... 117.4

LENGTH OF CYLINDER   45"
CUTOUT   90°
ONLY STRINGERS RIVETED

DISTANCE FROM HORIZONTAL DIAMETER, INCHES.

16 12 8 4 0 -4 -8 -12 -16 -20 -24 -28
STRAIN X 10⁴

FIG. 15. STRAIN DIAGRAM OF CYLINDER 19 BAND D.

o....STRINGERS   1-9
X....   "   10-16

MOMENTS   IN.LB. X 10³

1....... 33.3   3...... 99.9
2....... 66.6   4...... 117.4

LENGTH OF CYLINDER   45"
CUTOUT   90°
ONLY STRINGERS RIVETED

DISTANCE FROM HORIZONTAL DIAMETER, INCHES.

16 12 8 4 0 -4 -8 -12 -16 -20
STRAIN X 10⁴

FIG. 16. STRAIN DIAGRAM OF CYLINDER 19 BAND G.

FIG. 17. Left diagram:

DISTANCE FROM HORIZONTAL DIAMETER, INCHES.

STRAIN X 10⁴

o... STRINGERS   1-9
×.... "   10-16

MOMENTS IN. LB. $\times 10^3$
1 ...... 37.4   4 ..... 127.4
2 ...... 73.2   5 ..... 153.1
3 ...... 106.6   6 ..... 168.9

LENGTH OF CYLINDER   45"
CUTOUT   45°
STRINGERS AND RINGS RIVETED

FIG. 17. STRAIN DIAGRAM OF CYLINDER 20—BAND A.

Right diagram:

o... STRINGERS   1-8
×.... "   10-16

MOMENTS IN. LB. $\times 10^3$
1 ...... 37.4   4 ..... 127.4
2 ...... 73.2   5 ..... 153.1
3 ...... 106.6   6,6A,6B ...168.9

6A .... STR. 1-8
6B .... STR. 10-16
6 .... AVERAGE

LENGTH OF CYLINDER   45"
CUTOUT   45°
STRINGERS AND RINGS RIVETED

FIG. 18. STRAIN DIAGRAM OF CYLINDER 20 BAND D.

FIG.19. STRAIN DIAGRAM OF CYLINDER 20 BAND G.
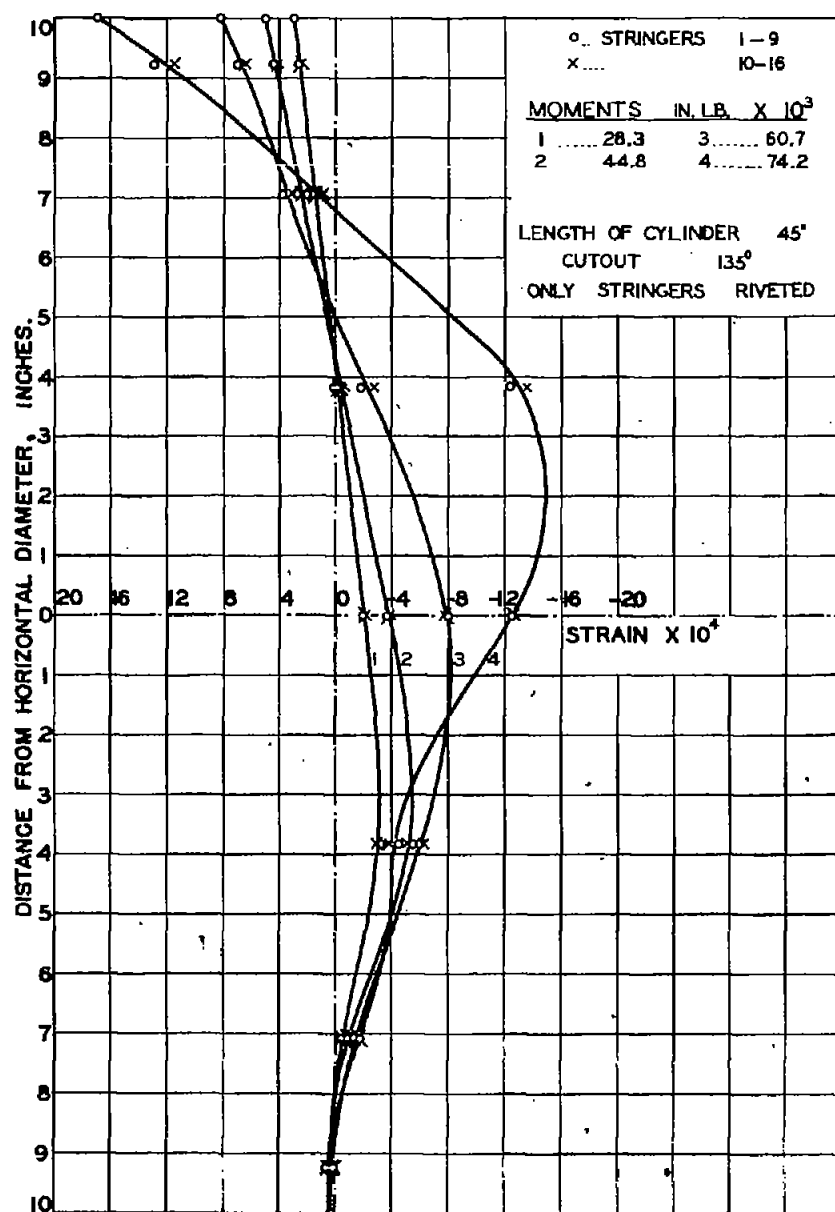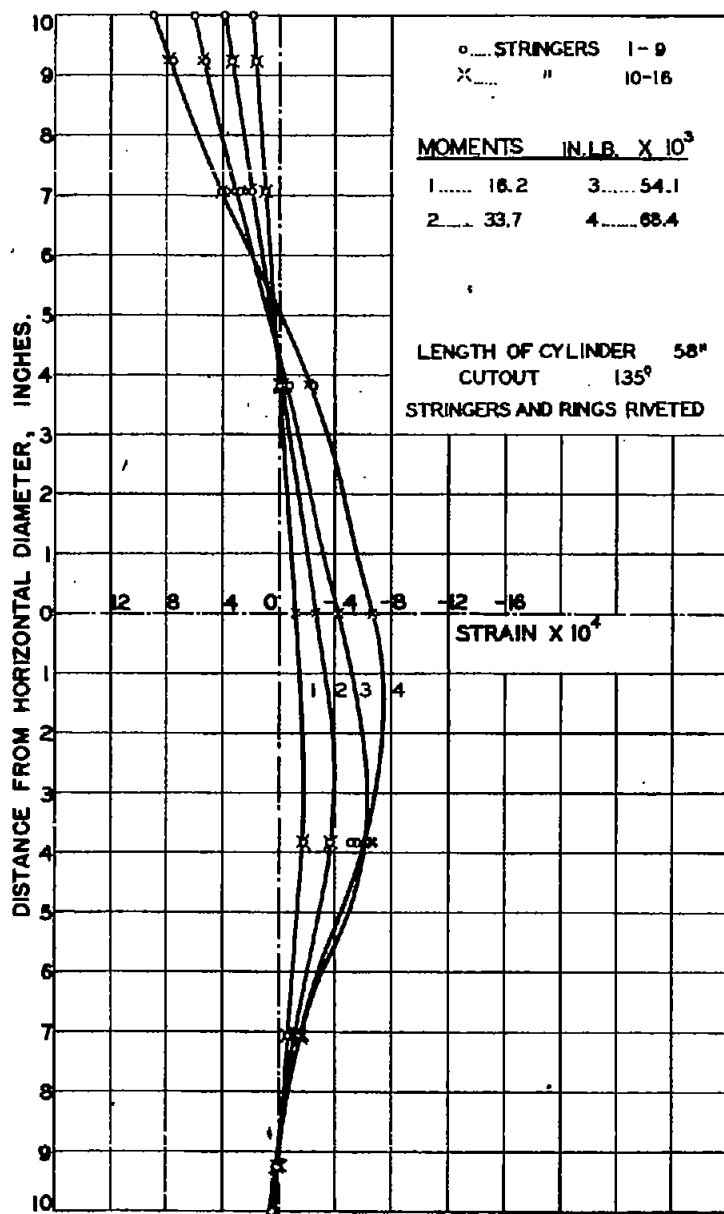
FIG.20. STRAIN DIAGRAM OF CYLINDER 21 BAND A.
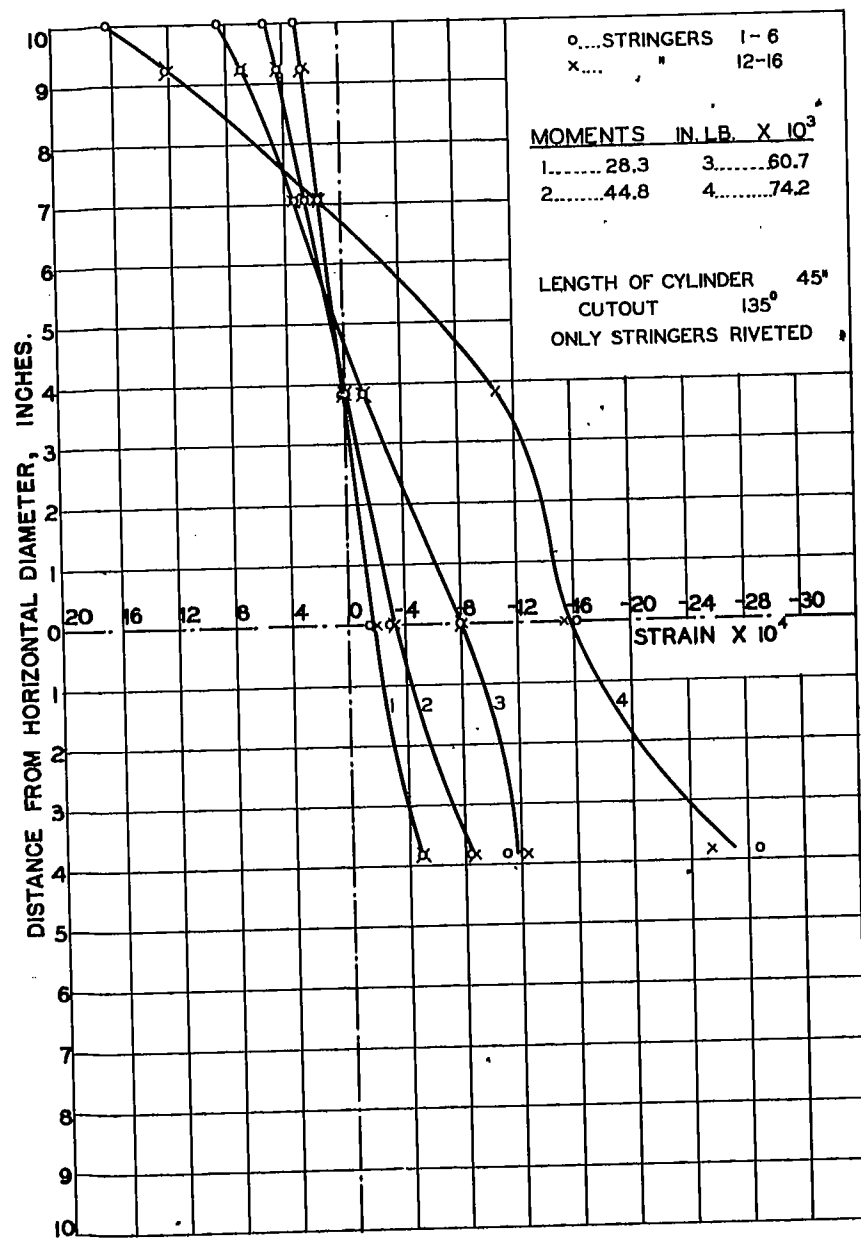
FIG. 21. STRAIN DIAGRAM OF CYLINDER 21 BAND D.
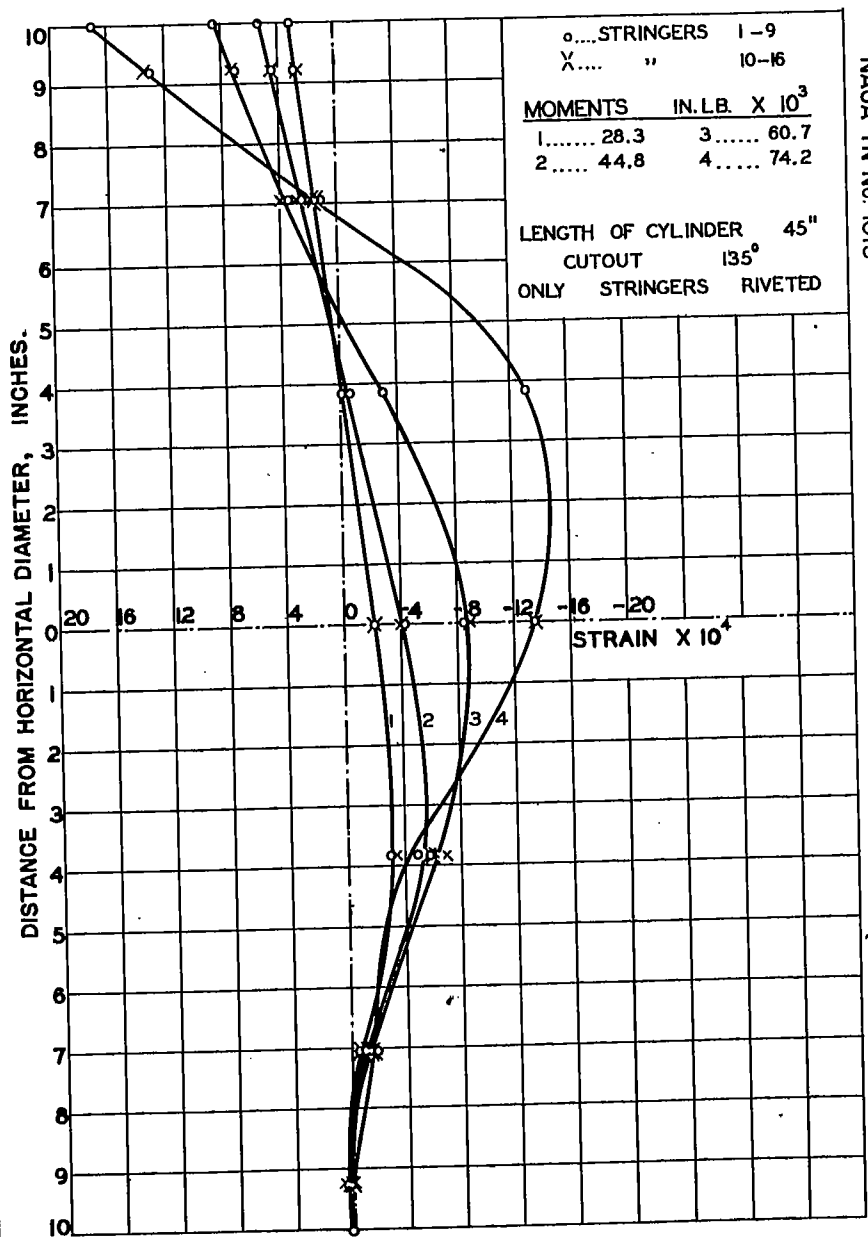
FIG. 22. STRAIN DIAGRAM OF CYLINDER 21 BAND G.
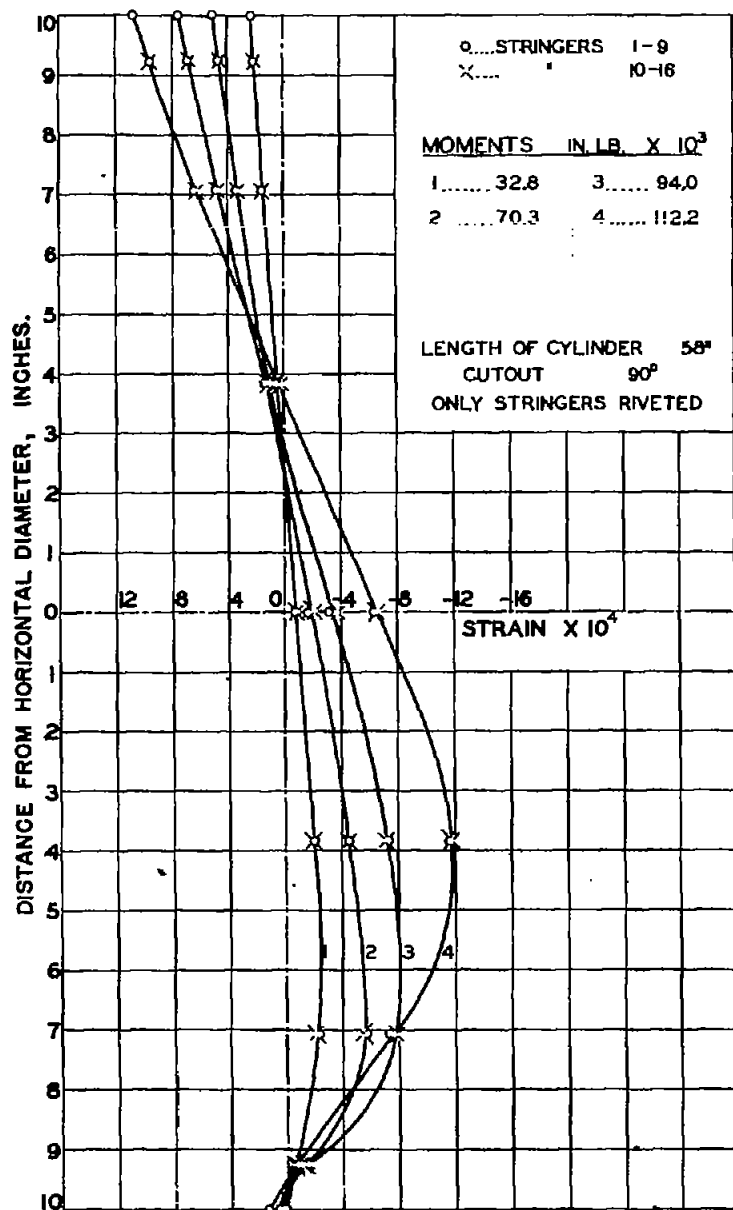
FIG.23. STRAIN DIAGRAM OF CYLINDER 22 BAND A.
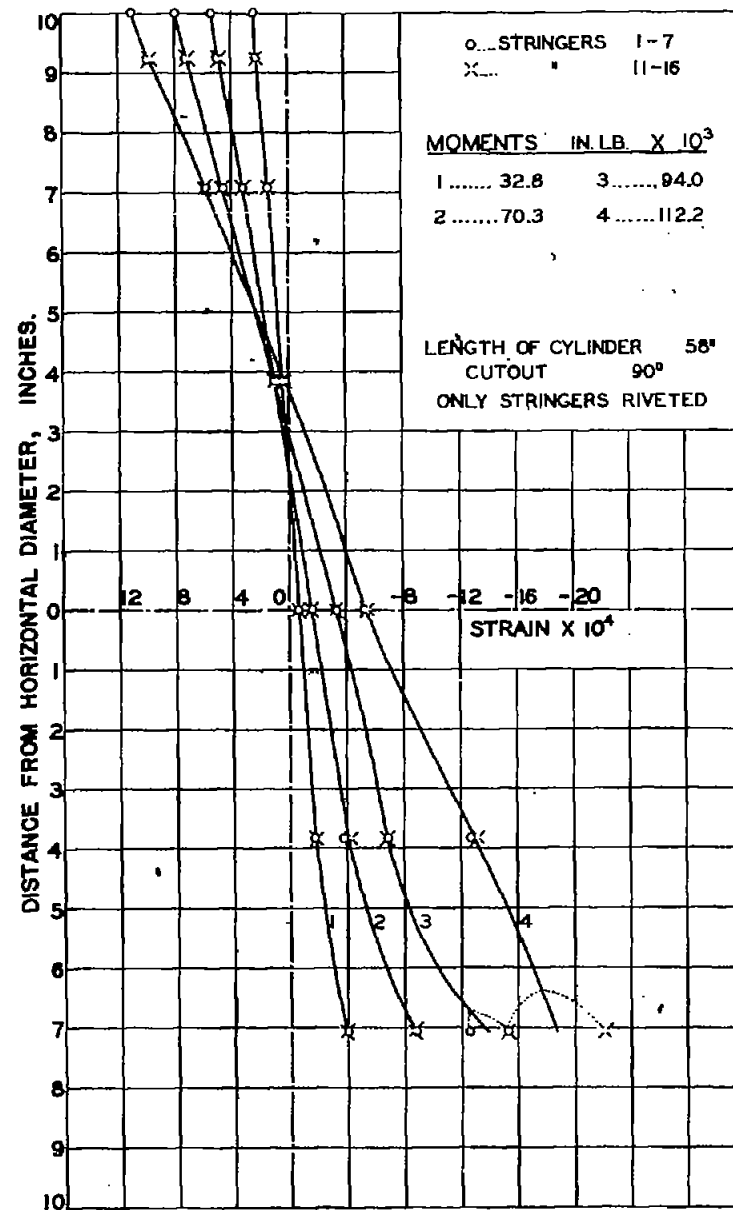
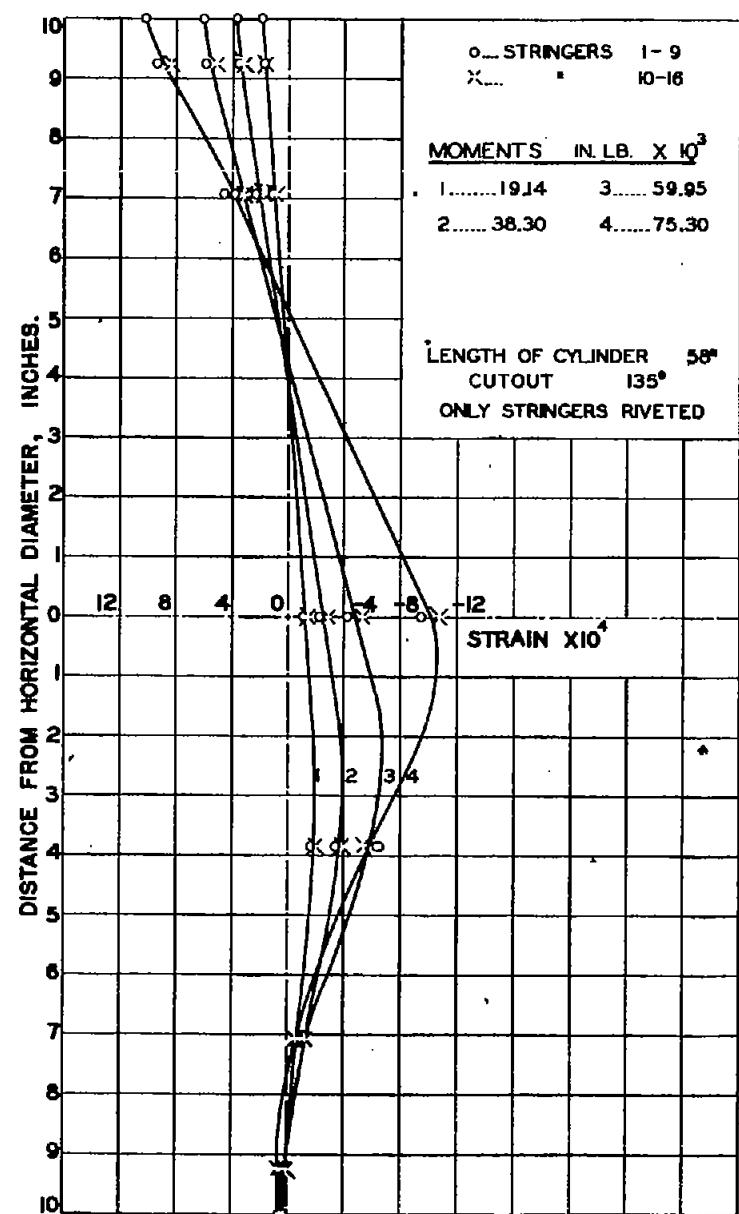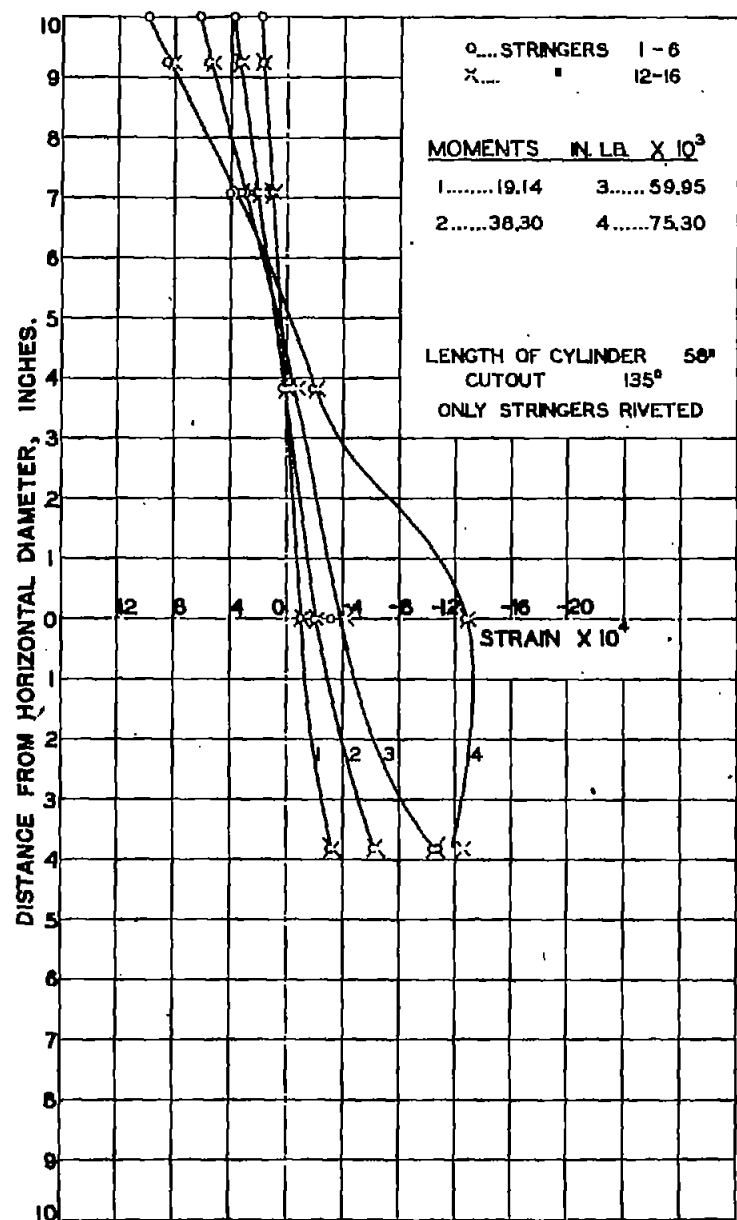FIG.24. STRAIN DIAGRAM OF CYLINDER 22 BAND E.
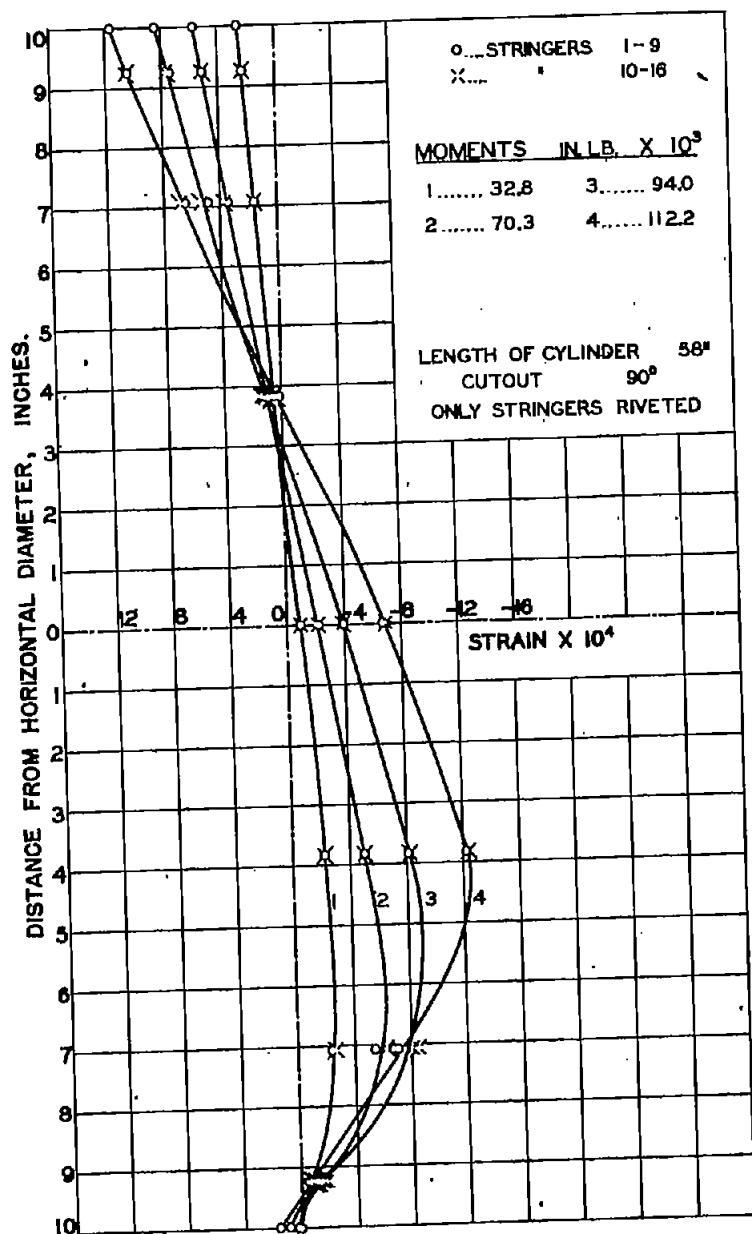
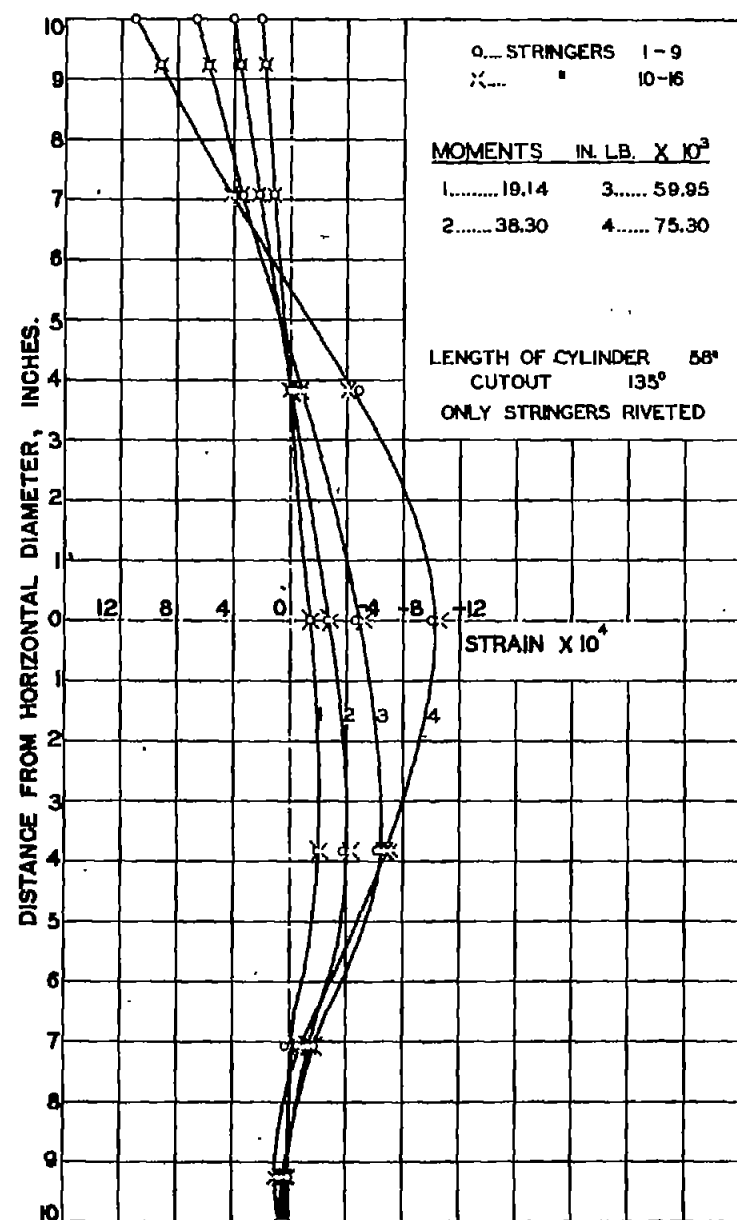FIG.25. STRAIN DIAGRAM OF CYLINDER 22 BAND I.
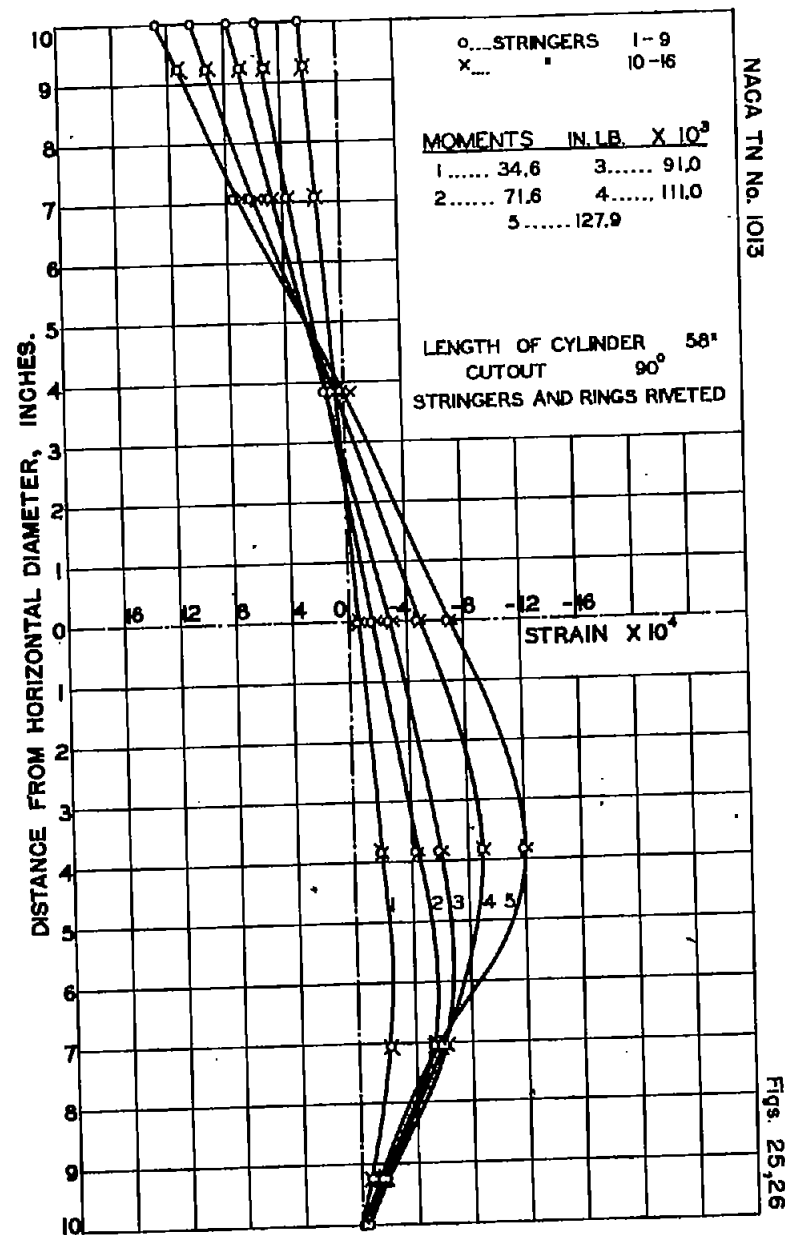
FIG.26. STRAIN DIAGRAM OF CYLINDER 23 BAND A.

FIG. 27. STRAIN DIAGRAM OF CYLINDER 23 BAND E.

FIG. 28. STRAIN DIAGRAM OF CYLINDER 23 BAND L.

o___ STRINGERS · 1-9
X___ " 10-16

MOMENTS   IN. LB. X 10³

1 ___ 16.2   3 ___ 54.1
2 ___ 33.7   4 ___ 68.4

LENGTH OF CYLINDER   58"
CUTOUT   135°
STRINGERS AND RINGS RIVETED

STRAIN X 10⁴

DISTANCE FROM HORIZONTAL DIAMETER, INCHES.

FIG. 29. STRAIN DIAGRAM OF CYLINDER 24 BAND A.

o___ SHEET AND STRINGER GAGES 1-6
X___ " " " " " 12-16

MOMENTS   IN. LB. X 10³

1 ___ 16.2   3 ___ 54.1
2 ___ 33.7   4 ___ 68.4

_____ NEGLECTING SHEET GAGES.
----- CONSIDERING SHEET GAGES.

LENGTH OF CYLINDER   58"
CUTOUT   135°
STRINGERS AND RINGS RIVETED

STRAIN X 10⁴

DISTANCE FROM HORIZONTAL DIAMETER, INCHES.

FIG. 30. STRAIN DIAGRAM OF CYLINDER 24   BAND E.

FIG. 31. STRAIN DIAGRAM OF CYLINDER 24 BAND I.

Within Fig. 31:

o — STRINGERS 1–9
X — " 10–16

MOMENTS IN.LB. X 10³

1...... 16.2   3.....54.1
2..... 33.7   4.....68.4

LENGTH OF CYLINDER 58"
CUTOUT 135°
STRINGERS AND RINGS RIVETED

STRAIN X 10⁴

DISTANCE FROM HORIZONTAL DIAMETER, INCHES.

FIG. 32. STRAIN DIAGRAM OF CYLINDER 25 BAND A.

Within Fig. 32:

o — STRINGERS 1–9
X — " 10–16

MOMENTS IN.LB. X 10³

1......19.14   3.....59.95
2......38.30   4.....75.30

LENGTH OF CYLINDER 58"
CUTOUT 135°
ONLY STRINGERS RIVETED

STRAIN X 10⁴

DISTANCE FROM HORIZONTAL DIAMETER, INCHES.

FIG. 33. STRAIN DIAGRAM OF CYLINDER 25 BAND E.

FIG. 34. STRAIN DIAGRAM OF CYLINDER 25 BAND I.

BANDS

	B	C			D			E			F
STR.13											
		ϵ_x	ϵ_c	γ	ϵ_x	ϵ_c	γ	ϵ_x	ϵ_c	γ	
(A)		-99	32	39	-98	31	51	-106	31	90	
(B)		-200	63	32	-207	62	54	-224	63	124	
STR.12											
		ϵ_x	ϵ_c	γ	ϵ_x	ϵ_c	γ	ϵ_x	ϵ_c	γ	
(A)		-168	53	23	-170	49	42	-173	49	73	
(B)		-346	104	36	-362	95	30	-367	101	122	
STR.11											
		ϵ_x	ϵ_c	γ	ϵ_x	ϵ_c	γ	ϵ_x	ϵ_c	γ	
(A)		-231	72	.95	-208	67	43	-280	93	199	
(B)		-393	128	210	-334	102	55	-248	-23	254	
STR.10											

ROWS (A)... M = 34,700 IN. LB.
ROWS (B)... M = 71,100 IN. LB.

STR. 9 — ALL STRAINS TO BE MULTIPLIED BY 10^{-6}

FIG. 35.   STRAINS CALCULATED FROM ROSETTE DATA.
CYLINDER 17

BANDS

	B	C			D			E			F
STR.13											
		σ_x	σ_c	τ	σ_x	σ_c	τ	σ_x	σ_c	τ	
(A)		-1032	27	158	-1023	18	206	-1116	-9	364	
(B)		-2090	35	129	-2174	-1	218	-2366	-48	501	
STR.12											
		σ_x	σ_c	τ	σ_x	σ_c	τ	σ_x	σ_c	τ	
(A)		-1755	30	93	-1792	-23	170	-1827	-33	295	
(B)		-3632	2	145	-3848	-157	121	-3885	-105	493	
STR.11											
		σ_x	σ_c	τ	σ_x	σ_c	τ	σ_x	σ_c	τ	
(A)		-2416	31	384	-2168	53	174	-2909	104	804	
(B)		-4092	117	848	-3501	21	222	-2941	-1124	1026	
STR.10											

ROWS (A)... M = 34,700 IN. LB.
ROWS (B)... M = 71,100 IN. LB.

STR. 9 — STRESSES GIVEN IN LB. PER SQ. IN.

FIG. 36.   STRESSES CALCULATED FROM ROSETTE DATA.
CYLINDER 17

BANDS

	C			D			E		
	ϵ_x	ϵ_c	γ				ϵ_x	ϵ_c	γ
(A)	−168	59	117				−160	51	120
(B)	−373	95	32				−367	121	247

STR. 14 — B ... E ... F
STR. 13

	C			D			E		
	ϵ_x	ϵ_c	γ	ϵ_x	ϵ_c	γ	ϵ_x	ϵ_c	γ
(A)	−294	94	143	?	?	122	−289	95	39
(B)	−497	172	294	?	?	145	−393	266	−248

STR. 12
STR. 11

ROWS (A)... M = 33,300 IN. LB.
ROWS (B)... M = 66,600 IN. LB.

STR. 10 — ALL STRAINS TO BE MULTIPLIED BY 10^{-6}

FIG. 37.   STRAINS CALCULATED FROM ROSETTE DATA.
CYLINDER 19

BANDS

	C			D			E		
	σ_x	σ_c	τ				σ_x	σ_c	τ
(A)	−1734	99	473				−1670	35	485
(B)	−3975	−195	129				−3816	126	998

STR. 14 — B ... E ... F
STR. 13

	C			D			E		
	σ_x	σ_c	τ	σ_x	σ_c	τ	σ_x	σ_c	τ
(A)	−3067	67	578	?	?	493	−3006	96	158
(B)	−5139	264	1187	?	?	586	−3614	1709	−1002

STR. 12
STR. 11

ROWS (A) ...M = 33,300 IN. LB.
ROWS (B) ...M = 66,600 IN. LB.

STR. 10 — STRESSES GIVEN IN LB. PER SQ. IN.

FIG. 38.   STRESSES CALCULATED FROM ROSETTE DATA.
CYLINDER 19

FIG. 39 — Strains (STR.13 to STR.12 region):

	B ϵ_x	B ϵ_c	B γ	C ϵ_x	C ϵ_c	C γ	D ϵ_x	D ϵ_c	D γ	E ϵ_x	E ϵ_c	E γ	F ϵ_x	F ϵ_c	F γ	G ϵ_x	G ϵ_c	G γ
(A)	-122	90	-88	-233	86	-145	-267	100	-37	-236	?	?	-224	56	-39	-232	174	-64
(B)	-218	146	-222	-222	83	-103	-316	146	-24	-324	88	-65	-380	95	-5	-328	496	-374

STR.12 to STR.11:

	C ϵ_x	C ϵ_c	C γ	G ϵ_x	G ϵ_c	G γ
(A)	-83	43	149	-90	33	-203
(B)	-218	128	281	25	-132	-187

STR.11 to STR.10:

	C ϵ_x	C ϵ_c	C γ	G ϵ_x	G ϵ_c	G γ
(A)	14	6	-79	10	6	95
(B)	27	92	6	17	3	209

STR.10 to STR.9:

	C ϵ_x	C ϵ_c	C γ	G ϵ_x	G ϵ_c	G γ
(A)	7	-1	-25	14	15	33
(B)	5	-4	-46	5	13	76

ROWS (A)...M = 19,140 IN. LB.
ROWS (B)...M = 38,300 IN. LB.
ALL STRAINS TO BE MULTIPLIED BY 10^{-6}

BANDS

FIG. 39.   STRAINS CALCULATED FROM ROSETTE DATA.
CYLINDER 25

FIG. 40 — Stresses (STR.13 to STR.12 region):

	B σ_x	B σ_c	B τ	C σ_x	C σ_c	C τ	D σ_x	D σ_c	D τ	E σ_x	E σ_c	E τ	F σ_x	F σ_c	F τ	G σ_x	G σ_c	G τ
(A)	-1096	616	-355	-2391	186	-586	-2735	230	-149	?	?	?	-2391	-129	-158	-2075	1205	-259
(B)	-2010	930	-897	-2274	189	-416	-3141	591	-97	-3434	-106	-263	-4056	-219	-20	-2068	4588	-1510

STR.12 to STR.11:

	C σ_x	C σ_c	C τ	G σ_x	G σ_c	G τ
(A)	-809	209	602	-924	69	-820
(B)	-2072	722	1135	-168	-1437	-755

STR.11 to STR.10:

	C σ_x	C σ_c	C τ	G σ_x	G σ_c	G τ
(A)	182	118	-319	136	104	384
(B)	630	1155	24	207	93	844

STR.10 to STR.9:

	C σ_x	C σ_c	C τ	G σ_x	G σ_c	G τ
(A)	77	13	-101	213	222	133
(B)	44	-29	-186	103	167	307

BANDS

ROWS (A)...M = 19,140 IN. LB.
ROWS (B)...M = 38,300 IN. LB.
STRESSES GIVEN IN LB. PER SQ. IN.

FIG. 40.   STRESSES CALCULATED FROM ROSETTE DATA.
CYLINDER 25
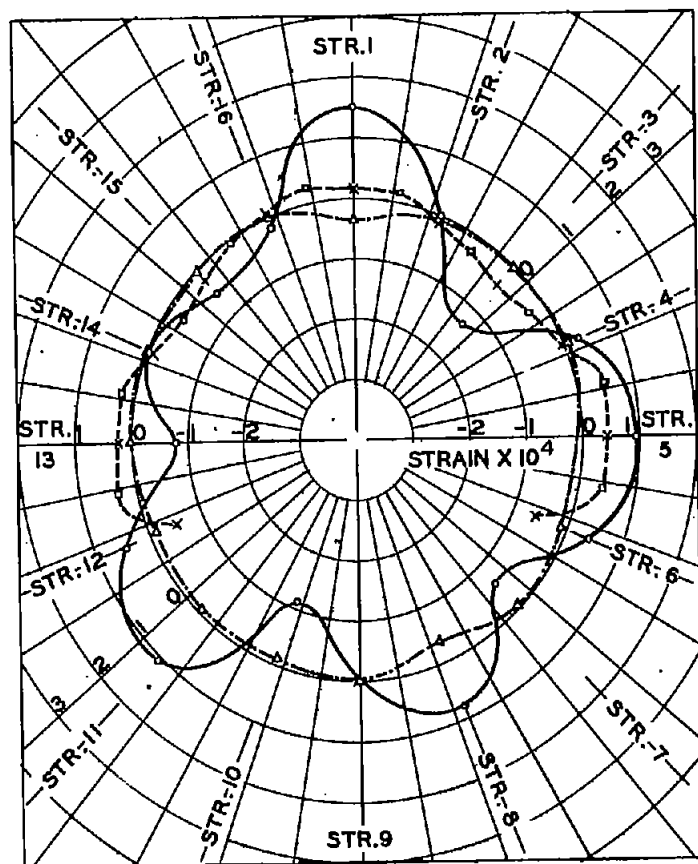
FIG. 41. INITIAL STRAIN IN CYLINDER 24
CAUSED BY TIGHTENING STRINGER GRIP
FITTINGS AND RING NO. 1.
——o—— BAND A   ———△——— BAND I
—×——□—— BAND E
STR. SHEET
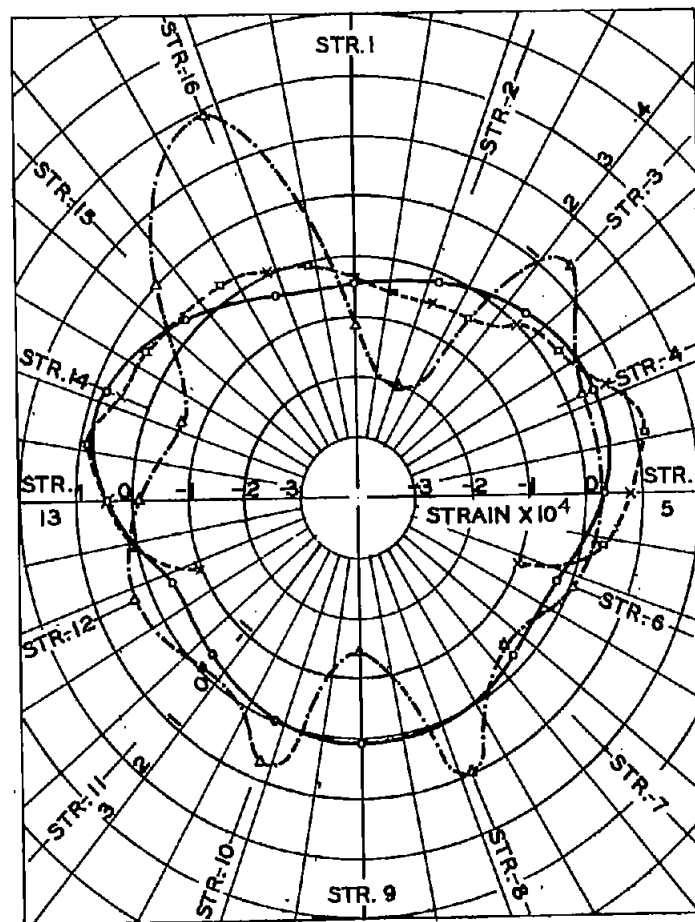
FIG. 42. INITIAL STRAIN IN CYLINDER 24
CAUSED BY TIGHTENING STRINGER GRIP
FITTINGS AND RING NO. 2.
——o—— BAND A   ——△—— BAND I
—×——□—— BAND E
STR. SHEET
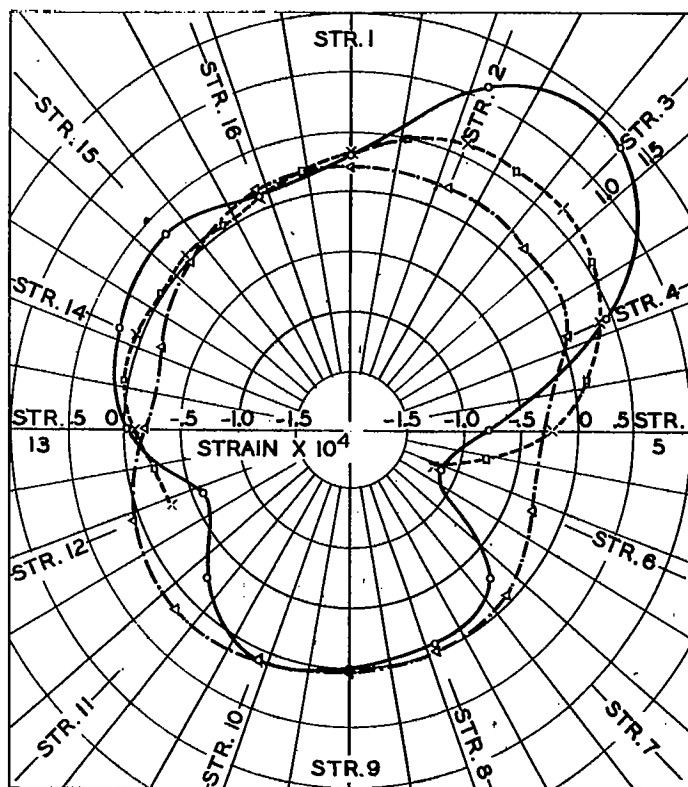
FIG. 43. INITIAL STRAIN IN CYLINDER 24
CAUSED BY TIGHTENING TO END STAND
———o——— BAND A —·—△—·— BAND I
—×—·—□—·— BAND E
STR.   SHEET
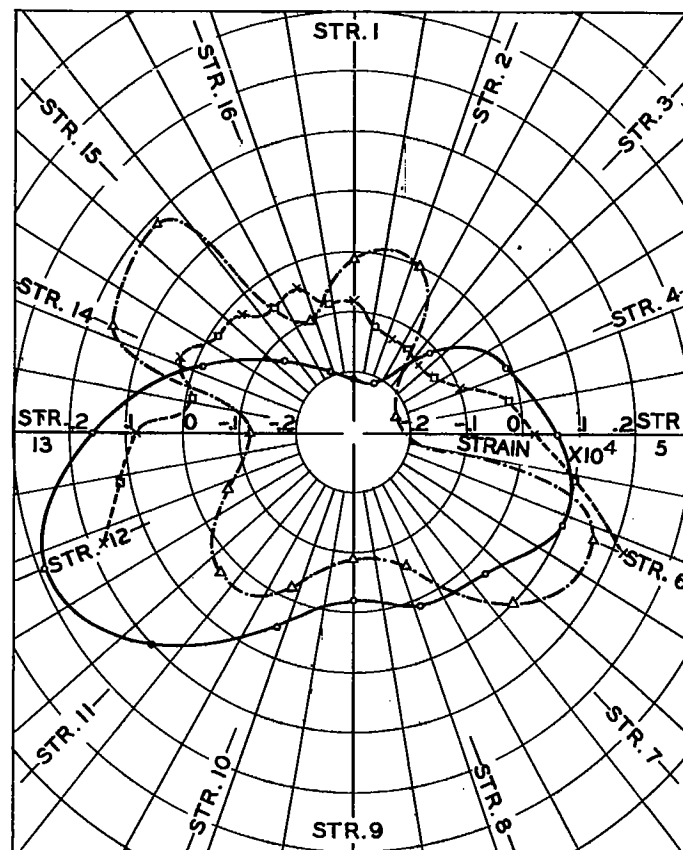
FIG. 44. INITIAL STRAIN IN CYLINDER 24
CAUSED BY TIGHTENING TO LOADING HEAD
———o——— BAND A —·—△—·— BAND I
—×—·—□—·— BAND E
STR.   SHEET
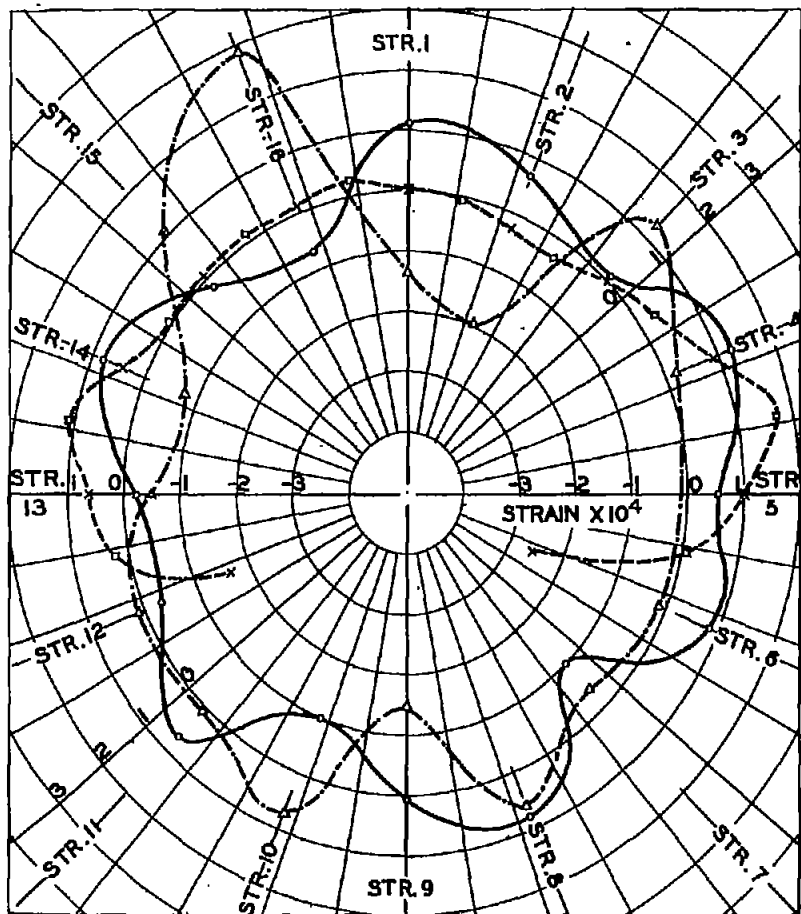
FIG.45. TOTAL INITIAL STRAIN IN CYLINDER 24

——○—— BAND A ——△—— BAND I
——×——□—— BAND E
STR. SHEET

MOMENT   35,000 IN. LB.

CYL. (BAND)	SYMBOL	LENGTH	REMARKS
16 (A,G AVE.)	——○——	45"	ONLY STR. BOLTED
17 (A,G AVE.)	——×——	45"	ONLY STR. RIVETED
18 (A,I AVE.)	———□———	58"	ONLY STR. RIVETED
20 (A,G AVE.)	——△——	45"	RINGS AND STR. RIVETED

DISTANCE FROM HORIZONTAL DIAMETER, INCHES.

STRAIN X 10⁴

NACA TN No. 1013

Figs. 45,46
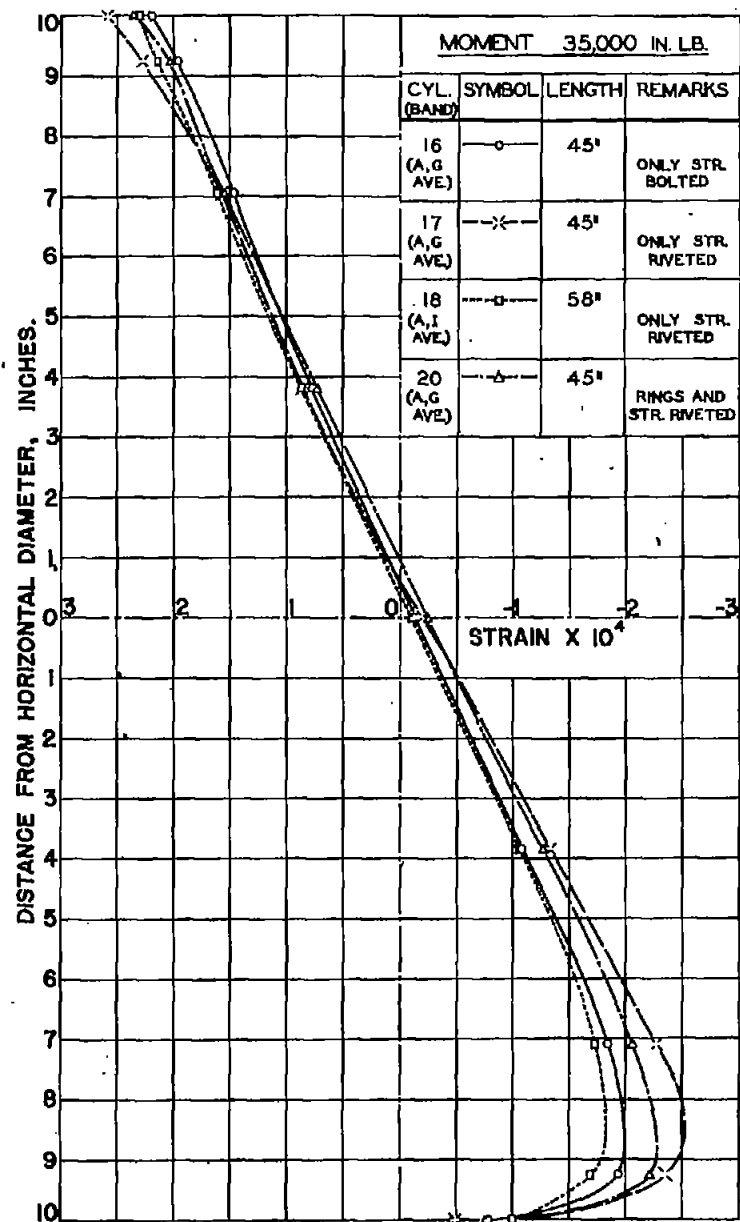
FIG. 46. COMPARISON OF STRAIN DIAGRAMS OF CYLINDERS WITH 45° CUTOUT – END BANDS.

CYL. (BAND)	SYMBOL	LENGTH	REMARKS
16 (D)	—o—	45"	ONLY STR. BOLTED
17 (D)	—x—	45"	ONLY STR. RIVETED
18 (E)	----□----	58"	ONLY STR. RIVETED
20 (D)	—△—	45"	RINGS AND STR. RIVETED

MOMENT   35,000 IN. LB.
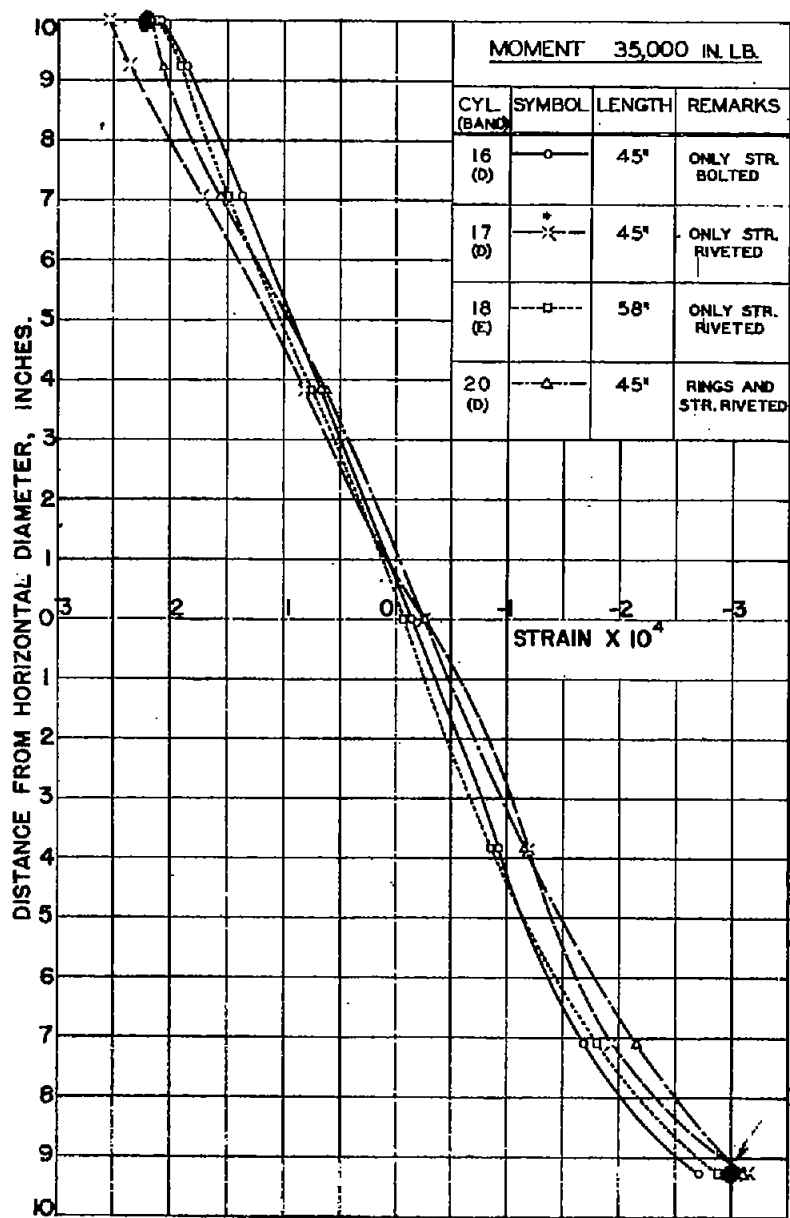
FIG. 47. COMPARISON OF STRAIN DIAGRAMS OF CYLINDERS WITH 45° CUTOUT — MIDDLE BANDS.

CYL. (BAND)	SYMBOL	LENGTH	REMARKS
19 (A, G AVE.)	—o—	45"	ONLY STR. RIVETED
22 (A, I AVE.)	—x—	58"	ONLY STR. RIVETED
23 (A, I AVE.)	----□----	58"	RINGS AND STR. RIVETED

MOMENT   35,000 IN. LB.
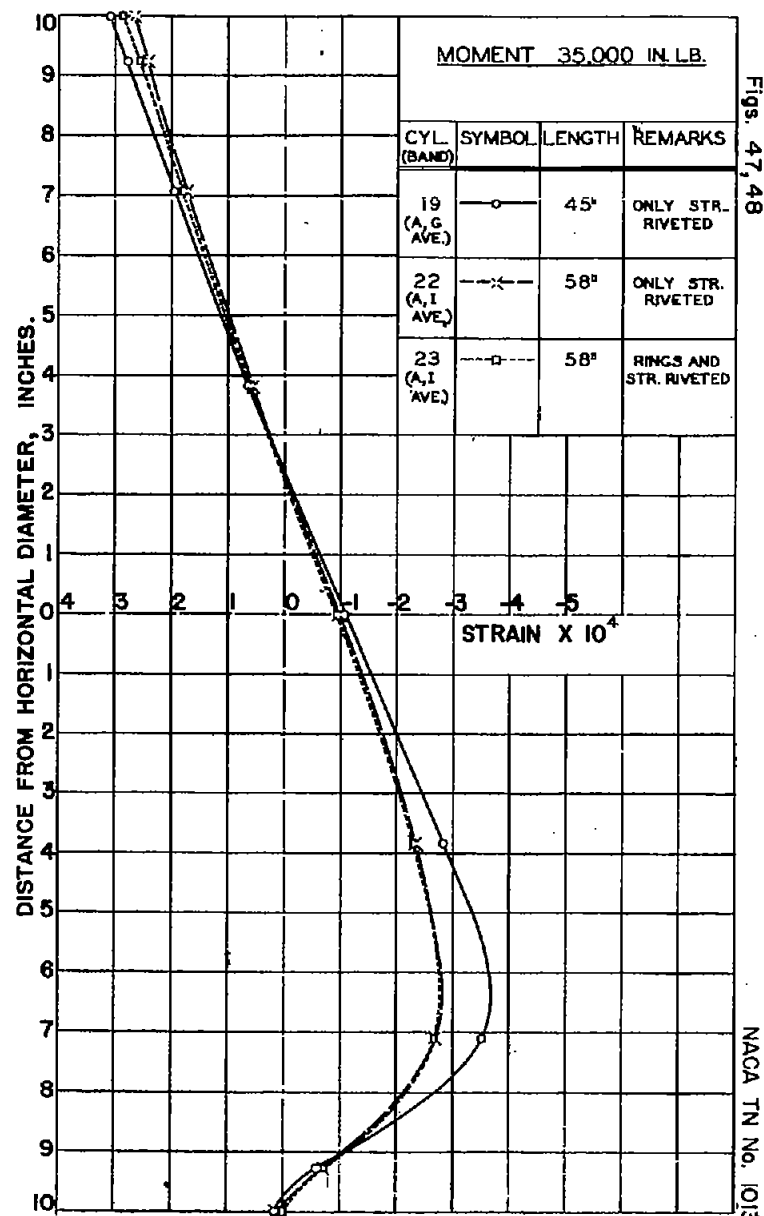
FIG. 48. COMPARISON OF STRAIN DIAGRAMS OF CYLINDERS WITH 90° CUTOUT — END BANDS.

MOMENT 35,000 IN. LB.

CYL. (BAND)	SYMBOL	LENGTH	REMARKS
19 (D)	—o—	45"	ONLY STR. RIVETED
22 (E)	—×—	58"	ONLY STR. RIVETED
23 (E)	—□—	58"	RINGS AND STR. RIVETED

STRAIN X 10⁴

DISTANCE FROM HORIZONTAL DIAMETER, INCHES.

FIG. 49. COMPARISON OF STRAIN DIAGRAMS OF CYLINDERS WITH 90° CUTOUT – MIDDLE BANDS.

MOMENT 35,000 IN. LB.

CYL. (BAND)	SYMBOL	LENGTH	REMARKS
21 (A, G AVE.)	—o—	45"	ONLY STR. RIVETED
24 (A, I AVE.)	—□—	58"	RINGS AND STR. RIVETED
25 (A, I AVE.)	—×—	58"	ONLY STR. RIVETED

STRAIN X 10⁴

DISTANCE FROM HORIZONTAL DIAMETER, INCHES.

FIG. 50. COMPARISON OF STRAIN DIAGRAMS OF CYLINDERS WITH 135° CUTOUT – END BANDS.

FIG. 51. COMPARISON OF STRAIN DIAGRAMS OF CYLINDERS WITH 135° CUTOUT — MIDDLE BANDS.

FIG. 52. STRAIN VARIATION ALONG STRINGER 7 - CYLINDER 18

MOMENTS IN. LB.

| 1. 35,600 | 3. 101,700 | 5. 142,300 |
| 2. 71,300 | 4. 126,100 | 6. 162,700 |
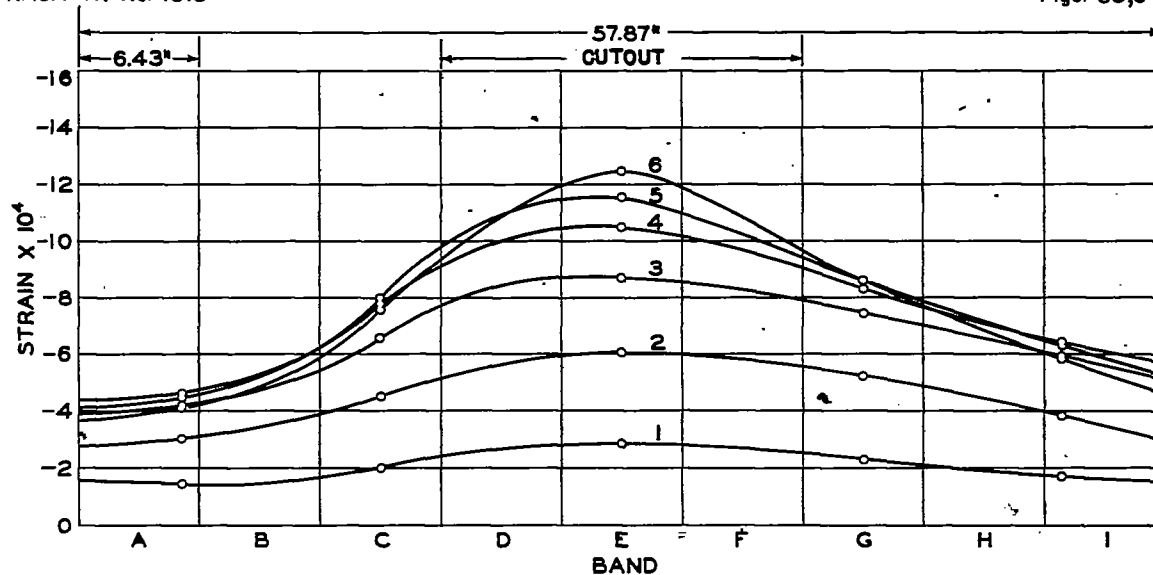
FIG.53. STRAIN VARIATION   ALONG STRINGER 8 - CYLINDER 18

MOMENTS IN. LB.

| 1. 35,600 | 3. 101,700 | 5. 142,300 |
| 2. 71,300 | 4. 126,100 | 6. 162,700 |
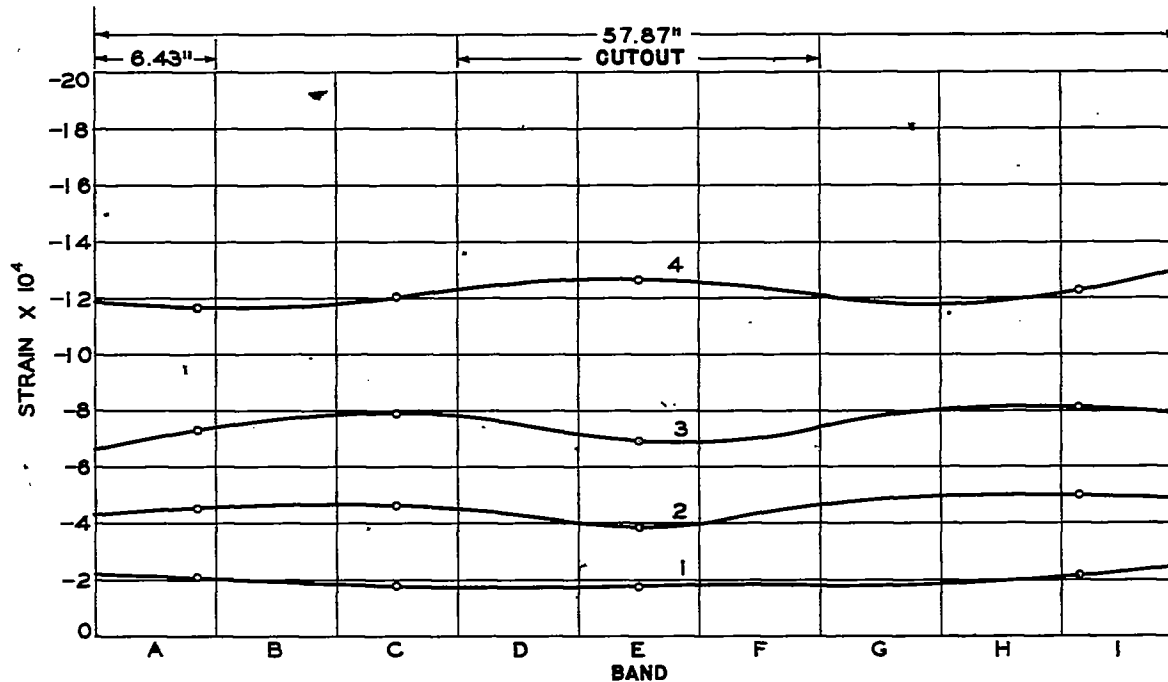
FIG.54. STRAIN VARIATION ALONG STRINGER 6-CYLINDER 22

MOMENT IN. LB.

| 1. 32,800 | 3. 94,000 |
| 2. 70,300 | 4. 112,200 |
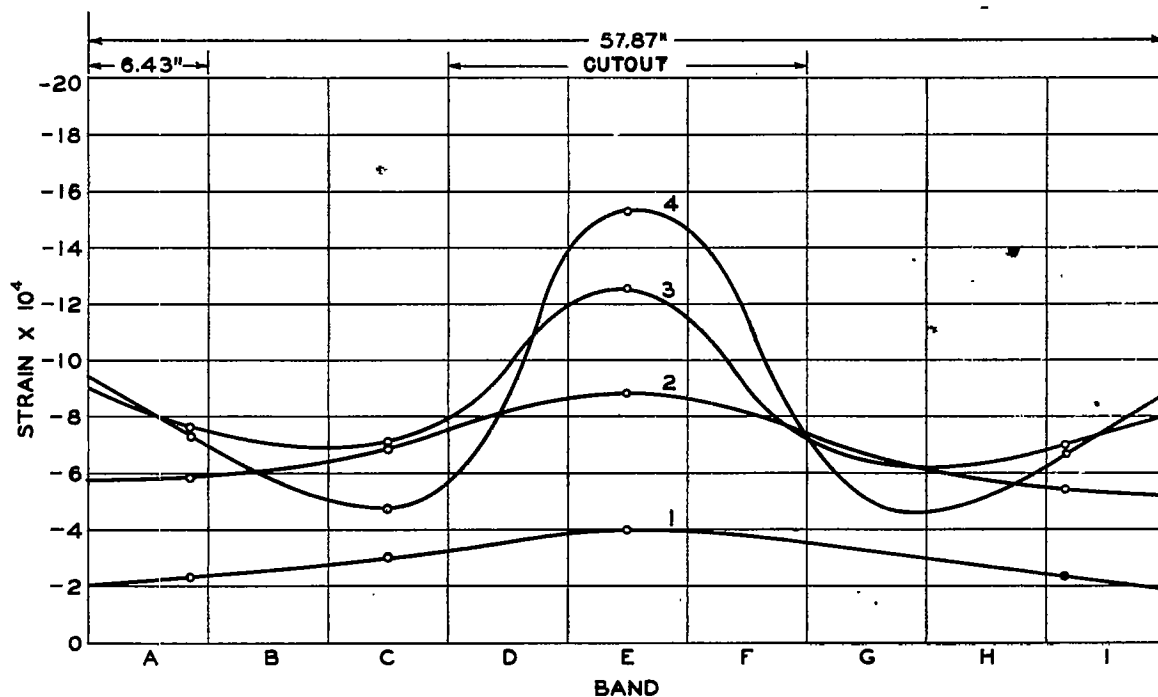
FIG.55. STRAIN VARIATION ALONG STRINGER 7-CYLINDER 22

MOMENT IN. LB.
1. 32,900   3. 94,000
2. 70,300   4. 112,200
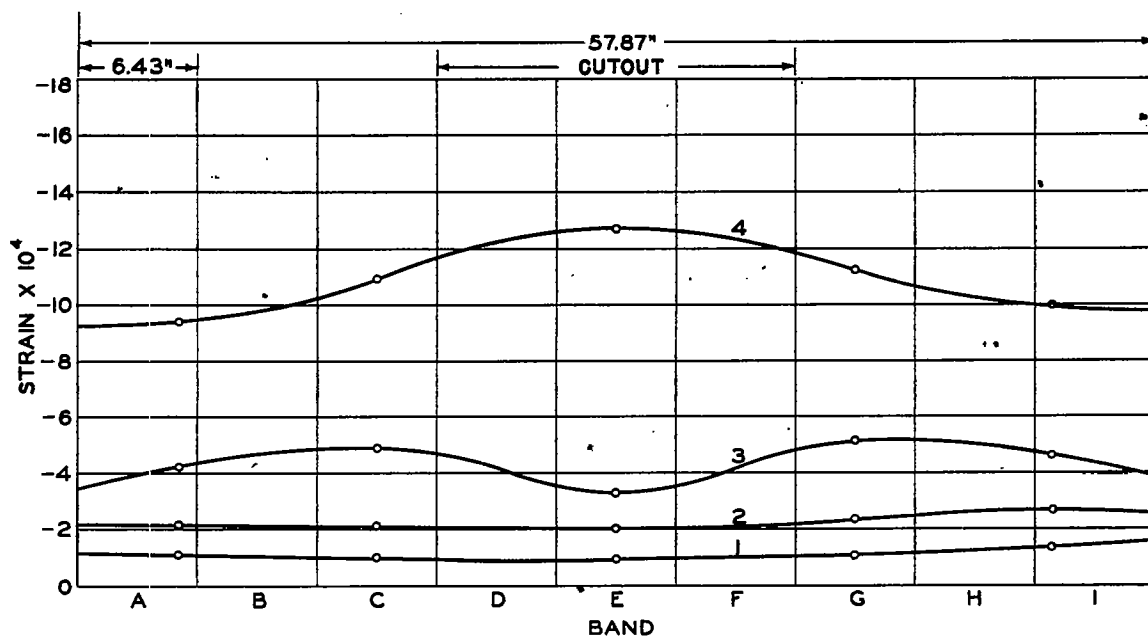
FIG.56. STRAIN VARIATION ALONG STRINGER 5-CYLINDER 25

MOMENTS IN. LB.
1. 19,140   3. 59,950
2. 38,300   4. 75,300
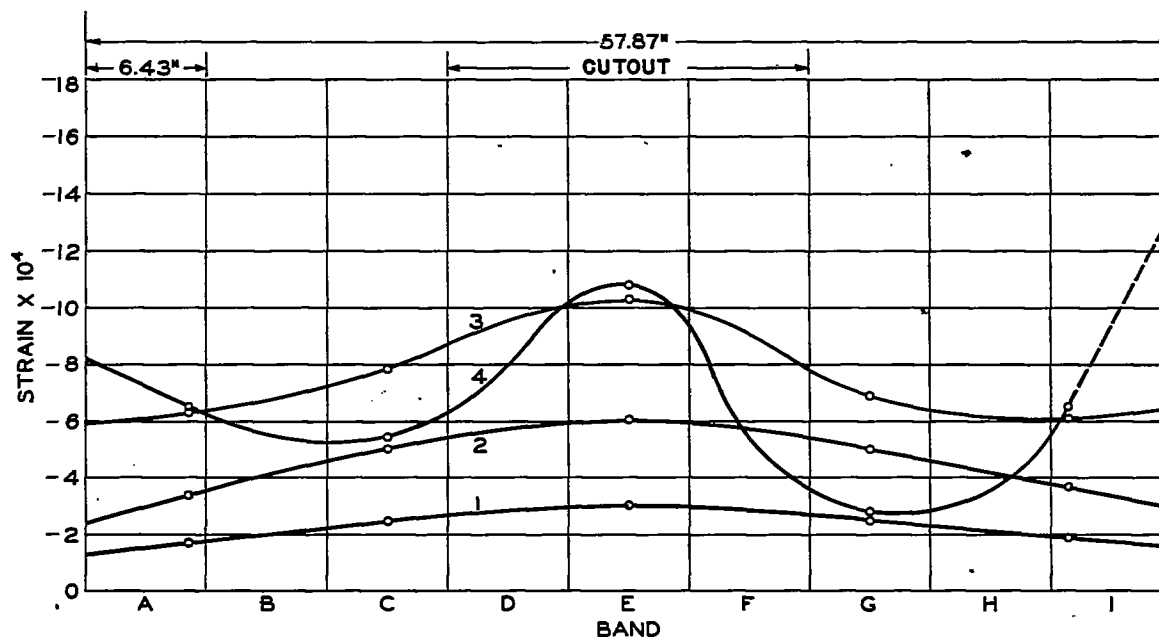
FIG.57. STRAIN VARIATION ALONG STRINGER 6-CYLINDER 25

MOMENTS IN. LB.

1. 19,140	3. 59,950
2. 38,300	4. 75,300
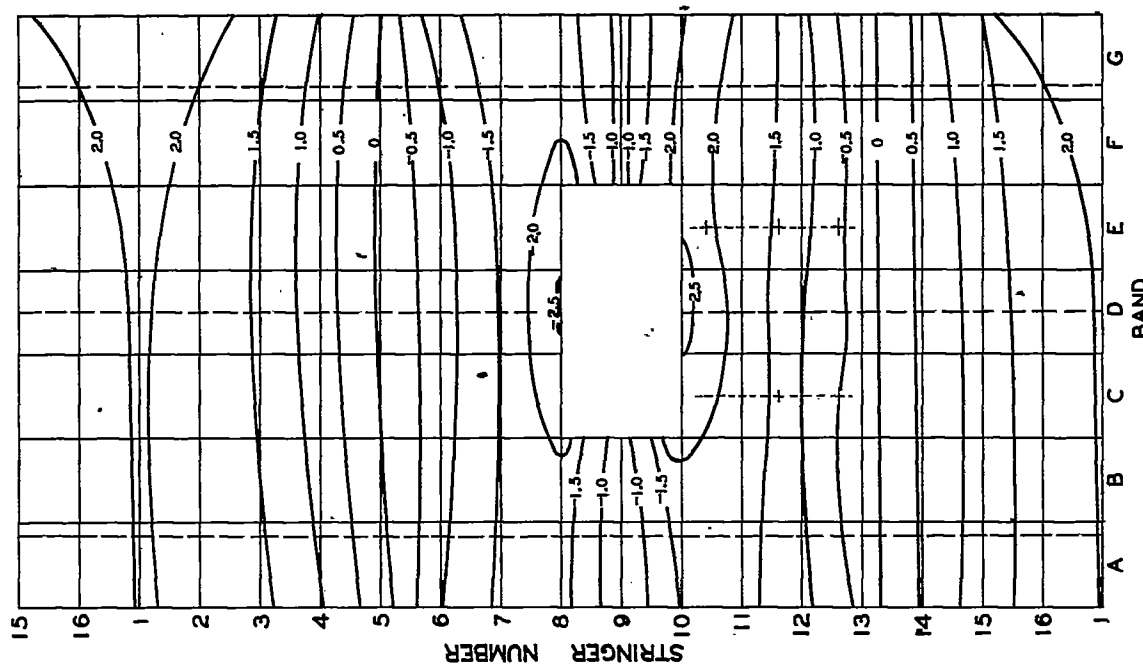
FIG. 58. STRAIN TRAJECTORIES FOR CYLINDER 16.

MOMENT 35000 IN. LB.

VALUES OF STRAIN TO BE MULTIPLIED BY 10^{-4}.

—·—+—·— INDICATES CENTERLINE OF STRAIN GAGES.
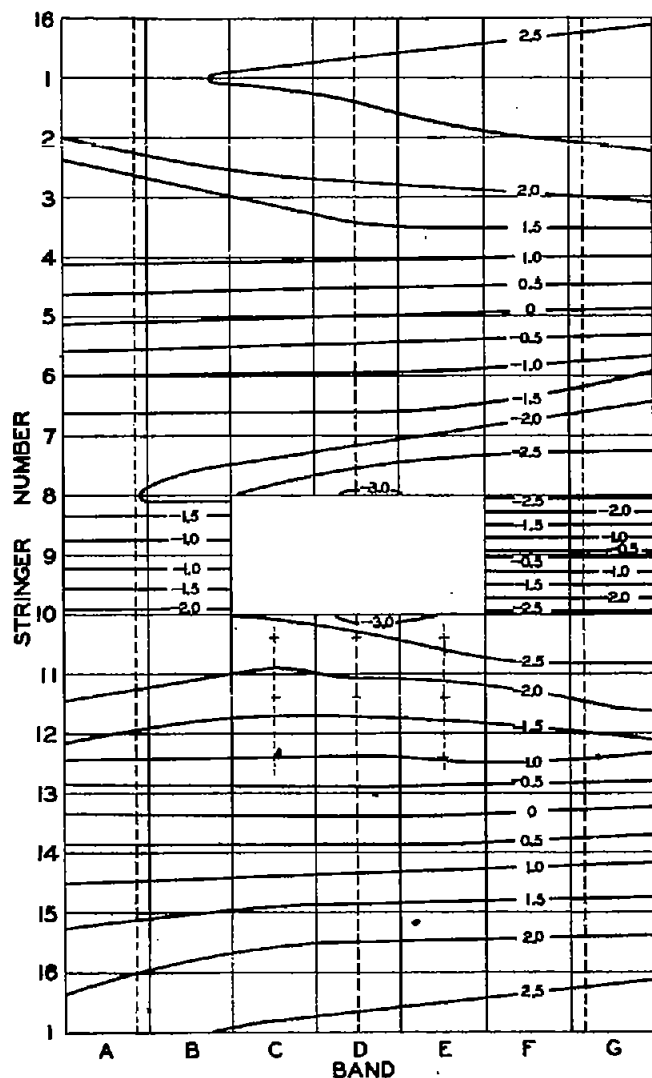
FIG. 59. STRAIN TRAJECTORIES FOR CYLINDER 17.
MOMENT 35000 IN. LB.
· VALUES OF STRAIN TO BE MULTIPLIED BY 10.$^{-4}$
---+---+--INDICATES CENTERLINE OF STRAIN GAGES.
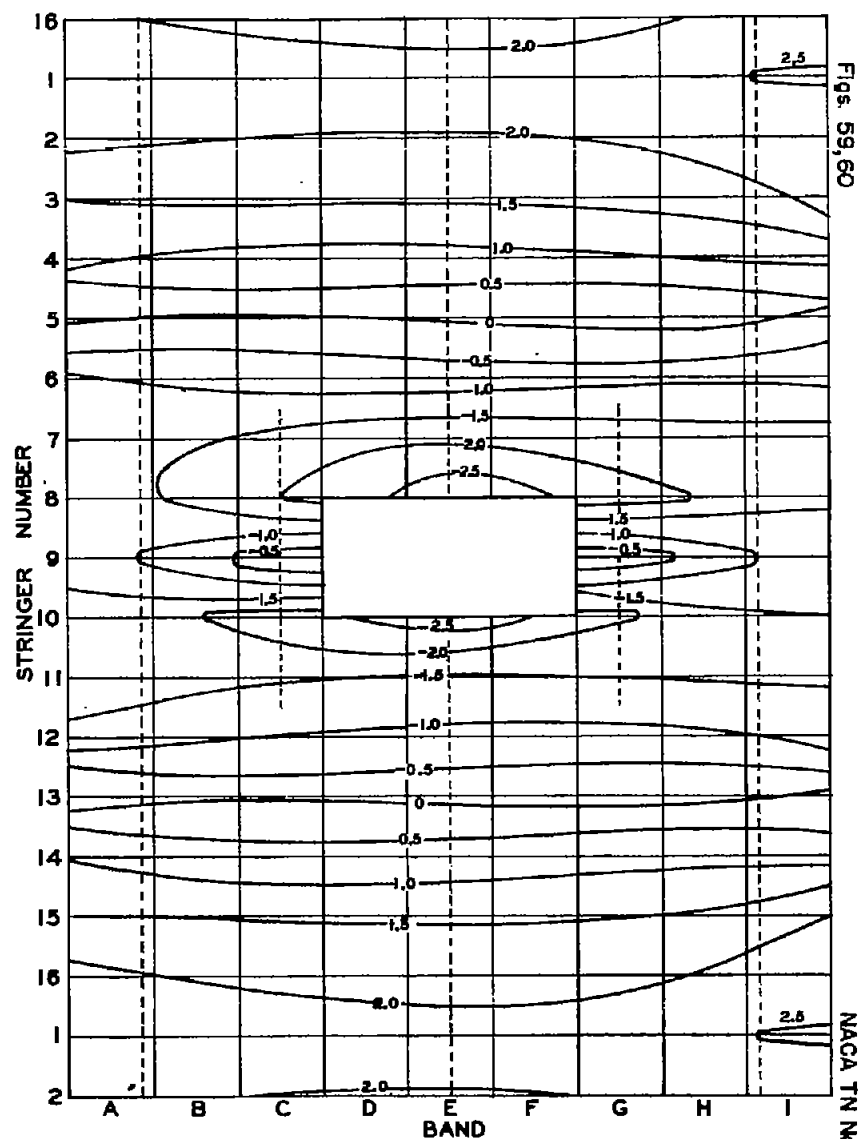
FIG. 60. STRAIN TRAJECTORIES FOR CYLINDER 18
MOMENT 35000 IN. LB.
VALUES OF STRAIN TO BE MULTIPLIED BY 10.$^{-4}$
----------INDICATES CENTERLINE OF STRAIN GAGES.
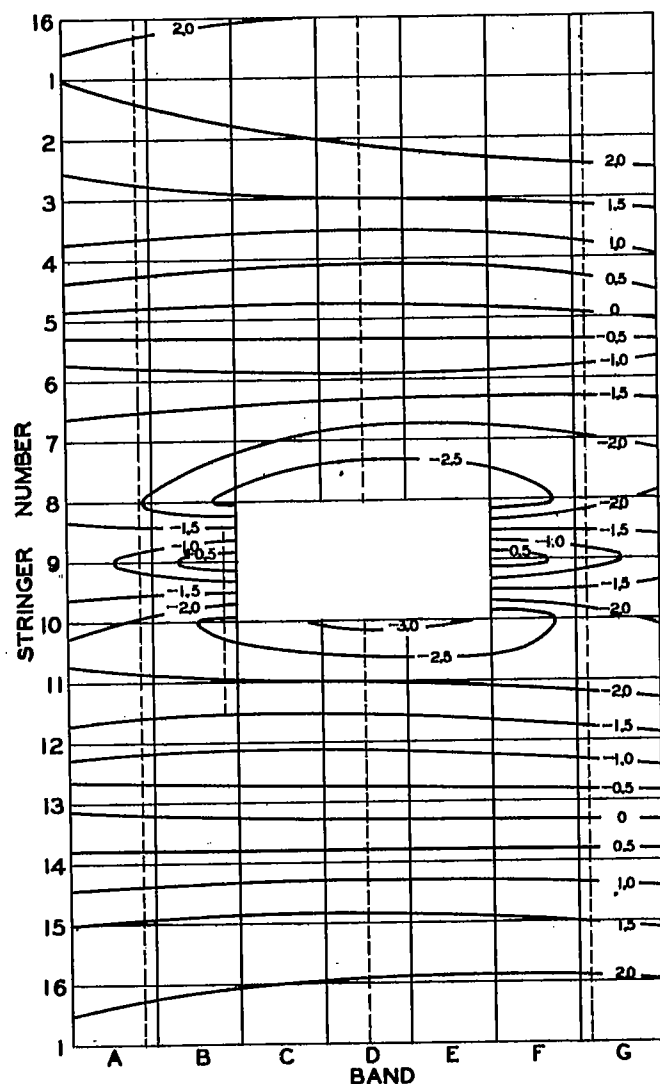
FIG. 61. STRAIN TRAJECTORIES FOR CYLINDER 20
MOMENT 35000 IN. LB.
VALUES OF STRAIN TO BE MULTIPLIED BY 10.$^{-4}$
— — — — — — —INDICATES CENTERLINE OF STRAIN GAGES.
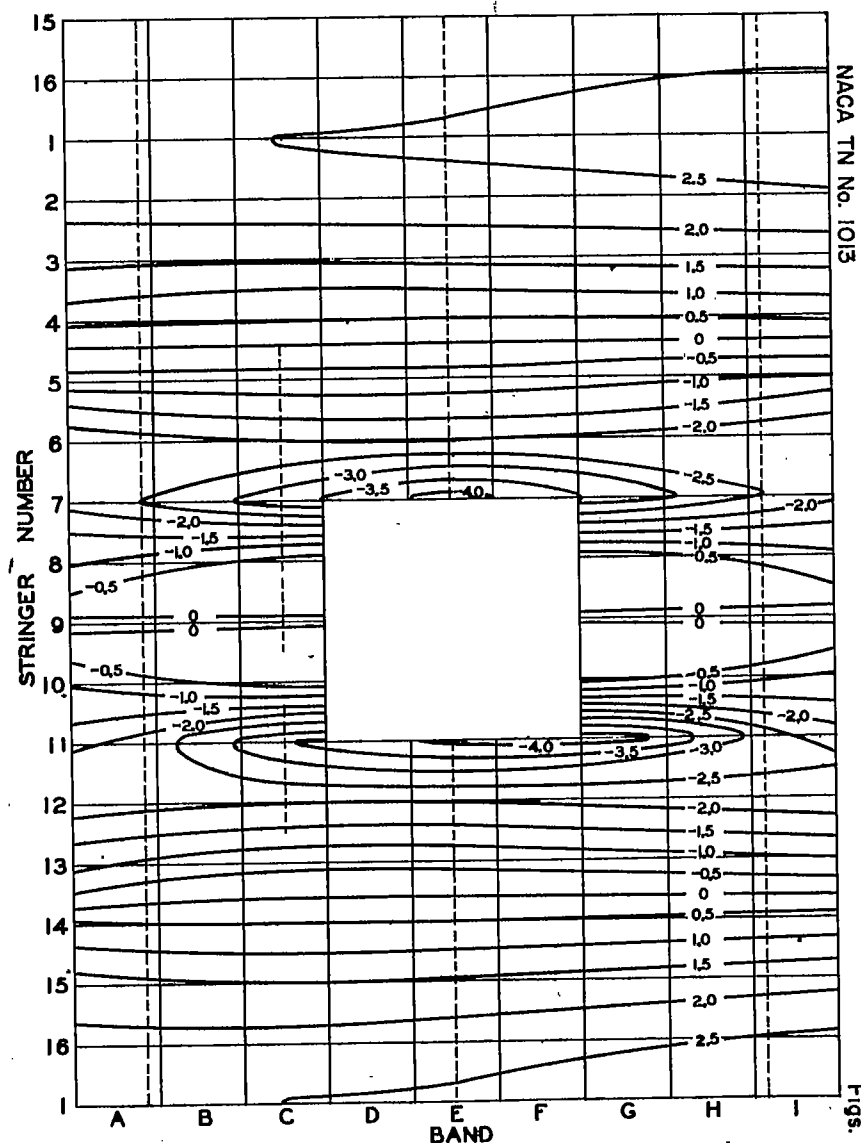
FIG. 62. STRAIN TRAJECTORIES FOR CYLINDER 22.
MOMENT 35000 IN. LB.
VALUES OF STRAIN TO BE MULTIPLIED BY 10,$^{-4}$
— — — — — — —INDICATES CENTERLINE · OF STRAIN GAGES.
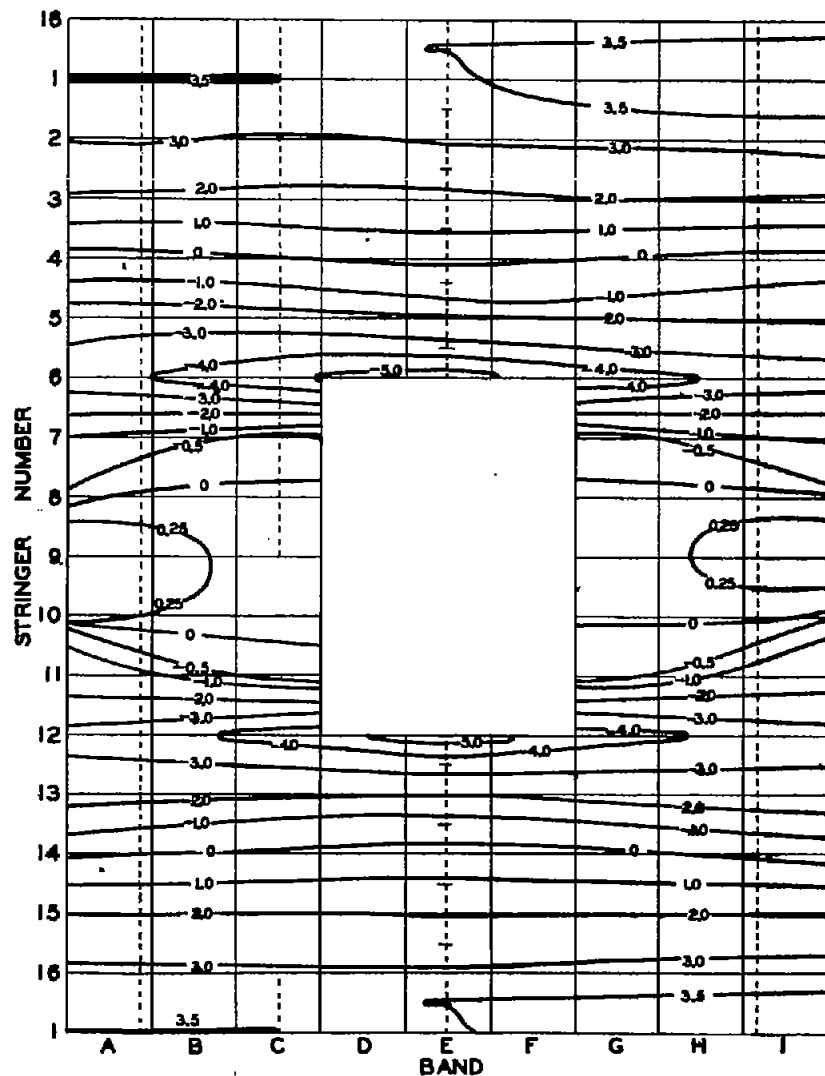
FIG. 63. STRAIN TRAJECTORIES FOR CYLINDER 24.
MOMENT 35000 IN. LB.
VALUES OF STRAIN TO BE MULTIPLIED BY 10^{-4}.
--+-----+-- INDICATES CENTERLINE OF STRAIN GAGES.
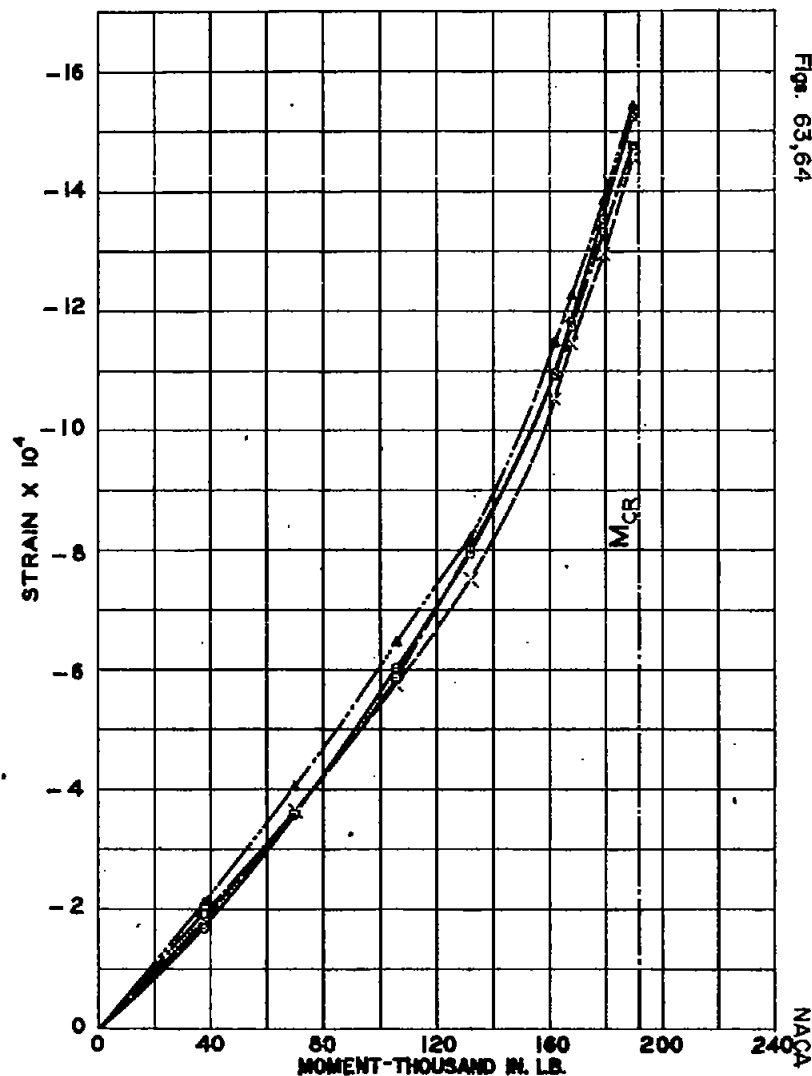
FIG. 64. STRINGER STRAIN VARIATION WITH MOMENT
CYLINDER 16

BAND A-STR. 7 —•—
BAND G-STR. 7 —•—
BAND A-STR. 11 --x--
BAND G-STR. 11 —x—
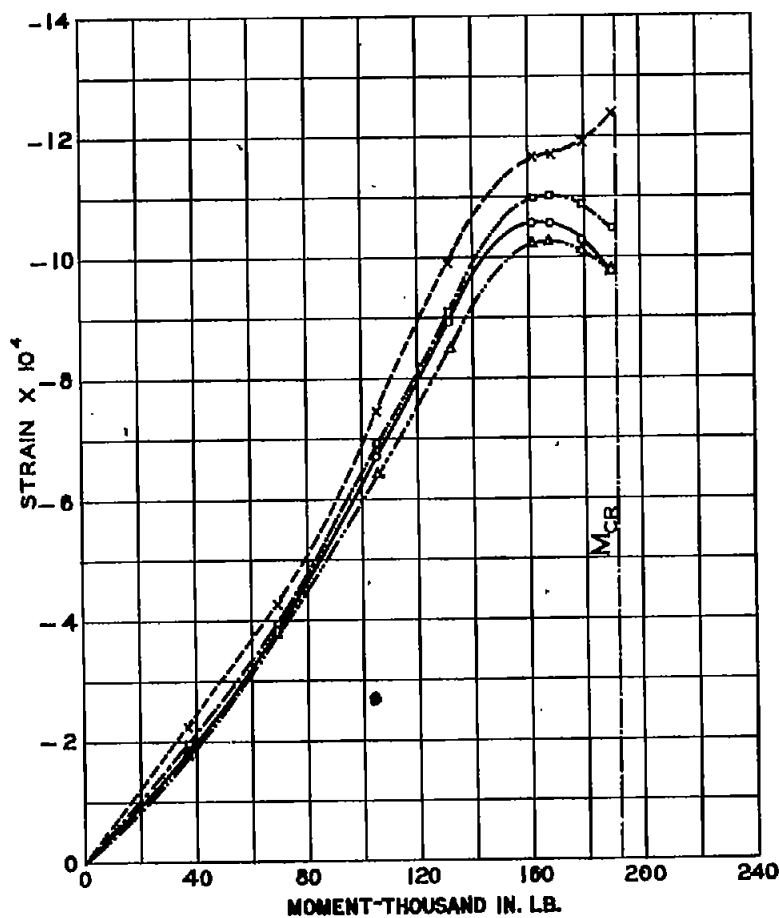
FIG.65. STRINGER STRAIN VARIATION WITH MOMENT
CYLINDER 16

BAND A-STR. 8 ——○——
BAND G-STR. 8 ——●——
BAND A-STR. 10 ——△——
BAND G-STR. 10 ——✕——

STRINGER I
STRINGER 7
STRINGER 8
STRINGER 10
STRINGER II
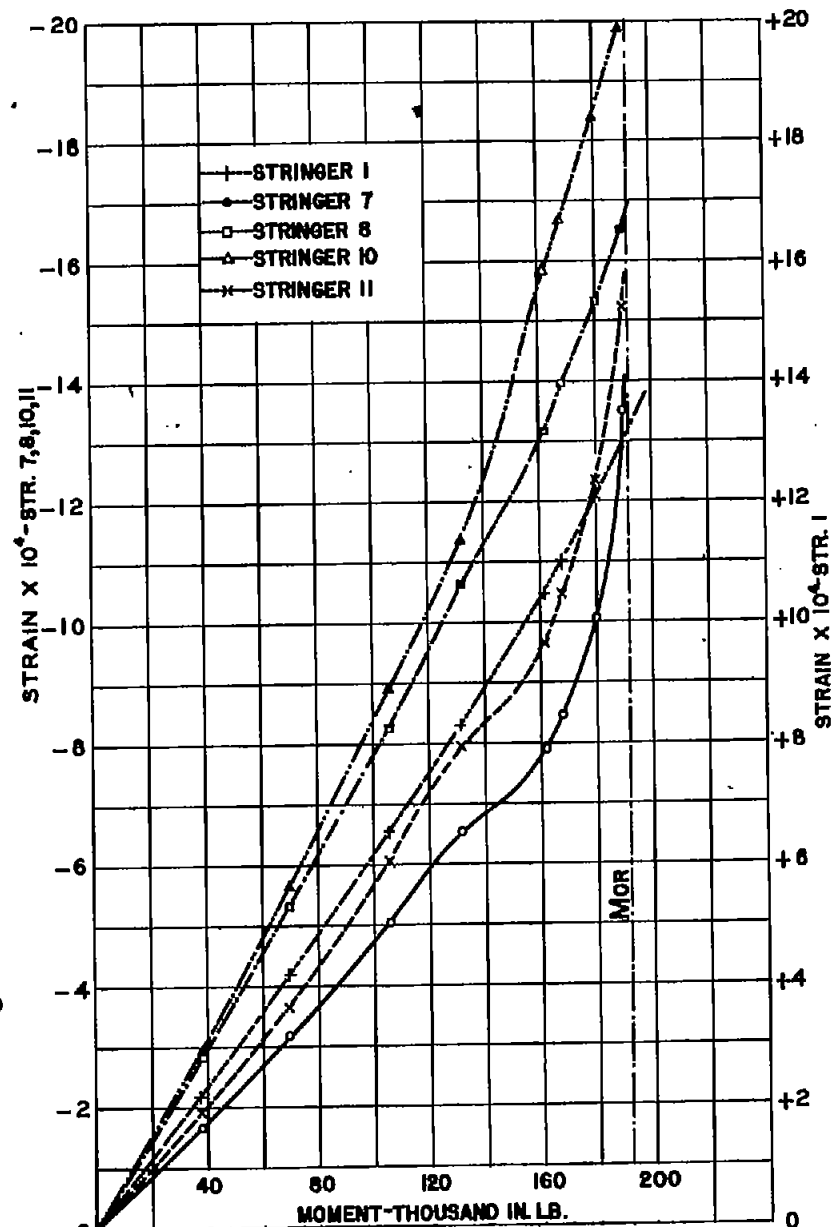
FIG.66. STRINGER STRAIN VARIATION WITH MOMENT
CYLINDER 16-BAND D
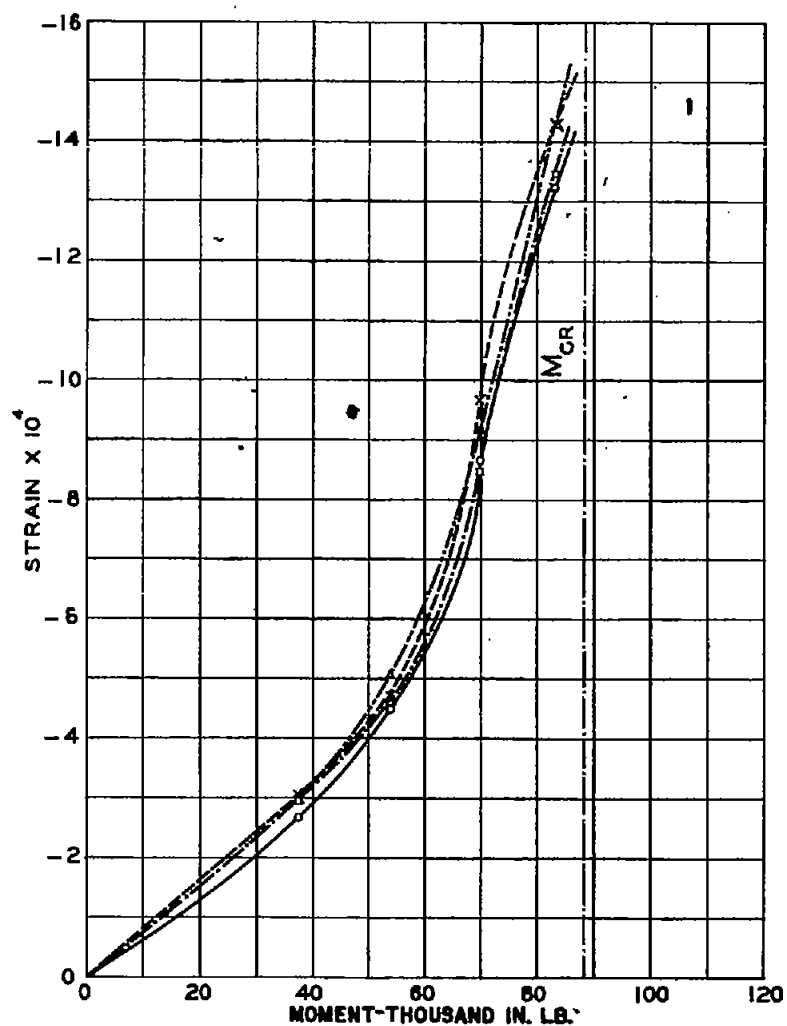
FIG.67. STRINGER STRAIN VARIATION WITH MOMENT
CYLINDER 21

—o— BAND A-STR. 5   —□— BAND A-STR. 13
—△— BAND G-STR. 5   --×-- BAND G-STR. 13
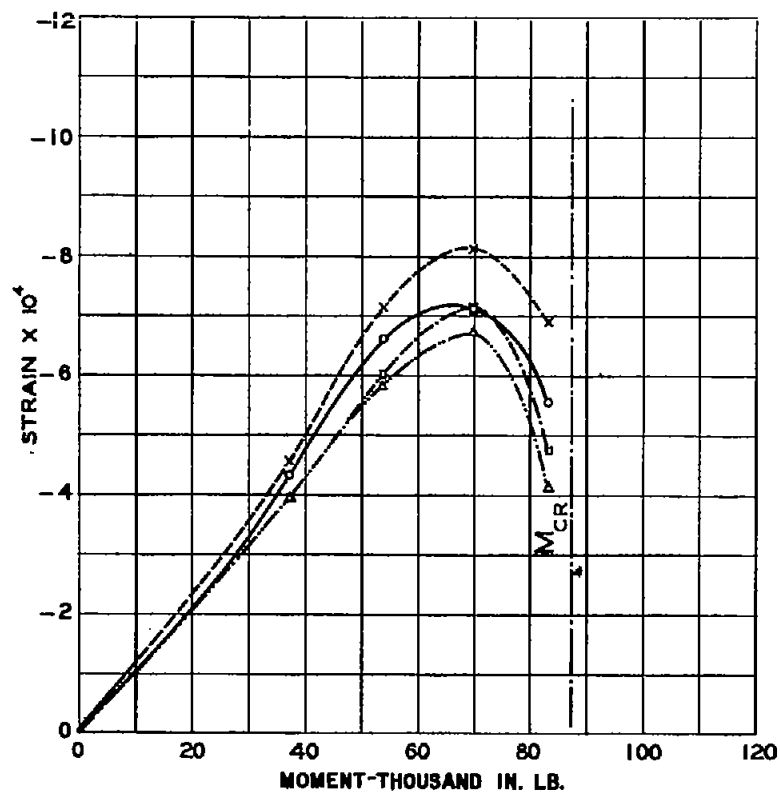
FIG.68. STRINGER STRAIN VARIATION WITH MOMENT
CYLINDER 21
—o— BAND A-STR. 6
--△-- BAND G-STR. 6
—□— BAND A-STR. 12
--×-- BAND G-STR. 12
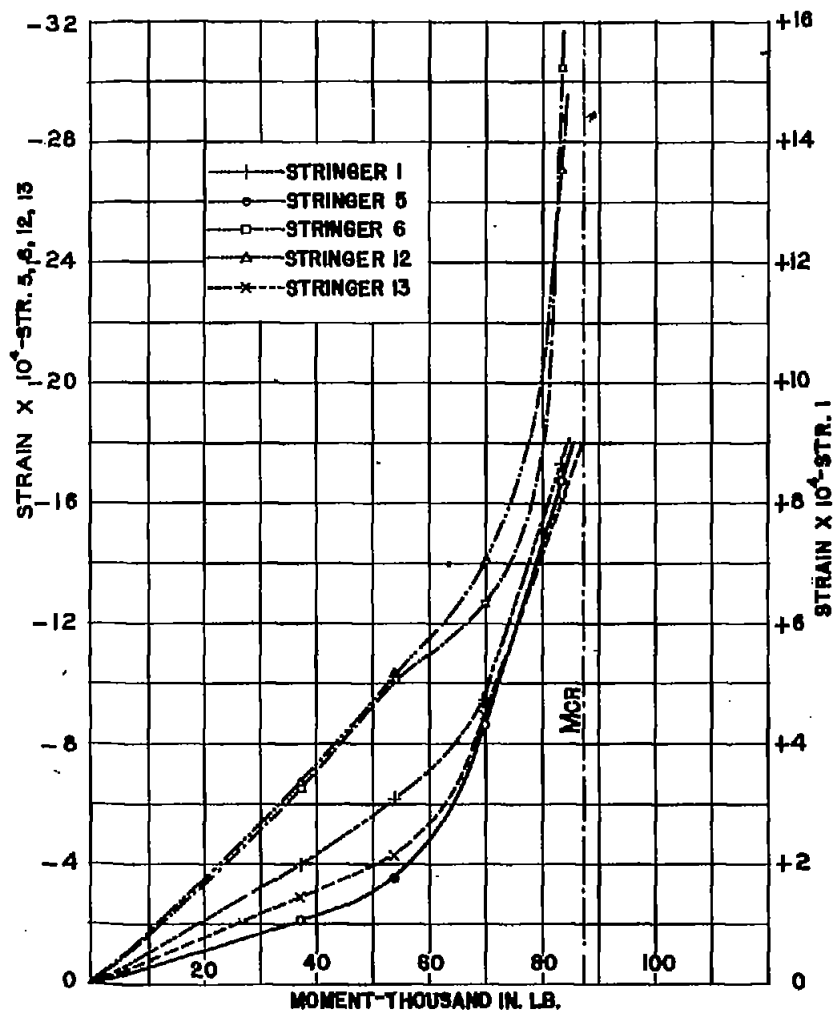
FIG.69. STRINGER STRAIN VARIATION WITH MOMENT
CYLINDER 21-BAND D

FIG.70. STRINGER STRAIN VARIATION WITH MOMENT
CYLINDER 22

STRINGER 1
STRINGER 5
STRINGER 6
STRINGER 12
STRINGER 13
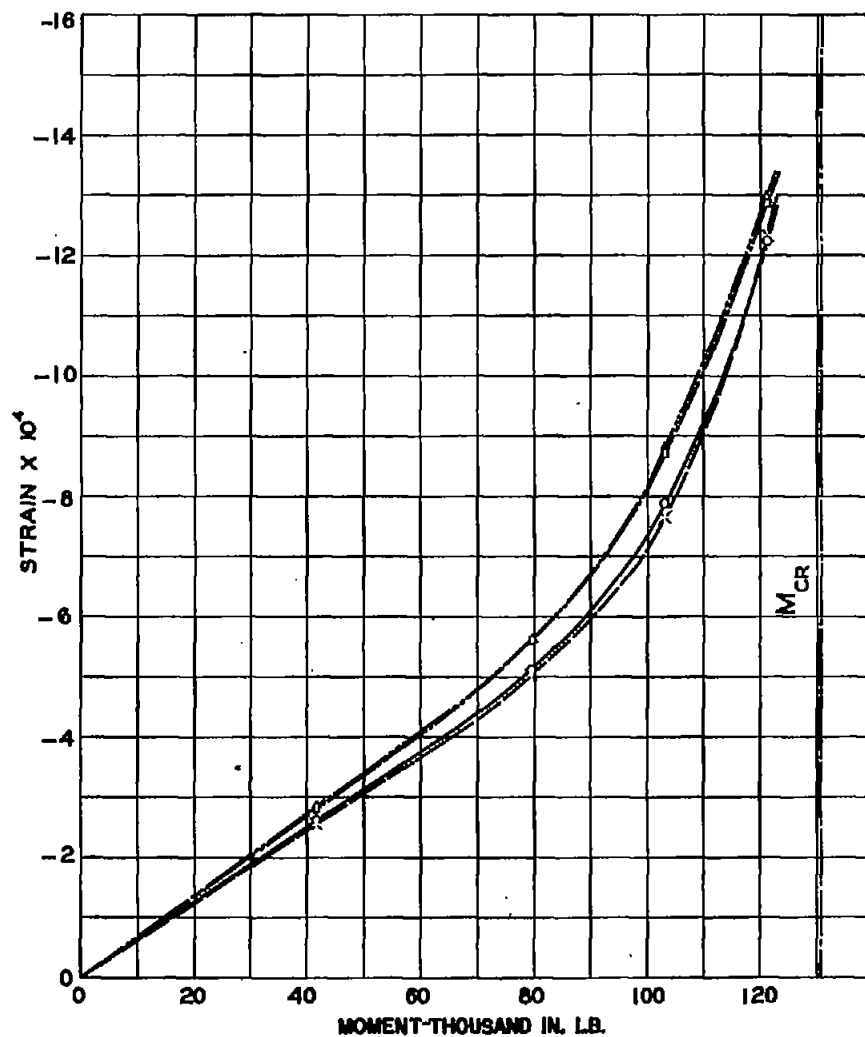
BAND A - STR. 6
BAND I - STR. 6
BAND A - STR. 12
BAND I - STR. 12
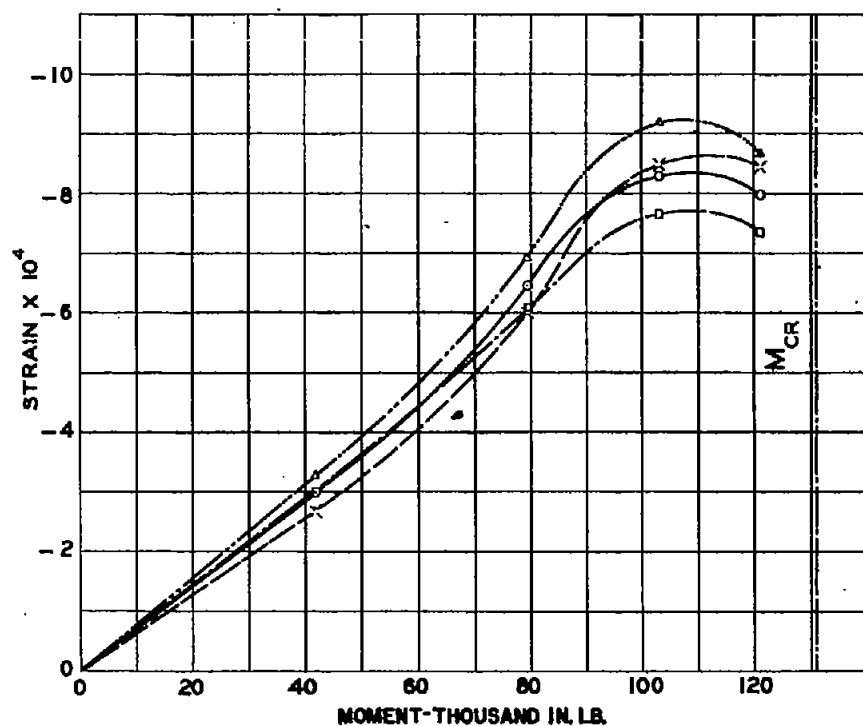
FIG.71. STRINGER STRAIN VARIATION WITH MOMENT
CYLINDER 22

—o— BAND A-STR. 7
—□— BAND I-STR. 7
--x-- BAND A-STR. 11
—△— BAND I-STR. 11
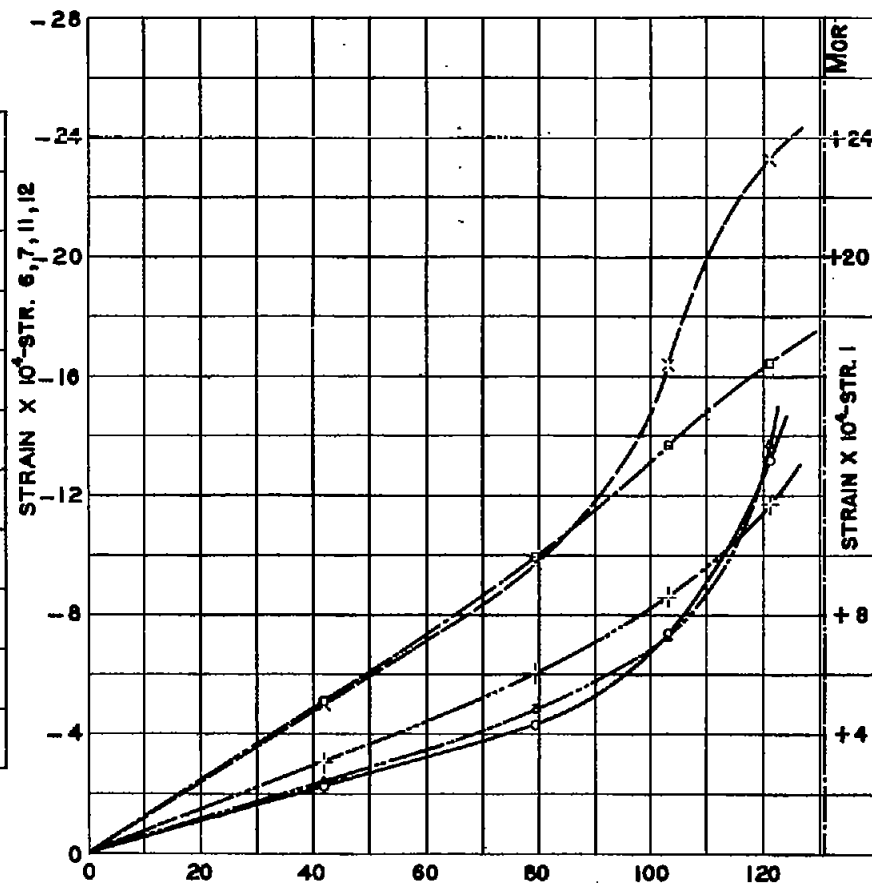
FIG.72. STRINGER STRAIN VARIATION WITH MOMENT
CYLINDER 22-BAND E

—+— STRINGER 1
—o— STRINGER 6
—□— STRINGER 7
--x-- STRINGER 11
—△— STRINGER 12
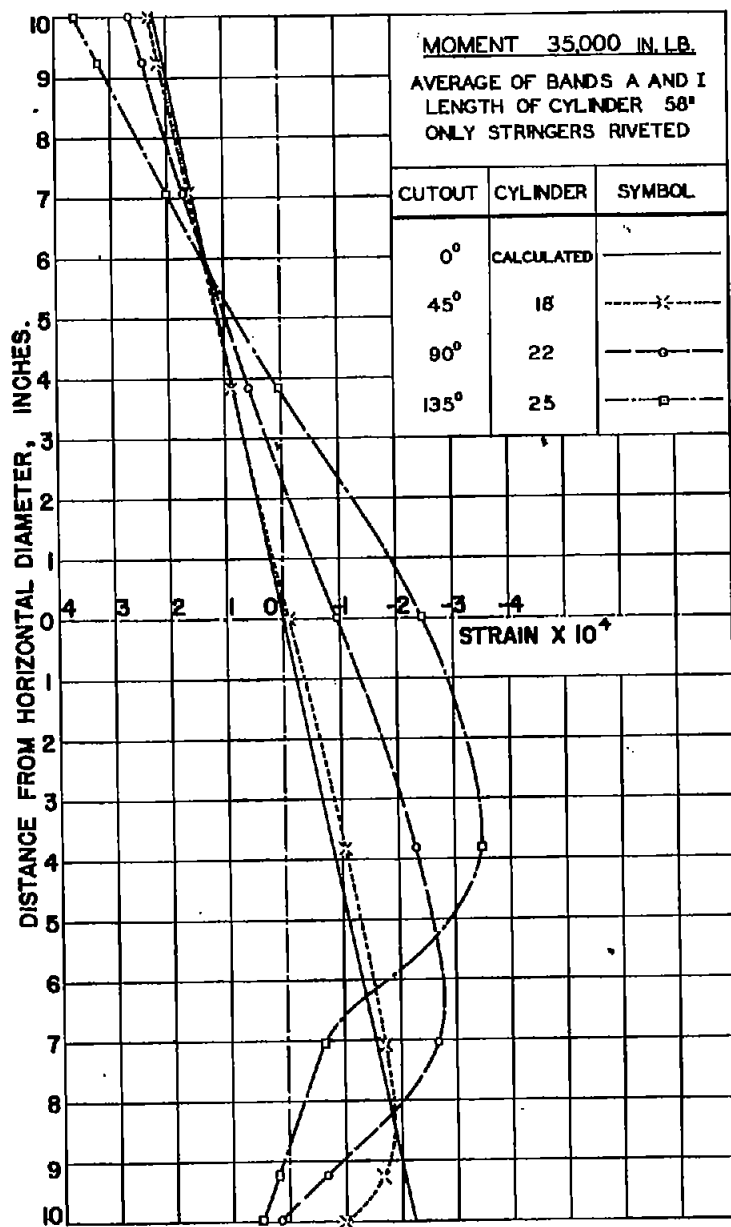
FIG. 73. EFFECT OF SIZE OF CUTOUT ON STRAIN
DISTRIBUTION — END BANDS.
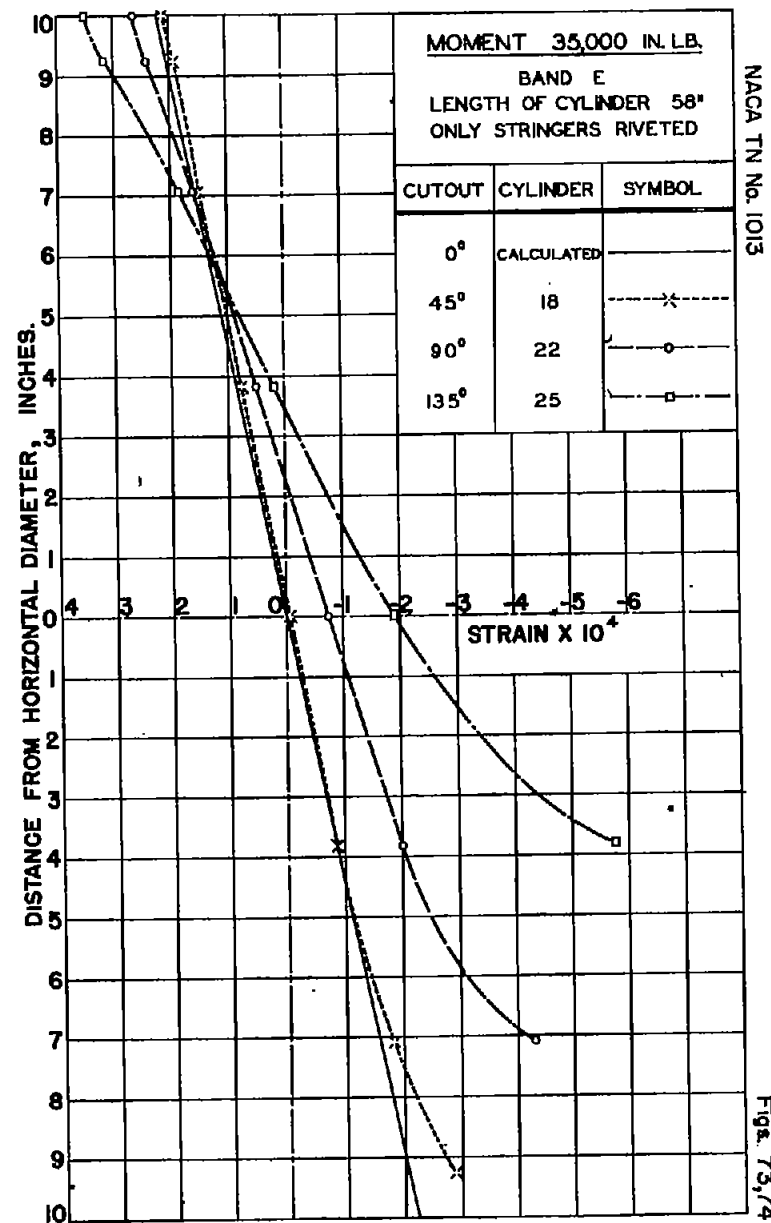
FIG. 74. EFFECT OF SIZE OF CUTOUT ON STRAIN
DISTRIBUTION — MIDDLE BANDS.

MOMENT 35000 IN. LB.

CURVE	1	NO CUTOUT
"	2	CUTOUT 45°
"	3	" 90°
"	4	" 135°

$$\epsilon = \frac{My_c}{EI_c}$$

DISTANCE FROM HORIZONTAL DIAMETER, INCHES.

STRAIN, $\epsilon \times 10^4$
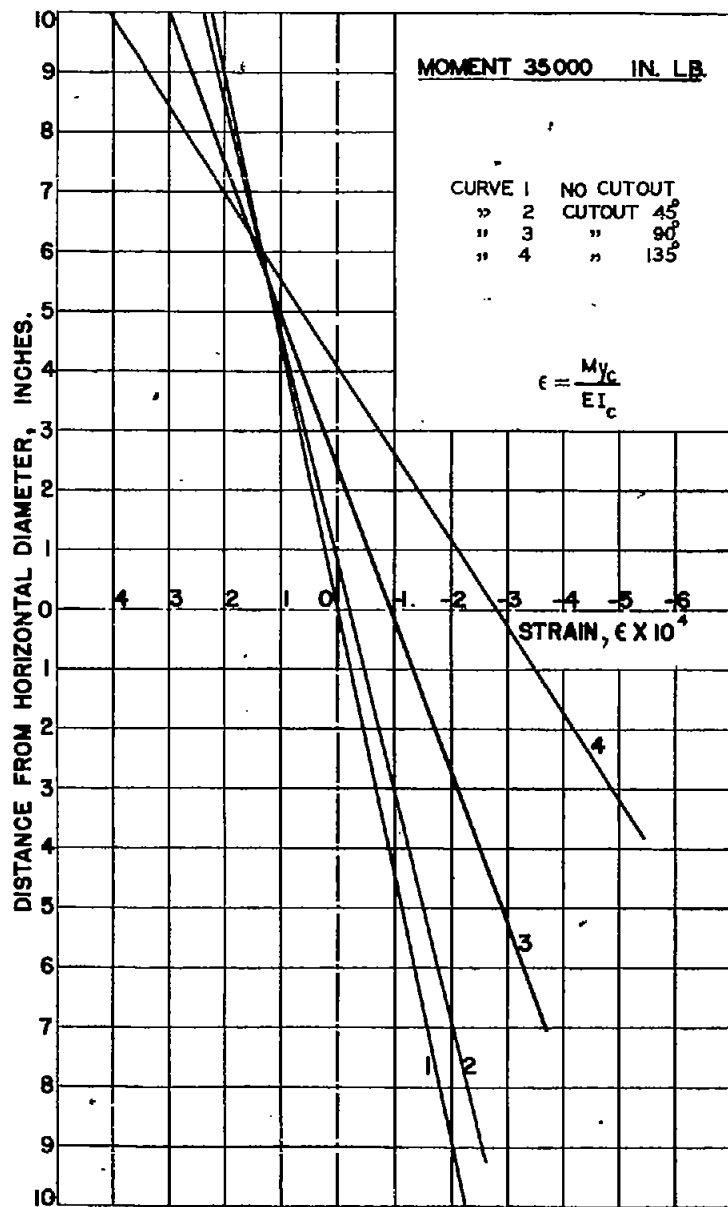
FIG. 75. EFFECT OF SIZE OF CUTOUT ON STRAIN
DISTRIBUTION — CALCULATED.

STRAIN $\times 10^4$

STR. 1
STR. 2,16
STR. 3,15
STR. 4,14
STR. 9
STR. 8,10
STR. 5,13
STR. 7,11
STR. 6,12
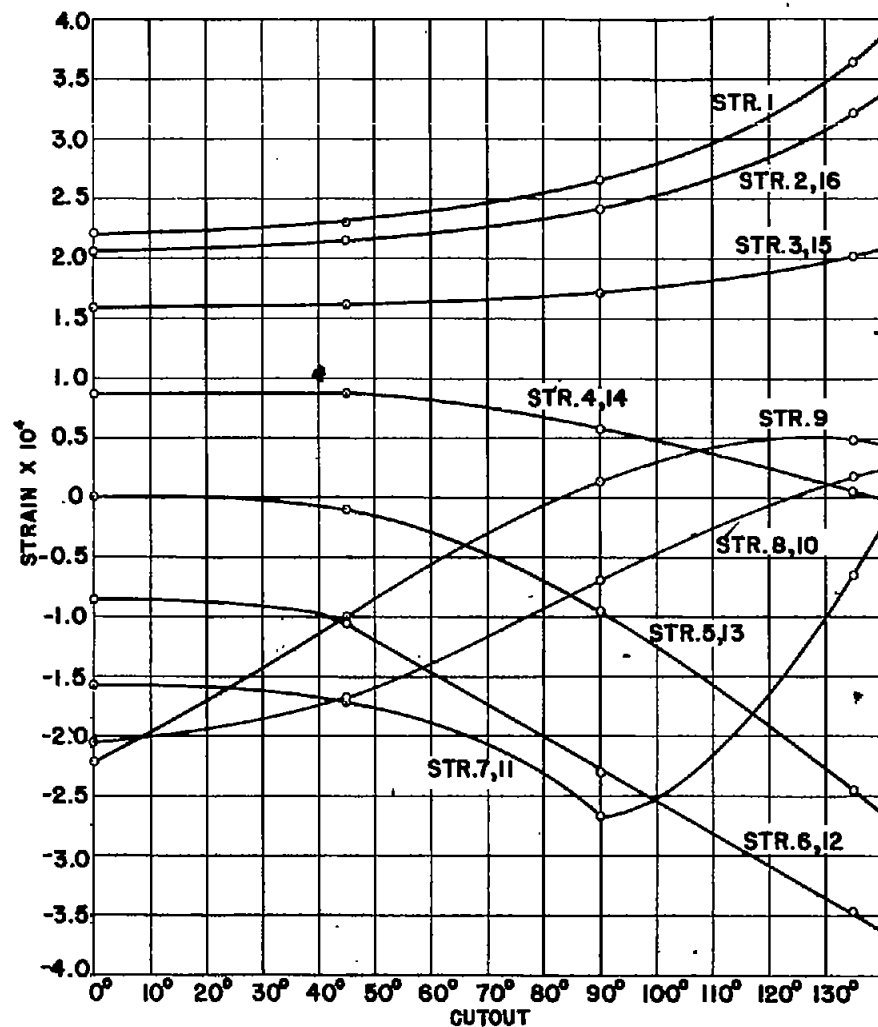
CUTOUT

FIG. 76. STRINGER STRAIN VARIATION WITH CUTOUT

END BANDS (AV. OF A, I)
CUTOUT 0°-CALCULATED
CUTOUT 45°-CYL. 18
CUTOUT 90°-CYL. 22
CUTOUT 135°-CYL. 25
MOMENT-35000 IN. LB.
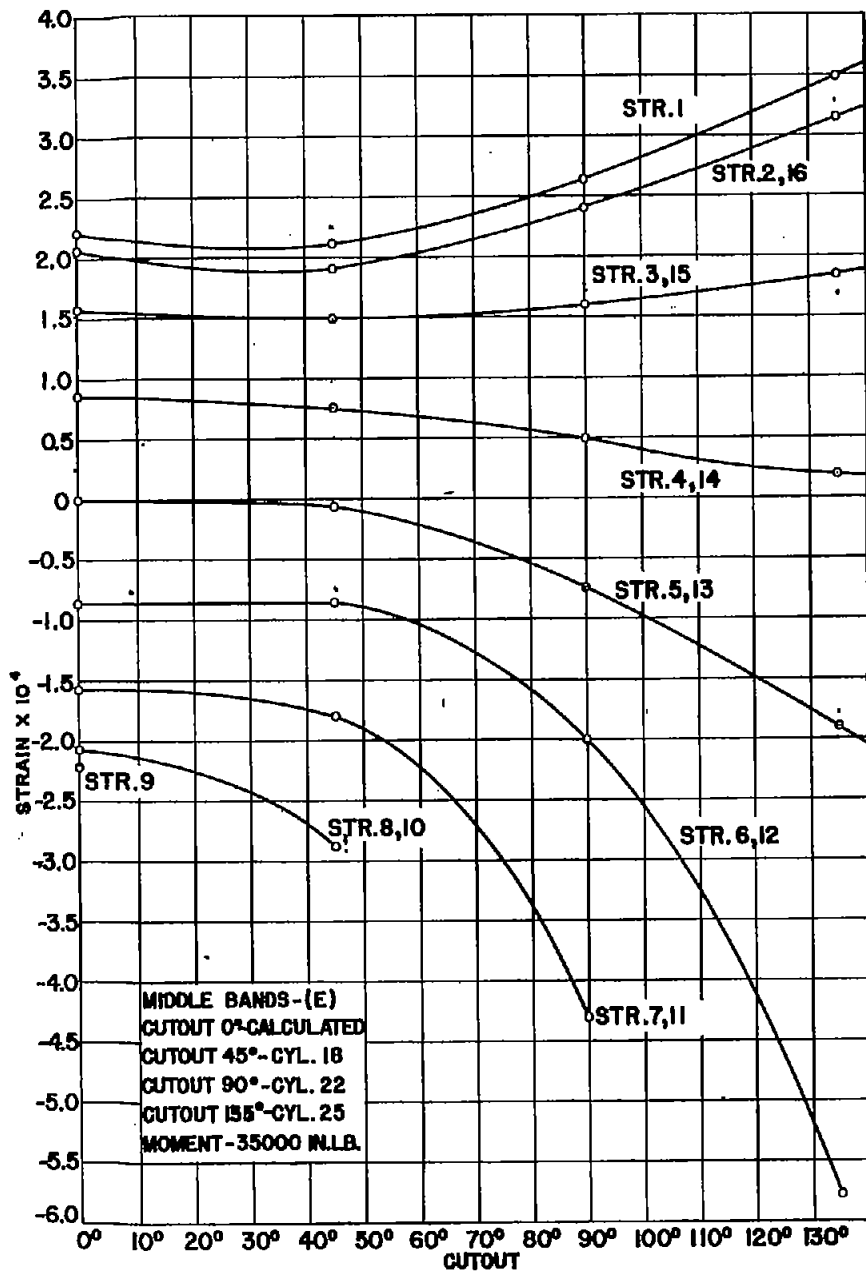
FIG. 77.   STRINGER STRAIN VARIATION WITH CUTOUT
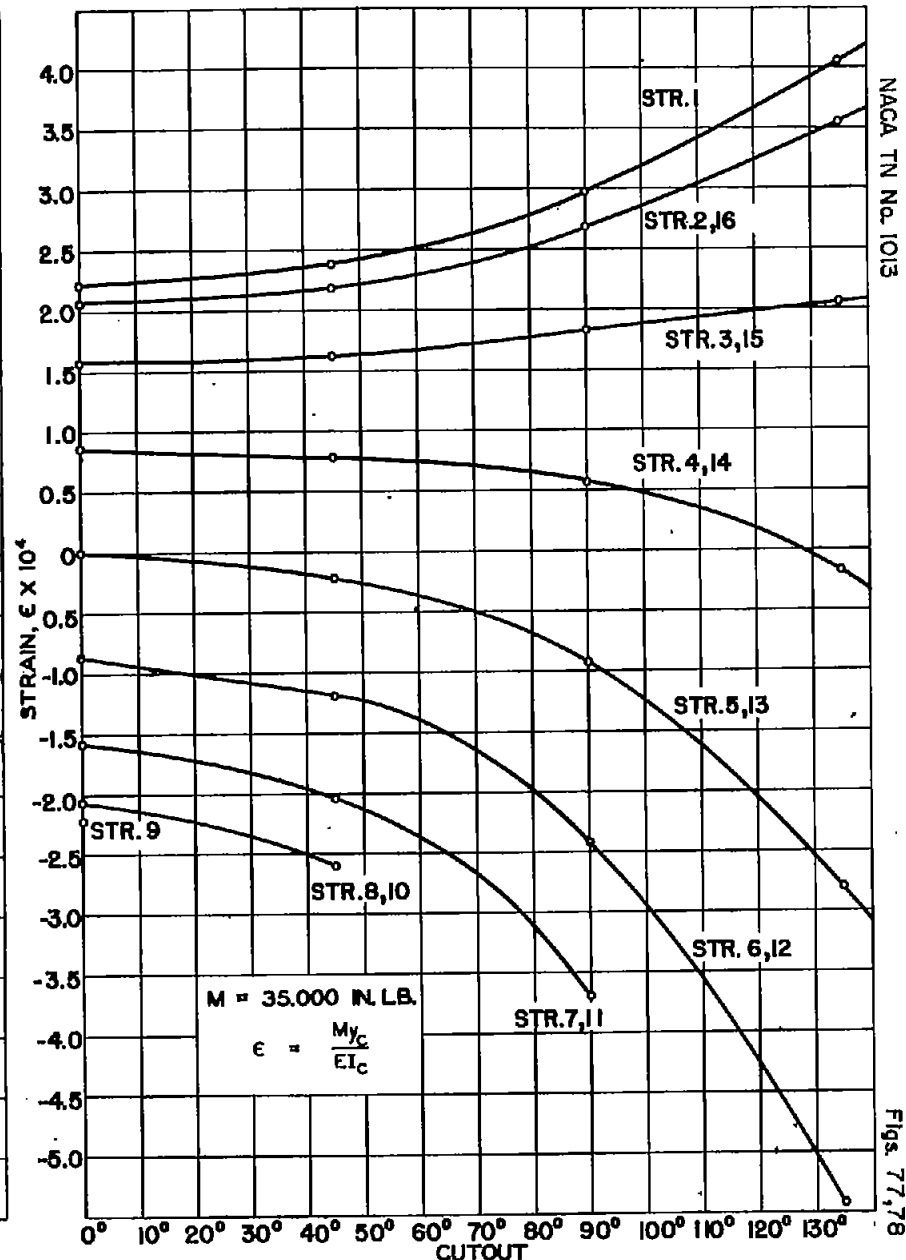
FIG. 78. CALCULATED STRINGER STRAIN VARIATION
WITH CUTOUT.

MIDDLE BANDS—(E)
CUTOUT 0°-CALCULATED
CUTOUT 45°-CYL. 18
CUTOUT 90°-CYL. 22
CUTOUT 155°-CYL. 25
MOMENT—35000 IN.LB.

$M = 35.000$ IN. LB.

$\epsilon = \dfrac{My_c}{EI_c}$

STRAIN × 10⁴

STRAIN, ϵ × 10⁴

CUTOUT

STR.1
STR.2,16
STR.3,15
STR.4,14
STR.5,13
STR.6,12
STR.7,11
STR.8,10
STR.9
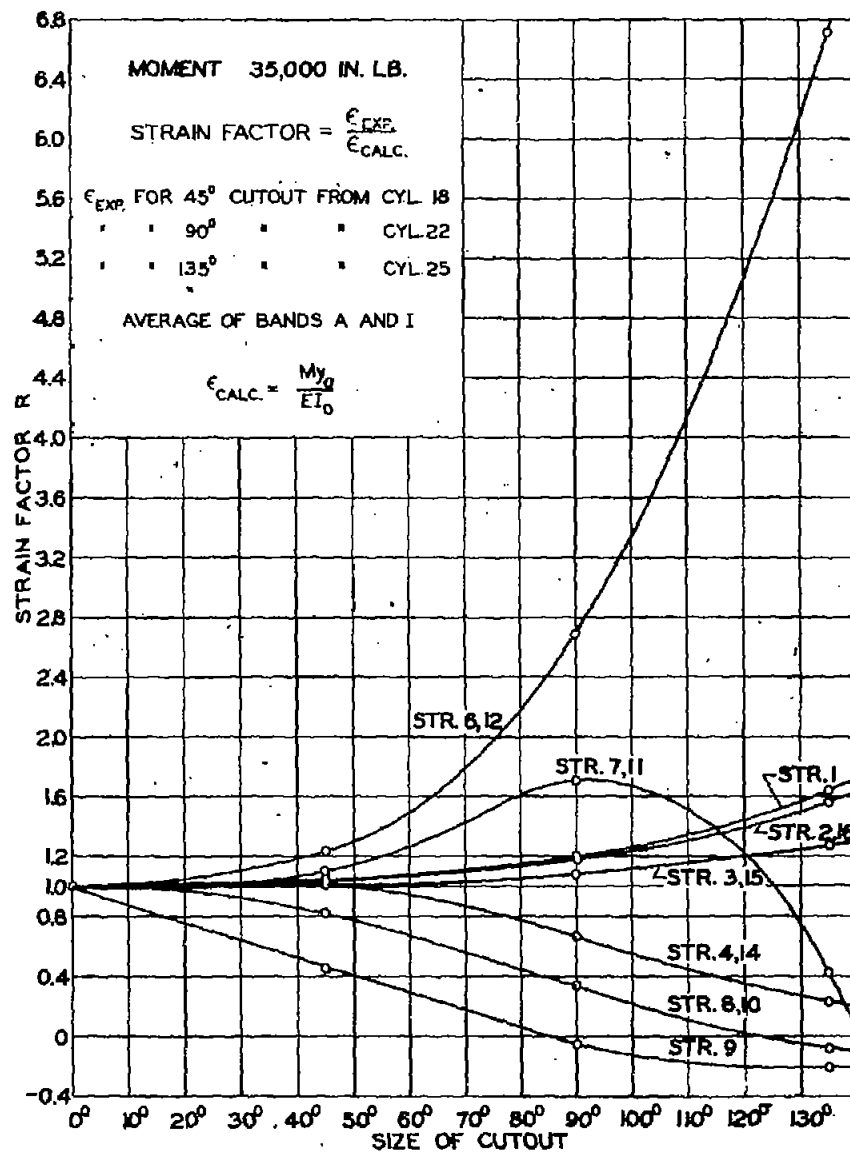
FIG. 79. STRAIN FACTORS FOR END BAND
BASED ON FULL SECTION.

FIG. 80. STRAIN FACTORS FOR MIDDLE BAND
BASED ON FULL SECTION.

FIG. 81. Chart — STRAIN FACTOR R vs SIZE OF CUTOUT

STR. 4,14
STR. 2,16
STR. 3,15
STR. 1
STR. 6,12
STR. 8,10
STR. 7,11
STR. 5,13

STRAIN FACTOR R

SIZE OF CUTOUT

0° 10° 20° 30° 40° 50° 60° 70° 80° 90° 100° 110° 120° 130°

1.2 1.1 1.0 0.9 0.8 0.7 0.6 0.5 0.4 0.3 0.2 0.1 0 -0.1 -0.2 -0.3

MOMENT   35,000 IN. LB.

$$\text{STRAIN FACTOR} = \frac{\epsilon_{EXP.}}{\epsilon_{CALC.}}$$

$\epsilon_{EXP.}$ FOR 45° CUTOUT FROM CYL. 18

"   "   90°   "   "   CYL. 22

"   "   135°   "   "   CYL. 25

AVERAGE OF BANDS A AND I

$$\epsilon_{CALC.} = \frac{My_C}{EI_C}$$
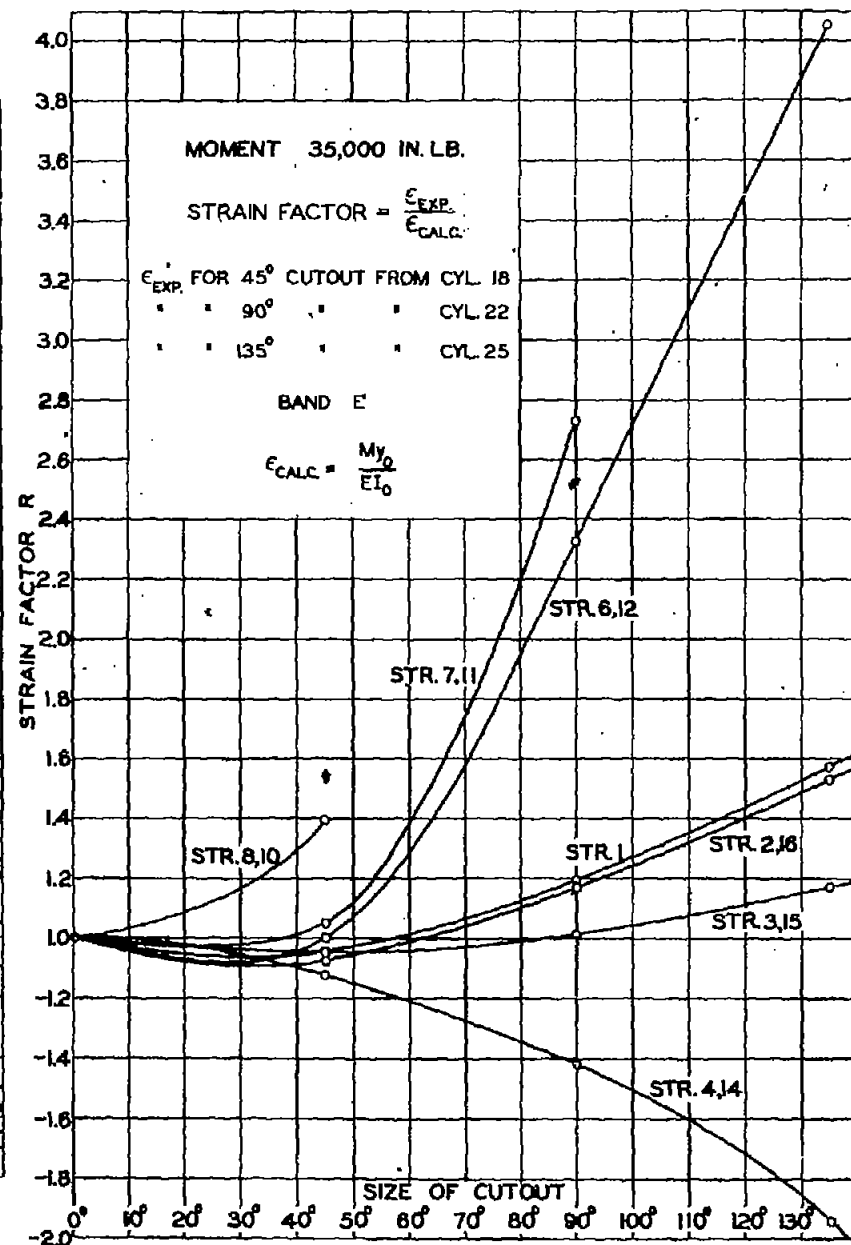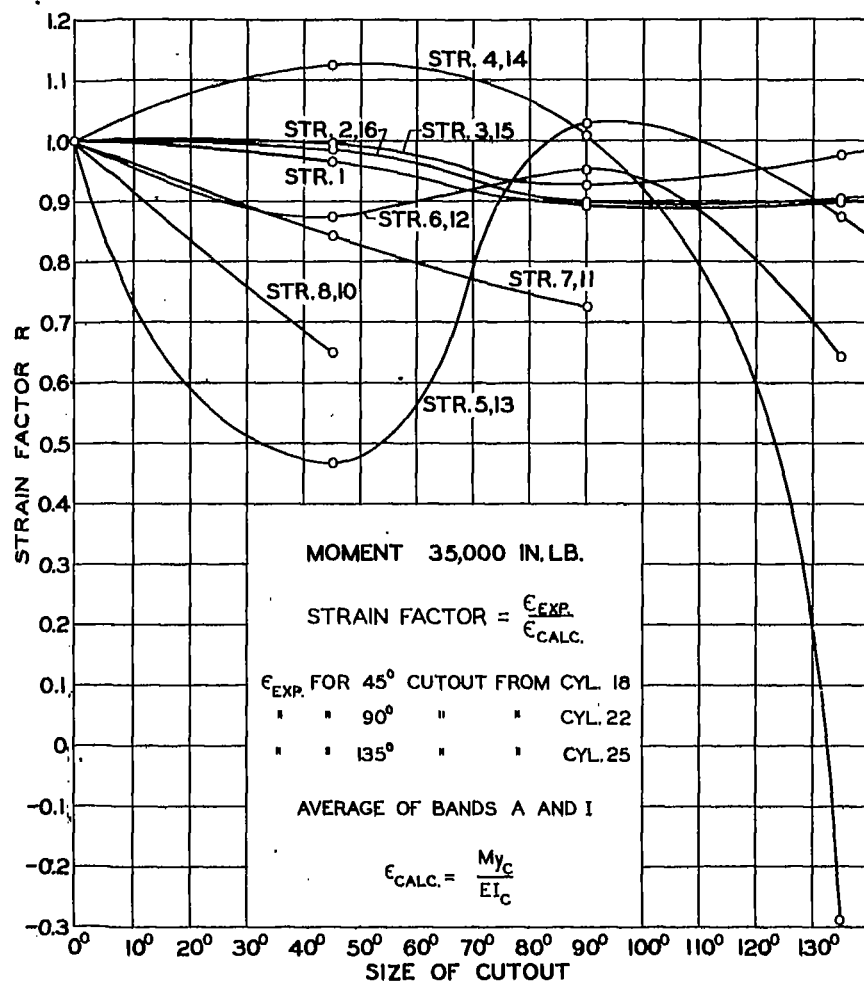
FIG. 81.   STRAIN FACTORS FOR END BAND
BASED ON SECTION WITH CUTOUT.

FIG. 82. Chart — STRAIN FACTOR R vs SIZE OF CUTOUT

STR. 8,10
STR. 3,15
STR. 7,11
STR. 1
STR. 2,16
STR. 6,12
STR. 5,13
STR. 4,14

STRAIN FACTOR R

SIZE OF CUTOUT

0° 10° 20° 30° 40° 50° 60° 70° 80° 90° 100° 110° 120° 130°

1.2 1.1 1.0 0.9 0.8 0.7 0.6 0.5 0.4 0.3 0.2 0.1 0 -0.1 -0.2 -0.3 -0.4 -0.5 -0.6 -0.7 -0.8 -0.9 -1.0 -1.1 -1.2

MOMENT   35,000 IN. LB.

$$\text{STRAIN FACTOR} \approx \frac{\epsilon_{EXP.}}{\epsilon_{CALC.}}$$

$\epsilon_{EXP.}$ FOR 45° CUTOUT FROM CYL. 18

"   "   90°   "   "   CYL. 22

"   "   135°   "   "   CYL. 25

BAND E

$$\epsilon_{CALC.} = \frac{My_C}{EI_C}$$
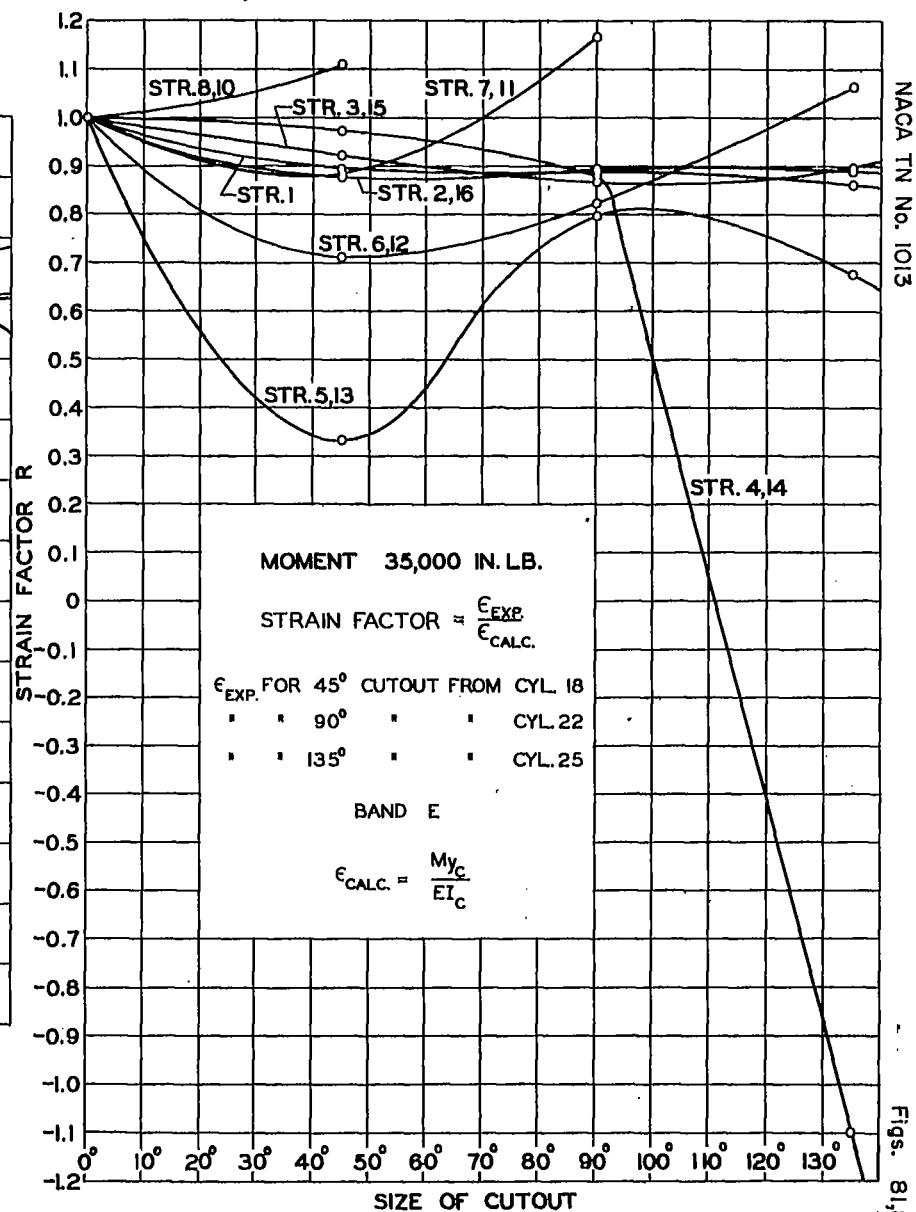
FIG. 82.   STRAIN FACTORS FOR MIDDLE BAND
BASED ON SECTION WITH CUTOUT.
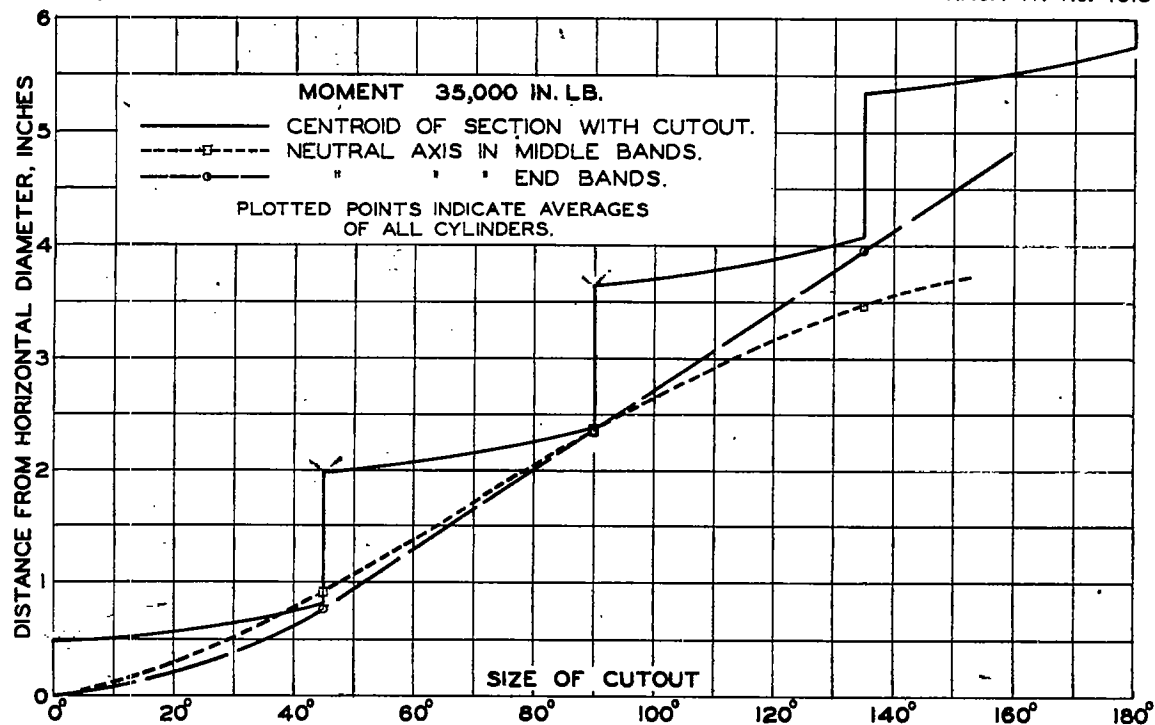
FIG. 83. EFFECT OF SIZE OF CUTOUT ON LOCATION OF NEUTRAL AXIS.
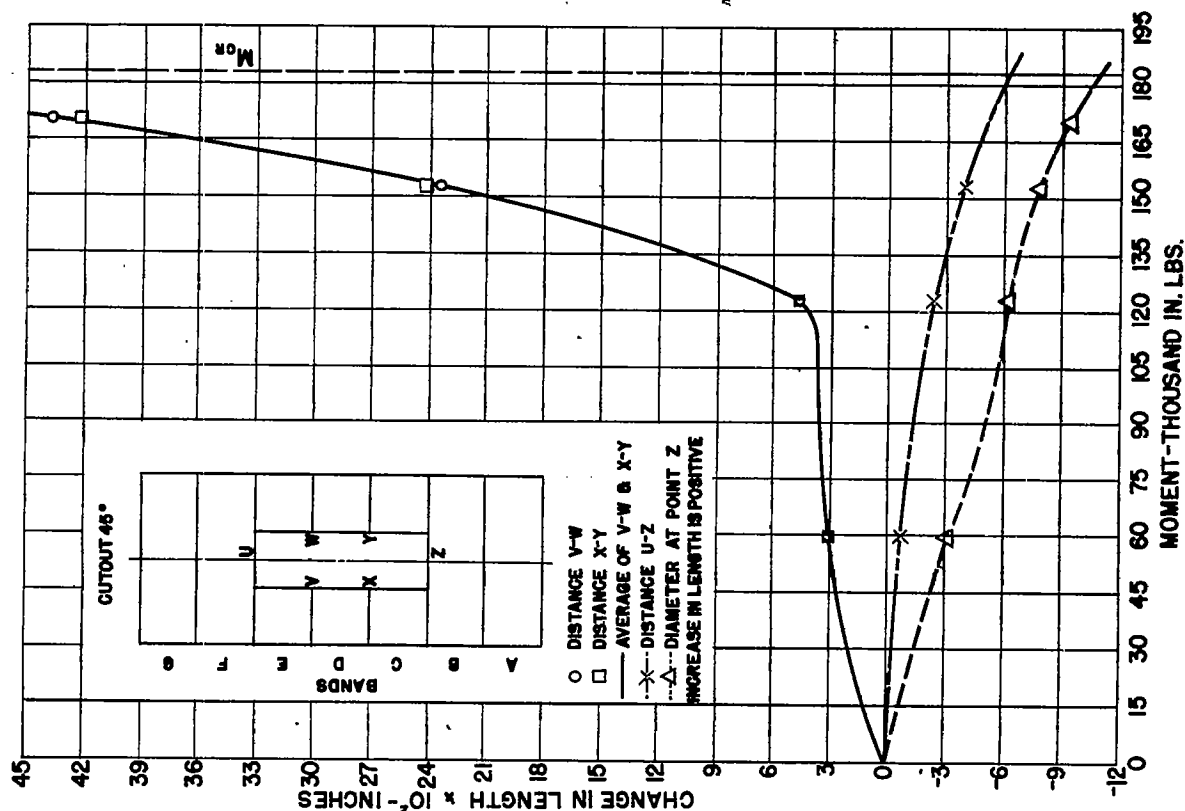
FIG. 84.

VARIATION IN DIMENSIONS OF CYLINDER 16 WITH MOMENT

FIG. 85.

CUTOUT 45°

BANDS

G
F
E
D
C
B
A

U
V W
X Y
Z

CHANGE IN LENGTH x 10^2 - INCHES

45
42
39
36
33
30
27
24
21
18
15
12
9
6
3
0
-3
-6
-9
-12

O   DISTANCE V-W
□   DISTANCE X-Y
—— AVERAGE OF V-W & X-Y
-X- DISTANCE U-Z
-△- DIAMETER AT POINT Z
INCREASE IN LENGTH IS POSITIVE

M$_{cr}$

0   15   30   45   60   75   90   105 120 135 150 165 180 195

MOMENT - THOUSAND IN. LBS.
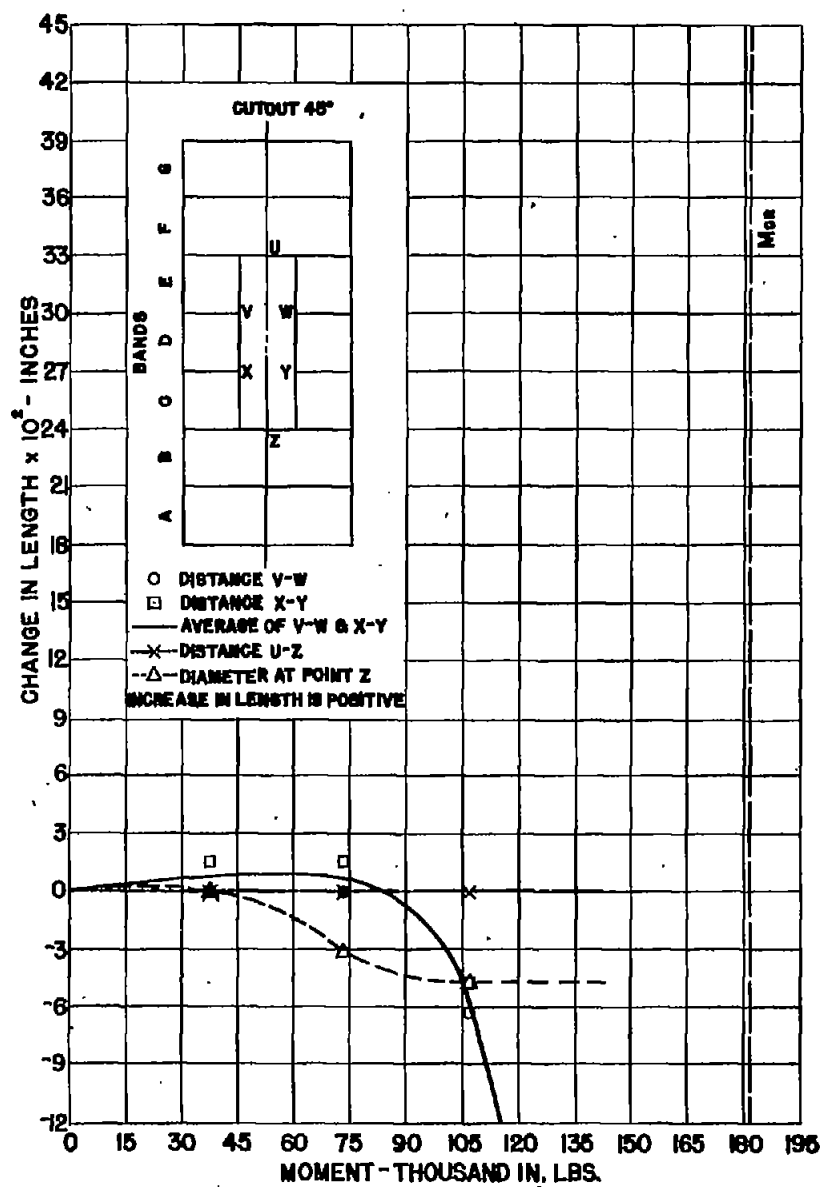
FIG. 85.

VARIATION IN DIMENSIONS OF CYLINDER 20 WITH MOMENT

CUTOUT	SYMBOL	CYLINDER	AVE. MAX. MOMENT
0°	—X—	11	289,000
45°	—△—	16,17,18,20	192,800
90°	---o---	19,22,23	135,800
135°	—□—	21,24,25	89,500

STRAIN X 10^4

-40
-38
-36
-34
-32
-30
-28
-26
-24
-22
-20
-18
-16
-14
-12
-10
-8
-6
-4
-2
0

PERCENTAGE OF M$_{CR.}$

10   20   30   40   50   60   70   80   90   100

FIG. 86. VARIATION WITH MOMENT OF MAXIMUM EXPERIMENTAL STRAIN.

STRAIN X10^4

SIZE OF CUTOUT, DEGREES

% OF M$_{CR}$

50	100	150	200	250	M FOR 0°
25	50	75	100	125	150	175	M FOR 45°
20	40	60	80	100	120	M FOR 90°
10	20	30	40	50	60	70	80	M FOR 135°

MOMENTS GIVEN IN THOUSAND IN. LB.

CURVES REPRESENT AVERAGE OF CYLINDERS 11 AND 16-25.

FIG. 87. EFFECT OF CUTOUT AND MOMENT
ON MAXIMUM EXPERIMENTAL STRAIN.

STRAIN X10^4

SIZE OF CUTOUT, DEGREES

% OF M$_{CR}$

50	100	150	200	250	M FOR 0°
25	50	75	100	125	150	175	M FOR 45°
20	40	60	80	100	120	M FOR 90°
10	20	30	40	50	60	70	80	M FOR 135°

MOMENTS GIVEN IN THOUSAND IN. LB.

AVERAGE OF EXPERIMENTAL M$_{CR}$ USED
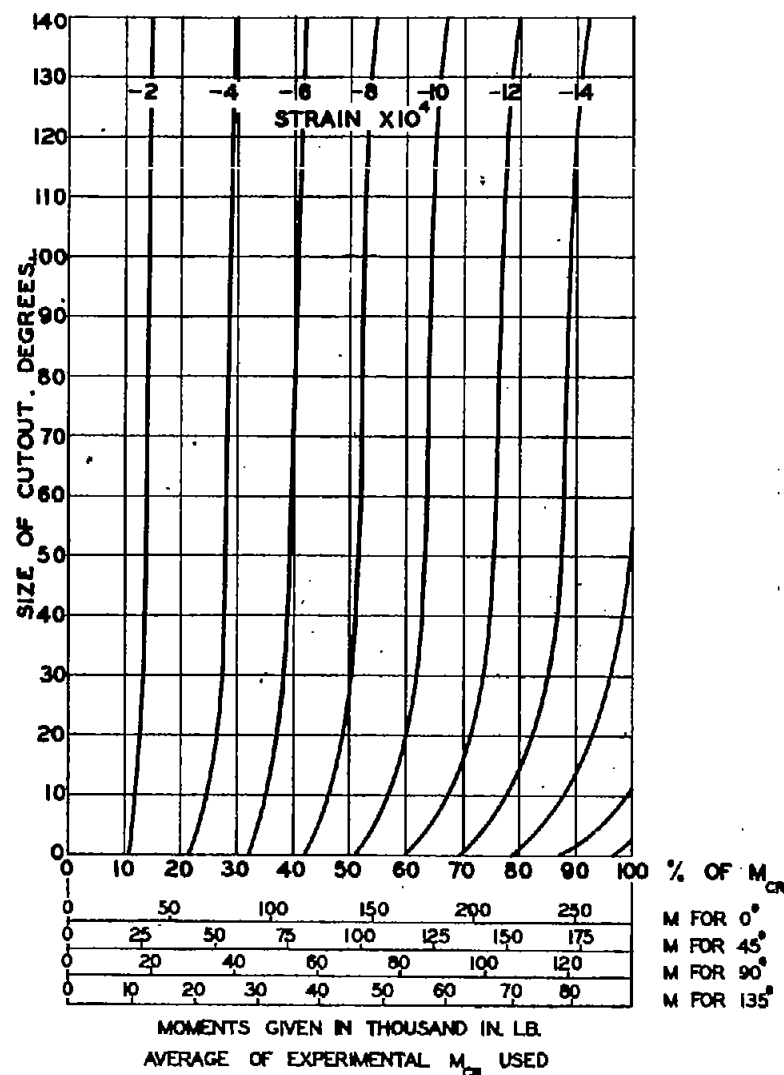
FIG. 88. CALCULATED EFFECT OF
CUTOUT AND MOMENT ON MAXIMUM STRAIN.

STRAIN FACTOR $= \dfrac{\text{MAX. } \epsilon_{\text{EXP.}}}{\text{MAX. } \epsilon_{\text{CALC.}}}$

$\epsilon_{\text{EXP.}}$—AVERAGE OF CYL.11 AND 16-25.

$\epsilon_{\text{CALC.}} = \dfrac{M y_c}{E I_c}$

AVERAGE OF EXPERIMENTAL $M_{\text{CR.}}$ USED.

CUTOUT 0° $M_{\text{CR.}}=$ 289,000 IN.LB.
CUTOUT 45° $M_{\text{CR.}}=$ 192,800 IN.LB.
CUTOUT 90° $M_{\text{CR.}}=$ 135,800 IN.LB.
CUTOUT 135° $M_{\text{CR.}}=$ 89,500 IN.LB.
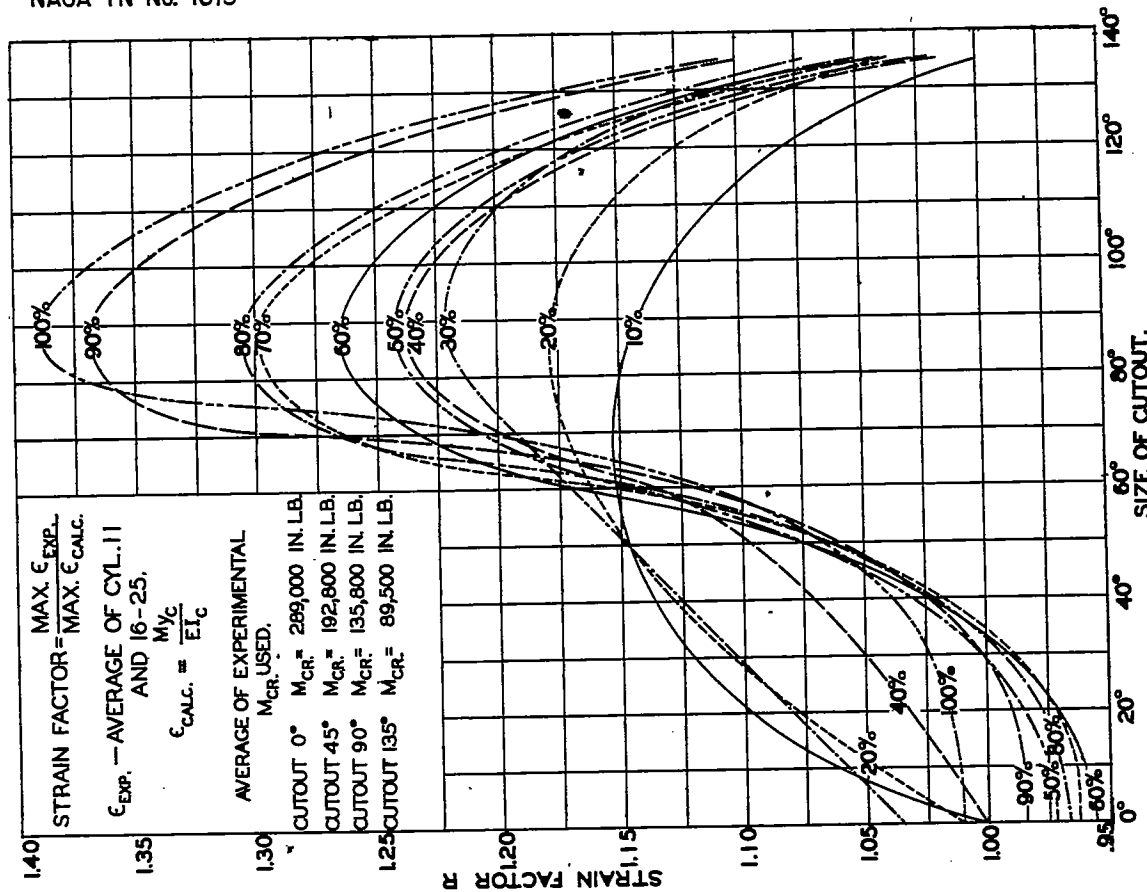
FIG. 89. STRAIN FACTORS.
PERCENTAGE OF MAXIMUM MOMENT INDICATED ON CURVES.
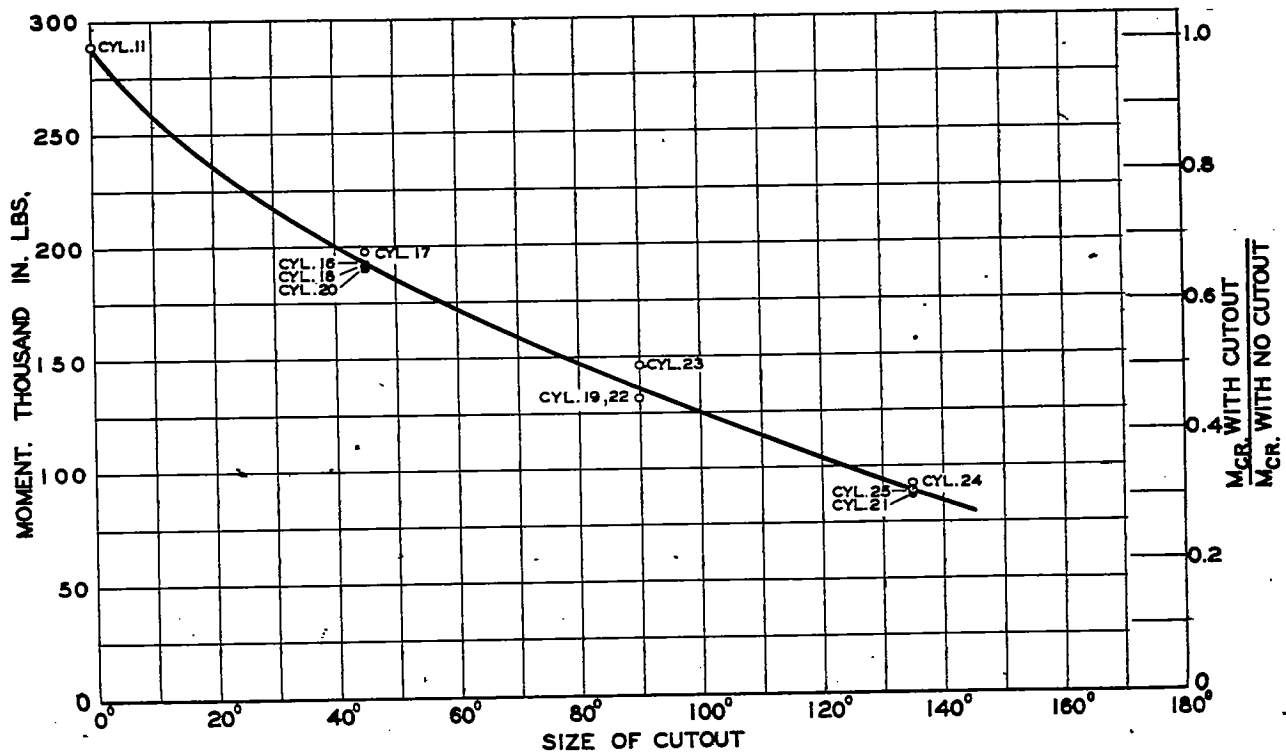
FIG.90. EFFECT OF SIZE OF CUTOUT ON CRITICAL MOMENT.
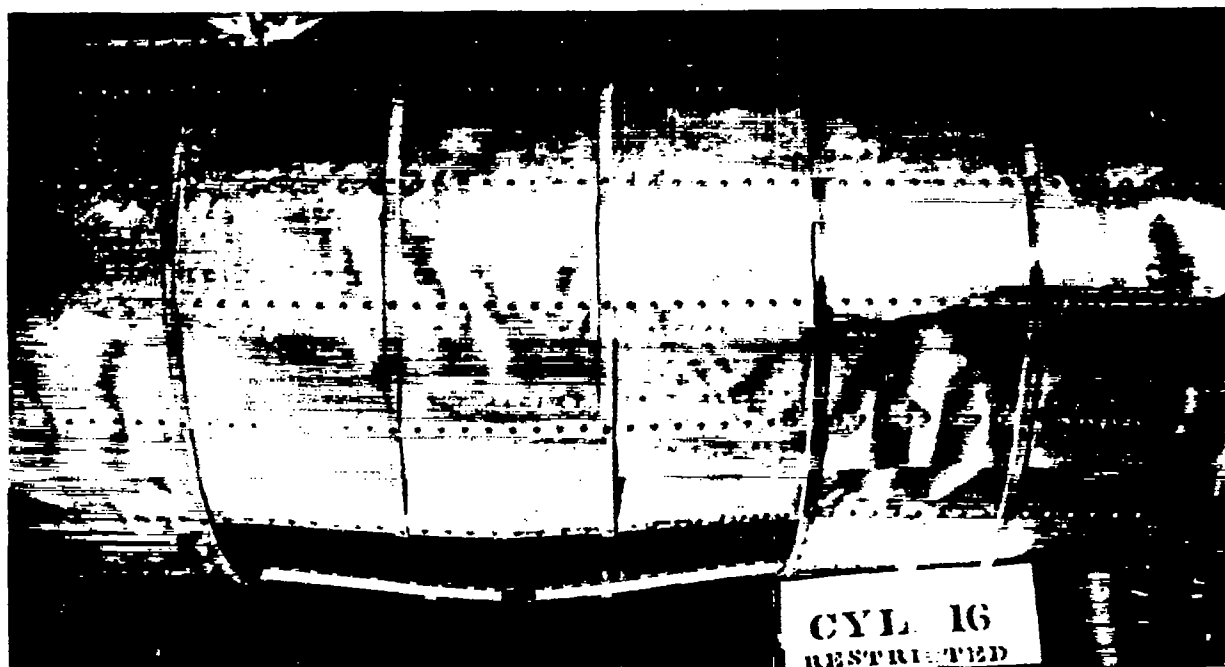
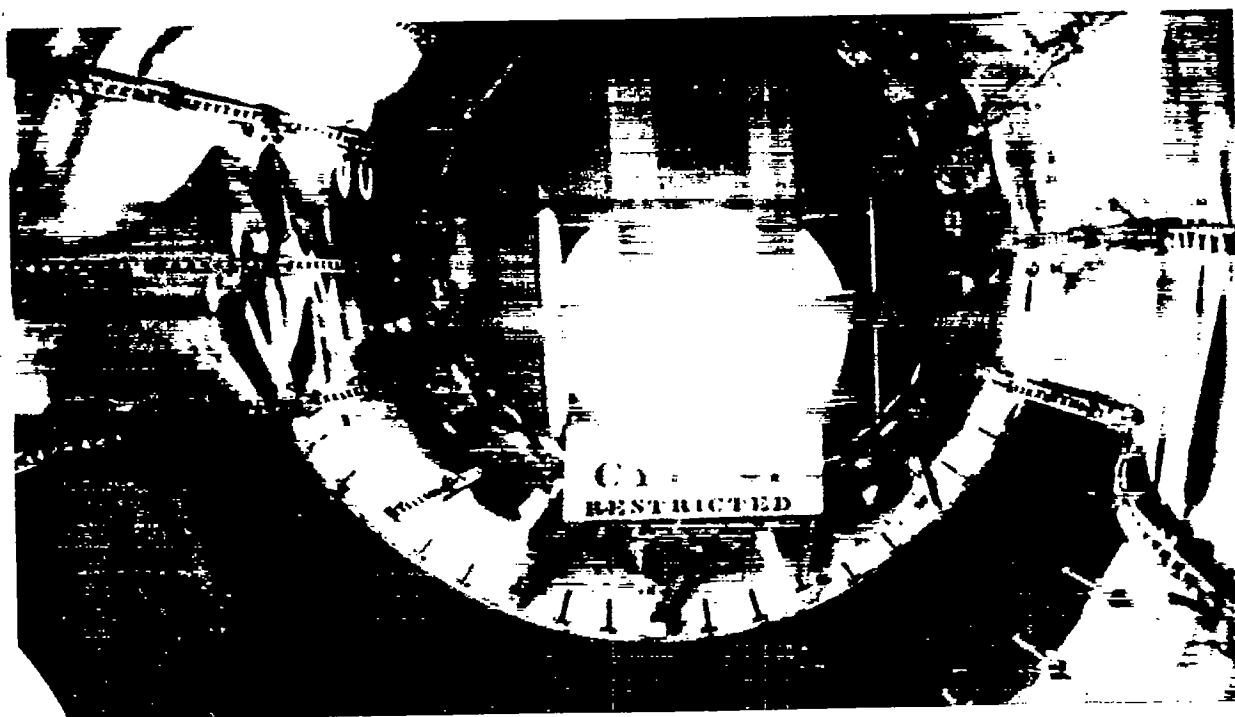Figure 91.- Side view of cylinder 16 after buckling.
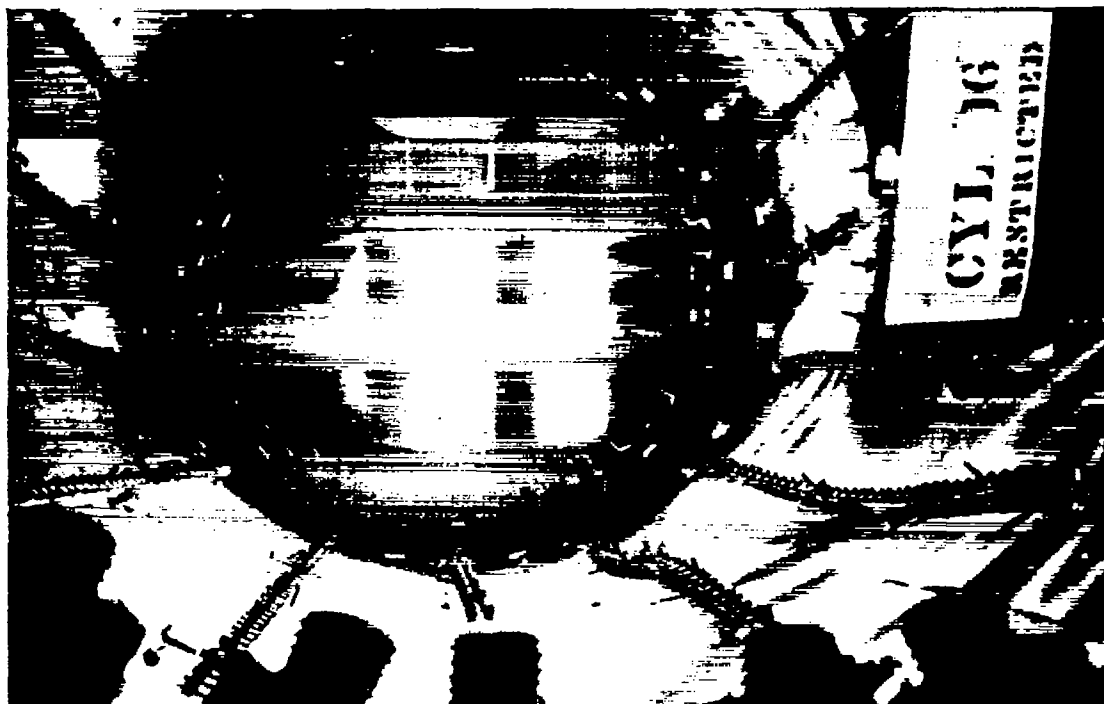
Figure 92.- Inside view of cylinder 16 after buckling.
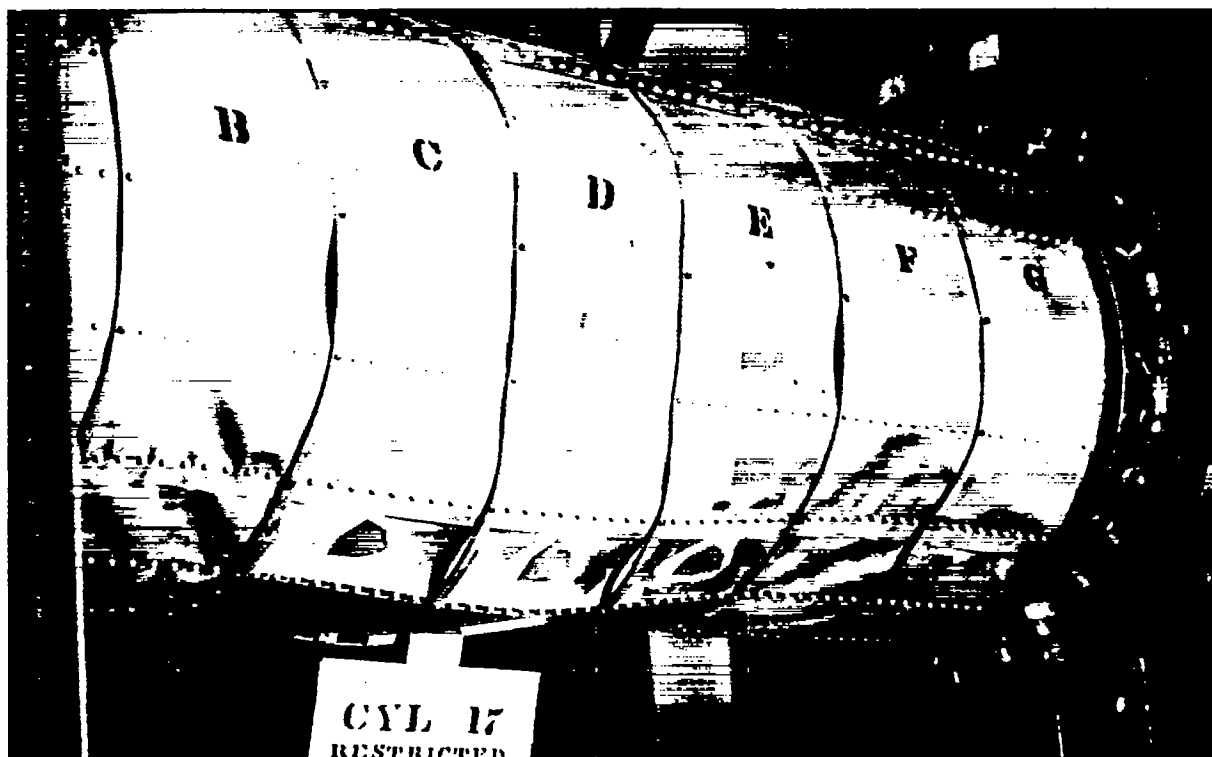
Figure 93.- Side view of cylinder 17 after buckling.
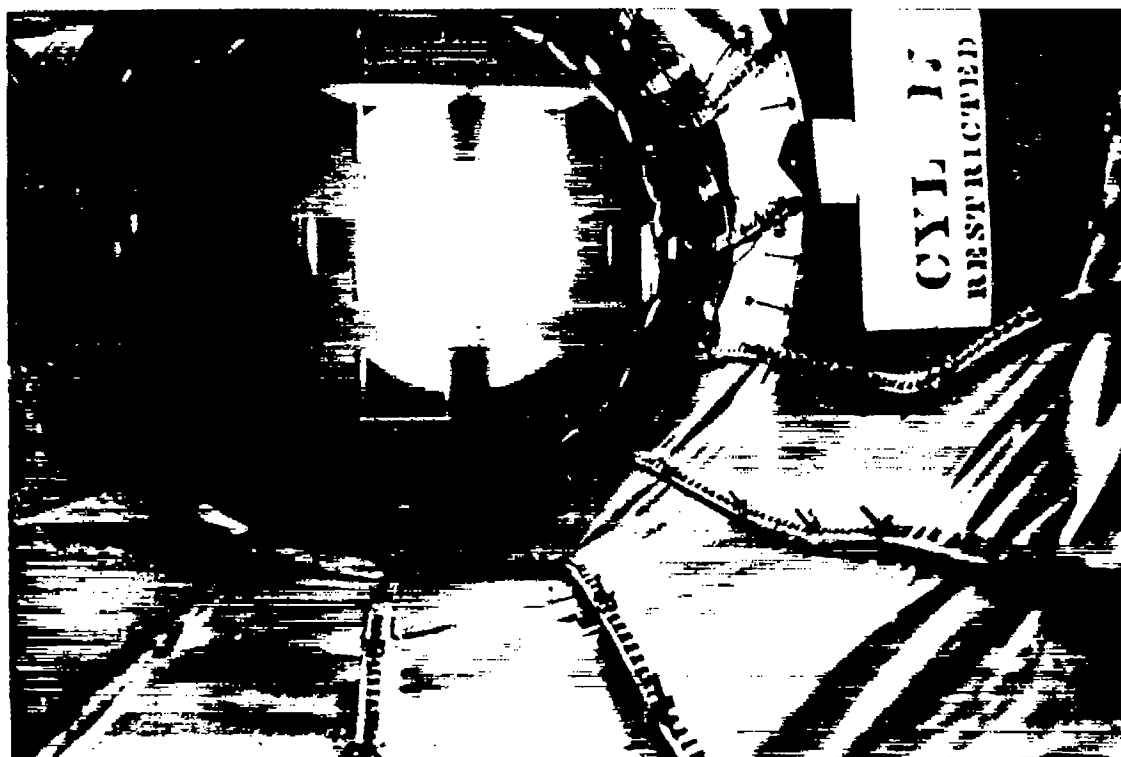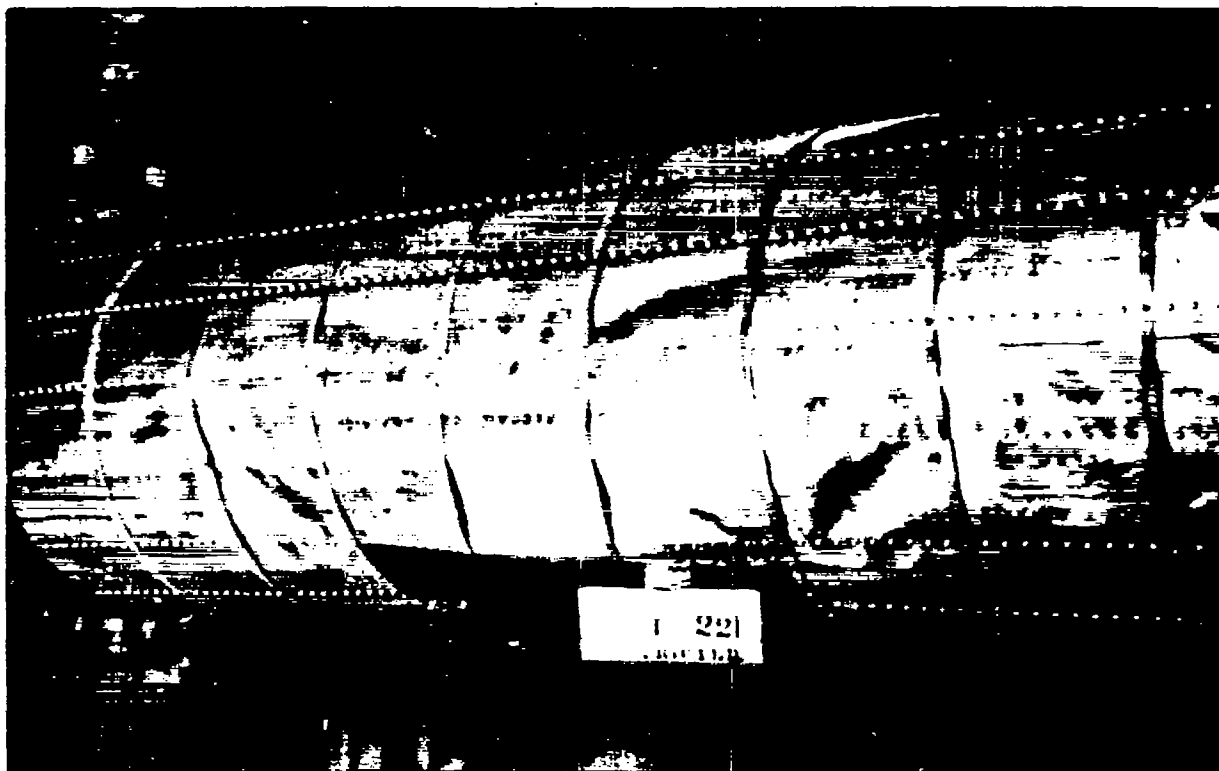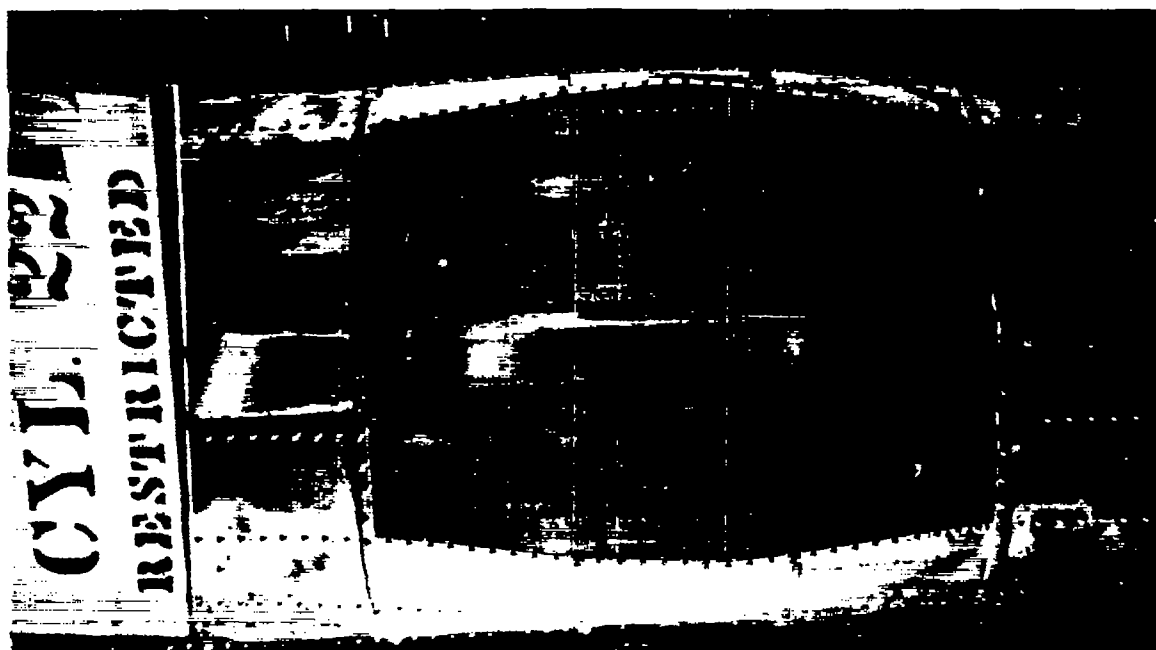

Figure 94.- Inside view of cylinder 17 after buckling.
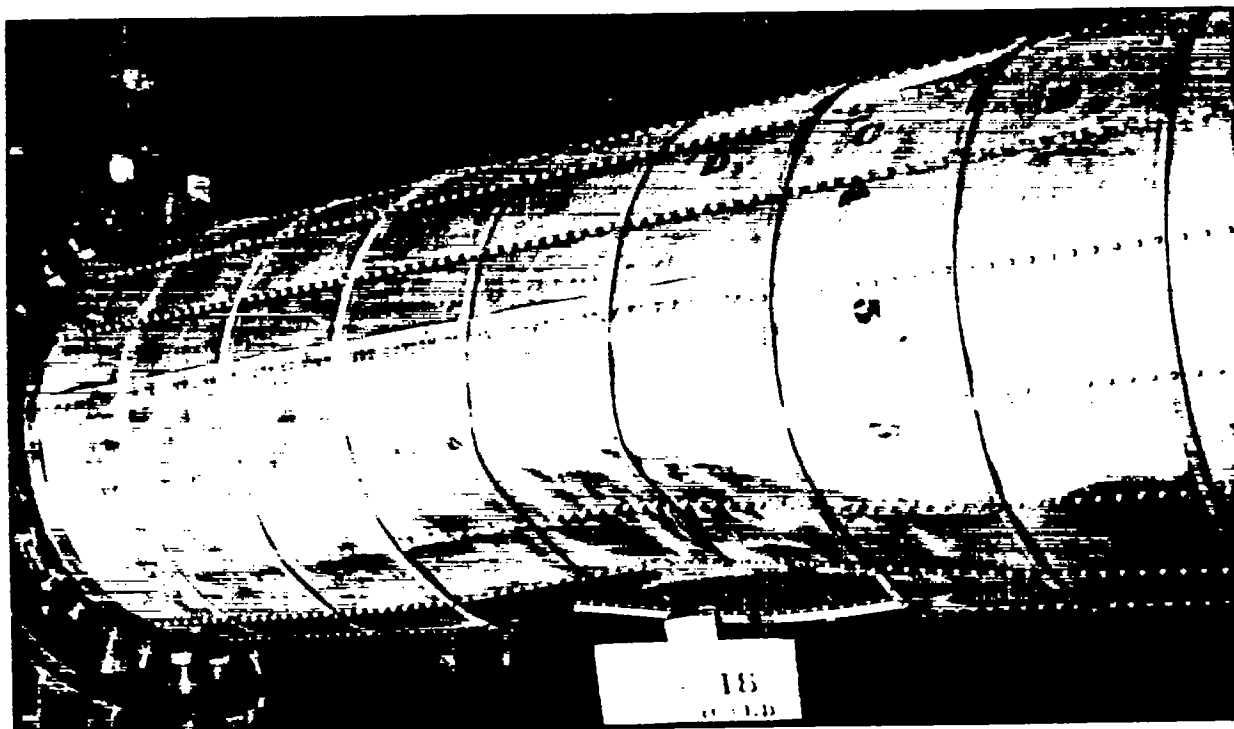
Figure 95.- Side view of cylinder 18 after buckling.
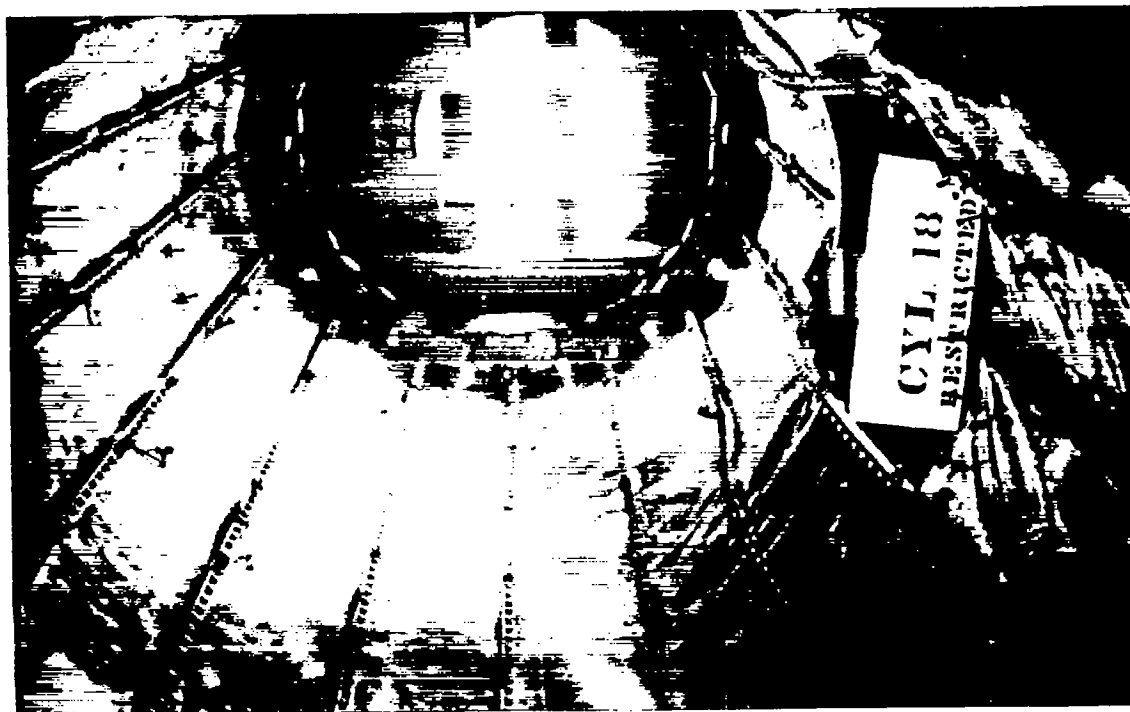
Figure 96.- Inside view of cylinder 18 after buckling.
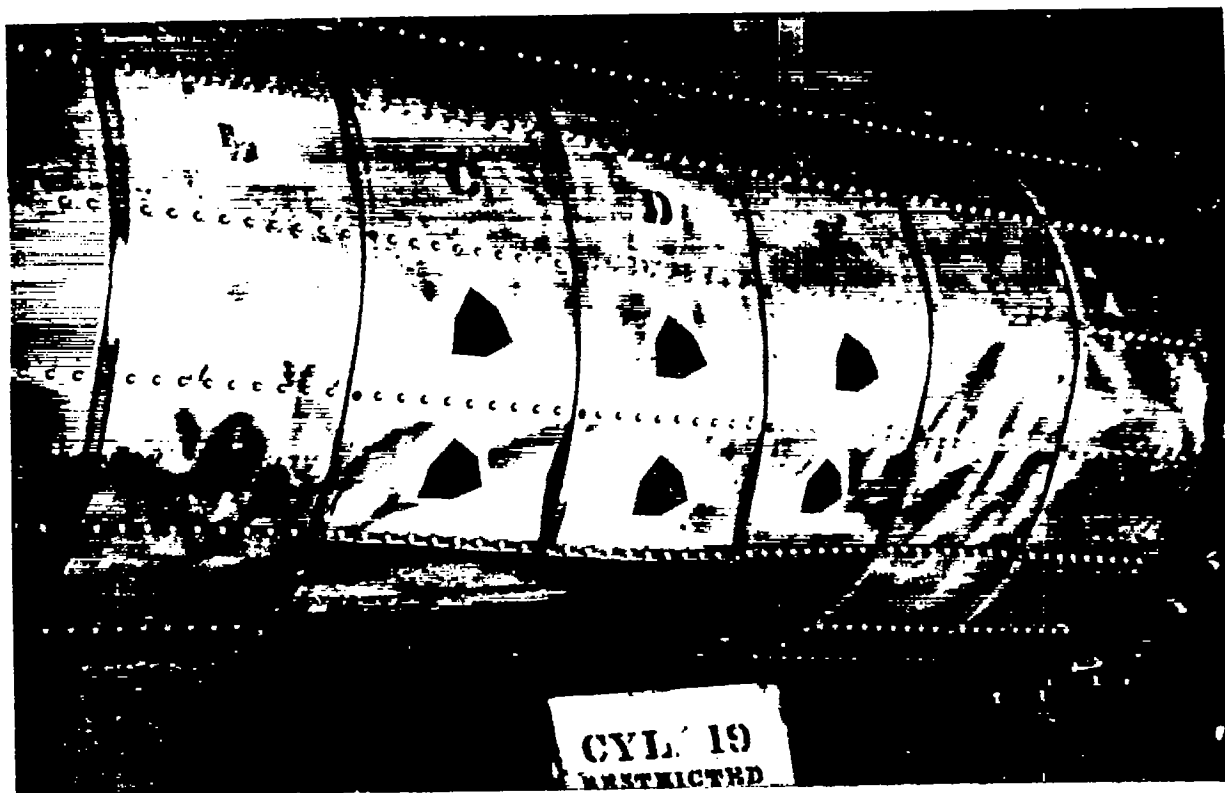
Figure 97.- Side view of cylinder 19 after buckling.
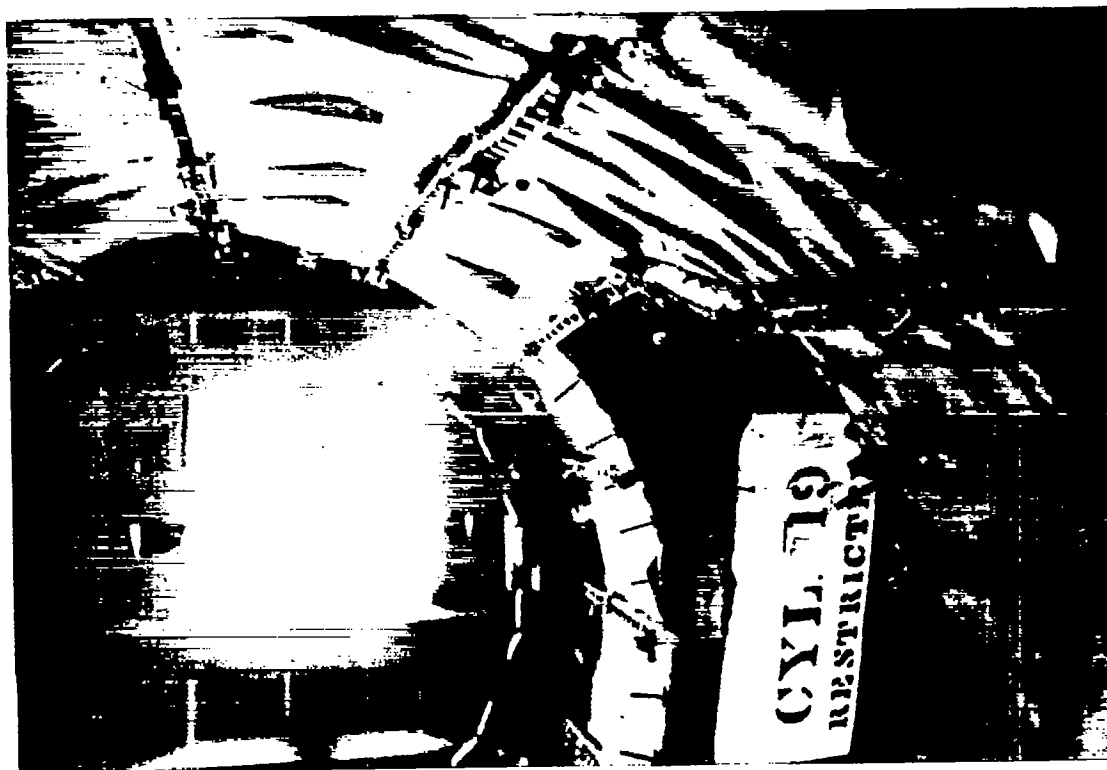
Figure 98.- Inside view of cylinder 19 after buckling.
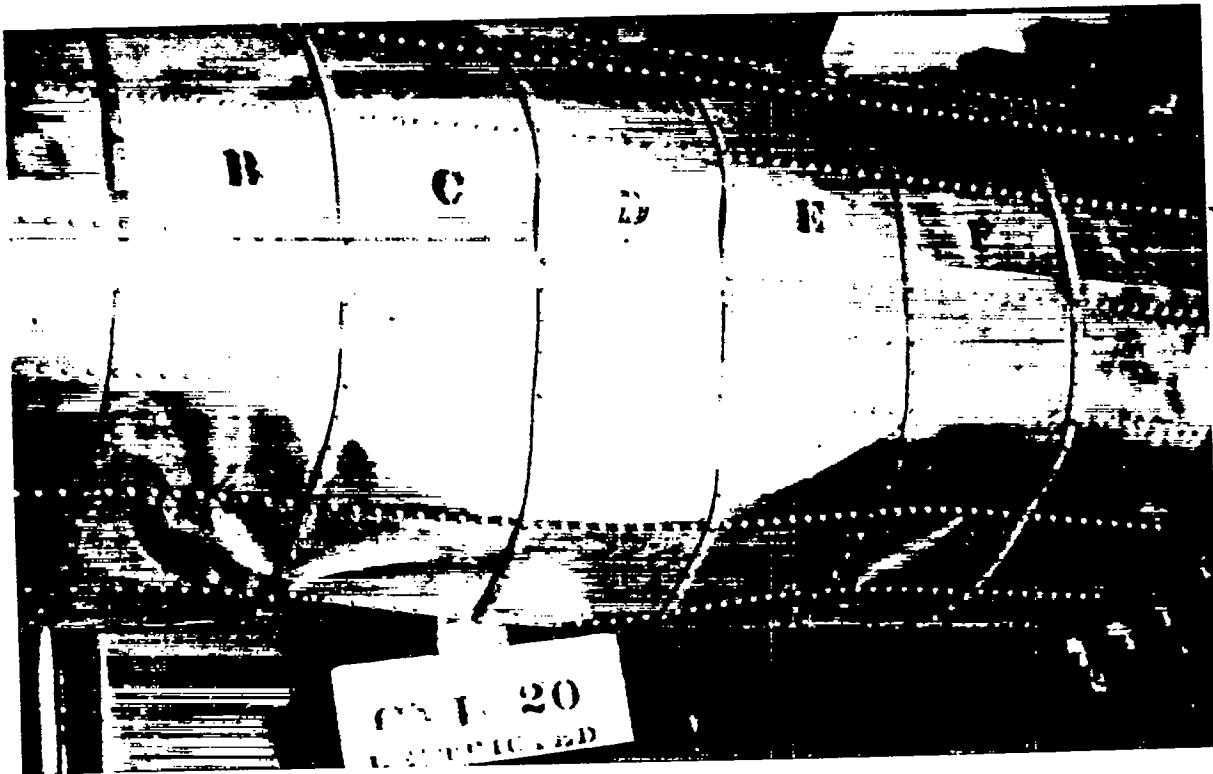
Figure 99.- Side view of cylinder 20 after buckling.
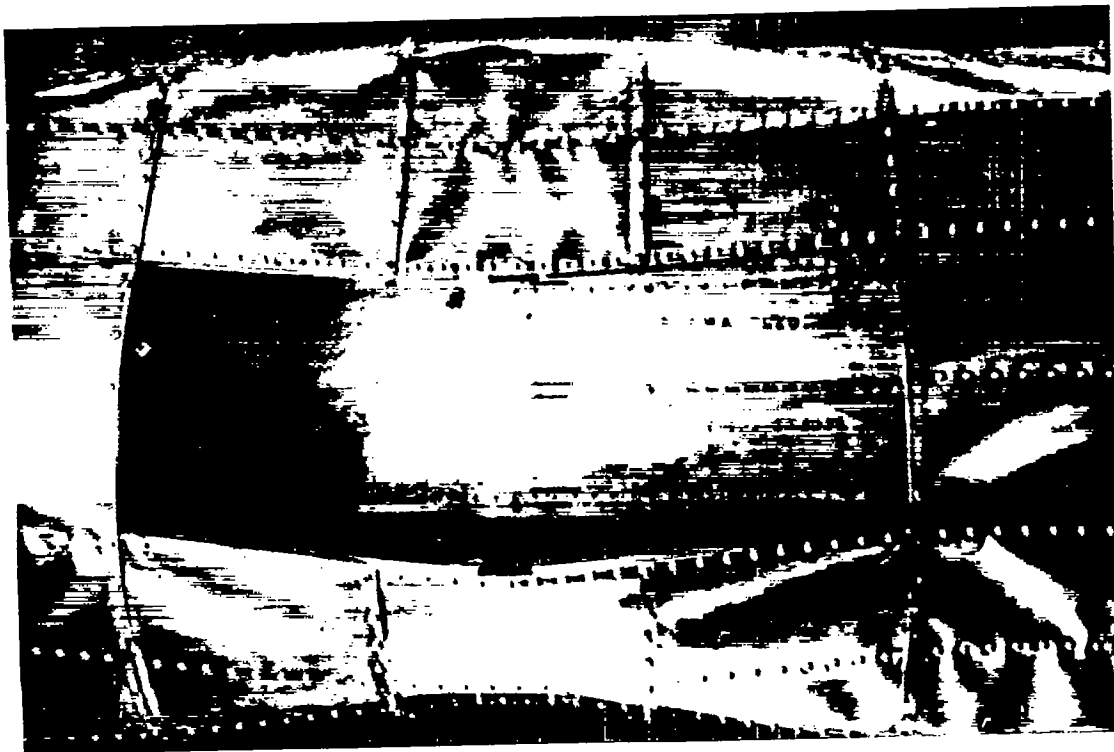
Figure 100.- View of cylinder 20 from below after buckling.
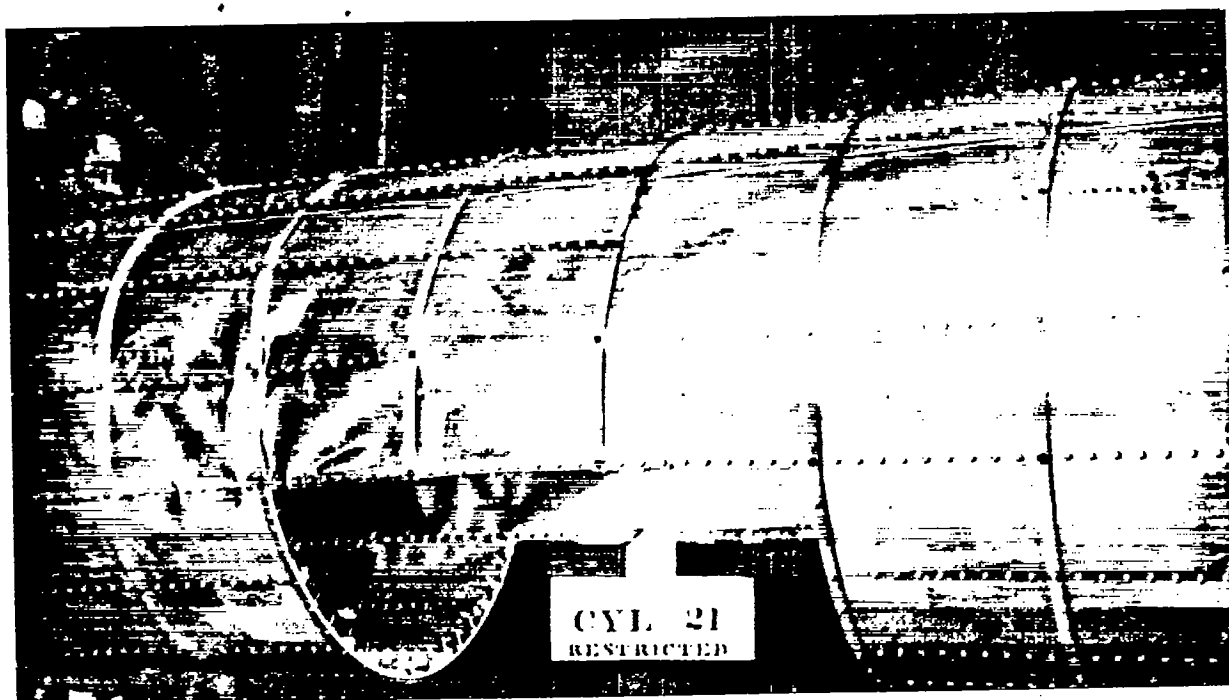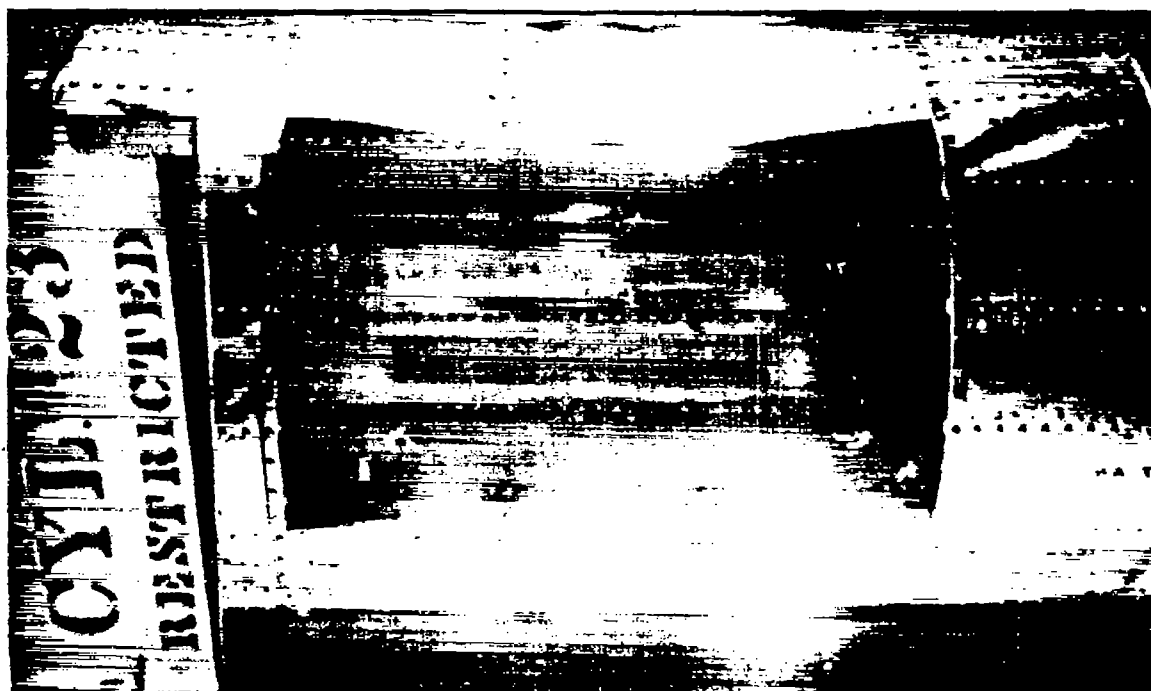
Figure 101.- Side view of cylinder 21 after buckling.

Figure 102.- Inside view of cylinder 21 after buckling.

Figure 103.- Side view of cylinder 22 after buckling.

Figure 104.- View of cylinder 22 from below after buckling.

Figure 105.- Inside view of cylinder 23 after buckling.

Figure 106.- View of cylinder 23 from below after buckling.
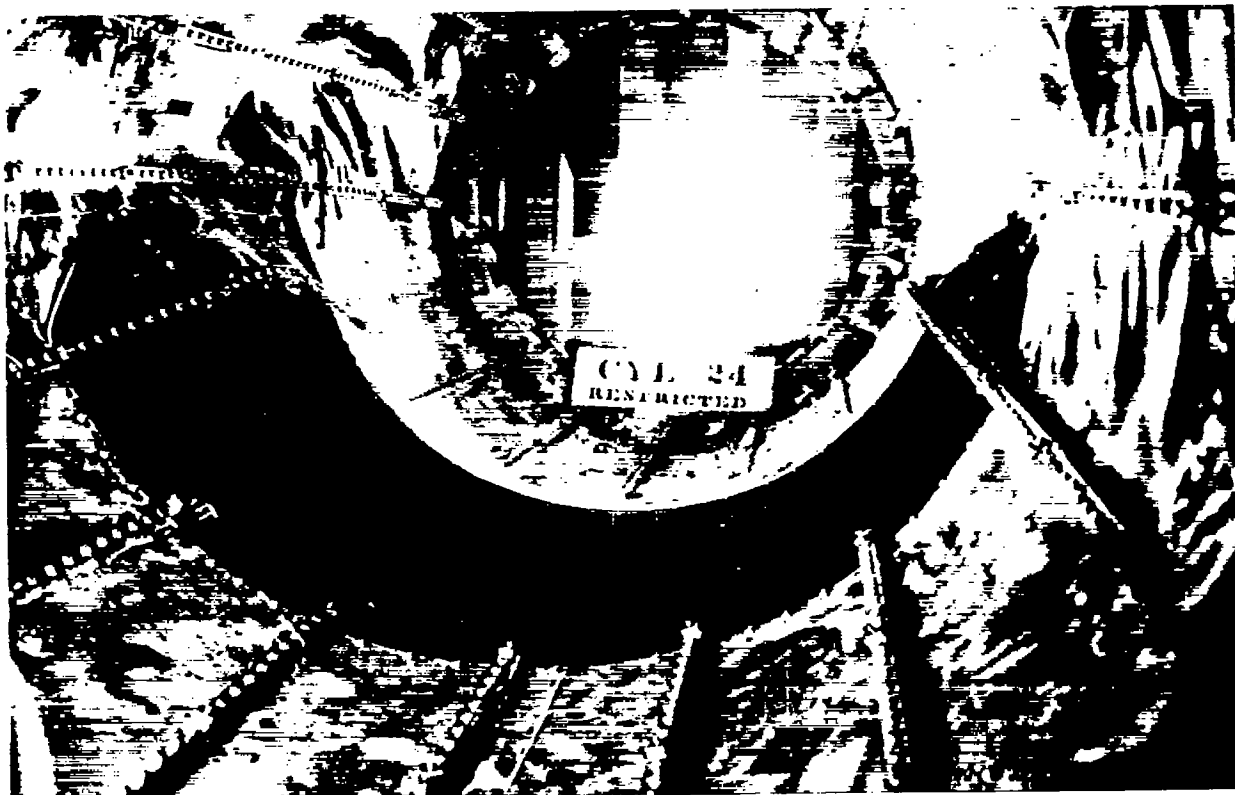
Figure 107.- Inside view of cylinder 24 after buckling.

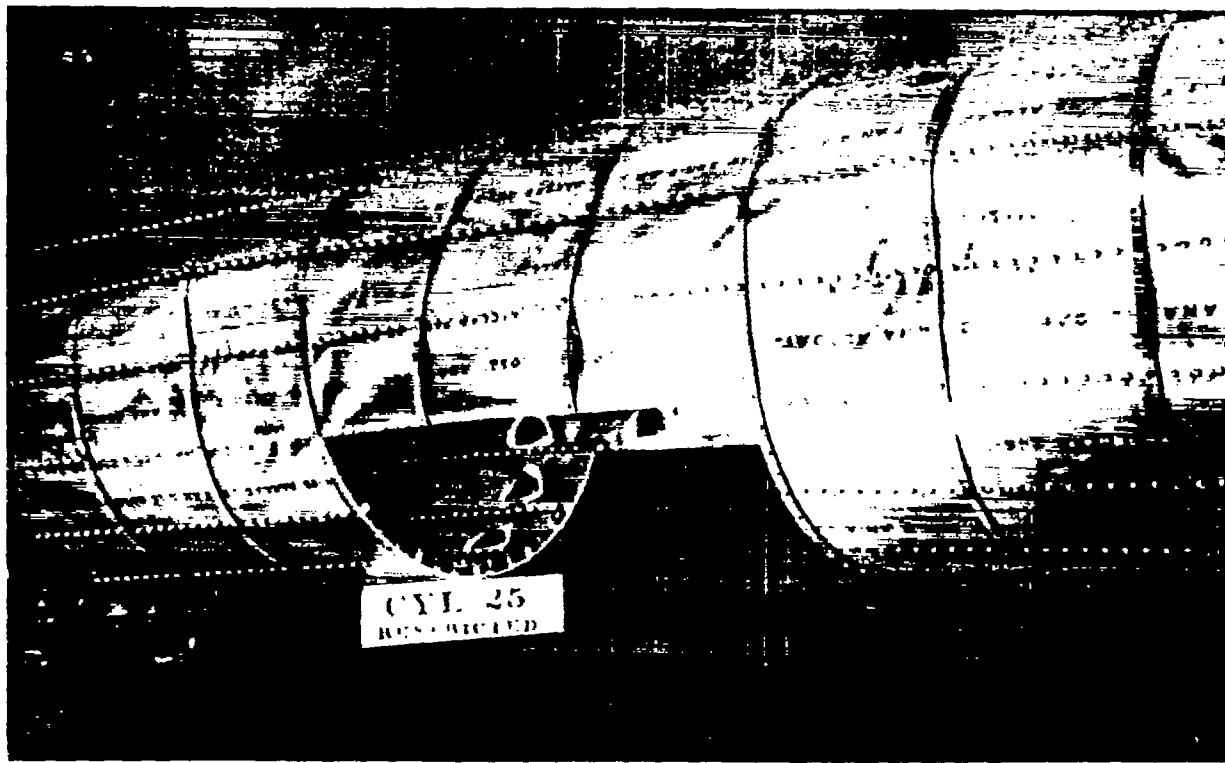Figure 108.- View of cylinder 24 from below after buckling.

Figure 109.- Side view of cylinder 25 after buckling.

Figure 110.- View of cylinder 25 from below after buckling.